The Dynamics of Stall and Surge Behavior in Axial-Centrifugal Compressors

by

William T. Cousins

Dissertation submitted to the Faculty of the
Virginia Polytechnic Institute and State University
in partial fulfillment of the requirements for the degree of

DOCTOR OF PHILOSOPHY
in
Mechanical Engineering

Walter F. O'Brien, Chairman
Eugene F. Brown
Milt W. Davis, Jr.
Wing F. Ng
Joseph A. Schetz

December 2, 1997
Blacksburg, Virginia

Key Words: Compressor, Stall, Surge, Unsteady-Flow, Dynamics, Axial, Centrifugal

The Dynamics of Stall and Surge Behavior in Axial-Centrifugal Compressors

by

William T. Cousins

Committee Chairman: Walter F. O'Brien

Department of Mechanical Engineering

ABSTRACT

The phenomena of stall and surge in axial-centrifugal compressors is investigated through high-response measurements of both the pressure field and the flowfield throughout the surge cycle. A unique high-response forward-facing and aft-facing probe provides flow information. Several axial-centrifugal compressors are examined, both in compressor rigs and engines. Extensive discussion is presented on the differences in axial and centrifugal rotors and their effect on the system response characteristics. The loading parameters of both are examined and data is presented that shows the increased tolerance of the centrifugal stage to instability. The dynamics of the compressor blade response are shown to be related to the transport time of a fluid particle moving through a blade passage. The data presented provides new insight into the dynamic interactions that occur prior to and during stall and surge. In addition, the inception of rotating stall and the inception of surge are shown to be the same phenomena. An analytical dynamic model (DYNTECC) is applied to one of the compression systems and the results are compared to data. The results show that the model can capture the global effects of rotating stall and surge. The data presented, along with the analytical results, provide useful information for the design of active and passive stall control systems.

ACKNOWLEDGEMENTS

As is always the case, there have been many people who have had an influence on the work that is contained in this dissertation. I would like to especially recognize my advisor, Dr. Walter O'Brien. It is certainly through his guidance and encouragement that this work is complete. In all the years of our relationship, he has never been one to insist on things being done in a certain way, but has always been there to encourage and provide the guidance when requested. He works with students as colleagues, not as boss and worker. I certainly owe him much for his support over the years and for helping to complete this work over a long distance. In addition, I would like to thank my committee, for their support and guidance in the completion of this work. Special thanks goes to Dr. Milt Davis at AEDC, for his guidance and support of the DYNTECC model. He has been interrupted many times with detailed modeling questions and has never failed to provide excellent support.

I would also like to thank AlliedSignal Engines, for permission to publish this material. Special thanks goes to Mark Jones, Ed Palmreuter, Bill Waterman, and Craig Thompson, for their support in this effort over the years. It is through the vision and acceptance of my ideas that this work proceeded. Tests such as those presented here require significant support. The laboratory support, especially from Paul Jobe and Manny Rubio has been superb, especially in light of my endless demands for data quality and the construction of specialized instrumentation. Thanks also to all those others at AlliedSignal for their encouragement and support of this work.

I would especially like to thank my Mom and Dad, who probably wondered if I would ever complete this work. It is through their many years of support and encouragement that I have had the desire to learn, and the drive to complete this work.

As always, there is a single person that stands out who has had a

greater effect on this work than anyone else, and that is my wife Nina. She has given me total support and encouragement, taking care of family duties to provide me with the environment and the time necessary to complete this effort. Above all that, the help in proofing this document into the late hours of the night can never be fully appreciated and recognized. And while they really don't yet understand what this is all about, I would like to thank Katie and Jonathan, my children, for their tolerance to Dad's frustrations and for their effort to keep the house quiet "so Dad could work."

I would like to dedicate this dissertation to my wife, Nina, whose love and consideration made this work possible.

TABLE OF CONTENTS

LIST OF FIGURES

LIST OF TABLES

NOMENCLATURE

A	area
c	absolute velocity
h	specific enthalpy
H	enthalpy
I	rothalpy
k	reduced frequency
p	pressure
Q	heat transfer rate
s	entropy
SW	shaft work
t	time
T	temperature
u	internal energy, velocity
U	blade velocity
v	average relative velocity
w	relative velocity
W	mass flow rate

ρ	density
τ	time constant

Subscripts

b	blade
B	boundaries
o	stagnation property
r	radial
rel	relative
REF	reference
s	static
ss	steady state
T	total
x	coordinate
θ	tangential

1.0 INTRODUCTION

The stability characteristic of the compression system is one of the major concerns in the design of gas turbines. When stability is not present, the resulting compression system instability is generally identified as either rotating stall or surge. When a compressor “stalls,” the flow over the blades of the compressor separates and the pressure rise capability and the flow capacity are both reduced. Rotating stall, typically a low-speed instability, is often thought of as being a blade-row based phenomena. During rotating stall, the flow over some of the airfoils separates and this separation propagates around the compressor annulus in the direction opposite rotor rotation. The rotation of the “stalled flow“ is induced by the change in the incoming air angle upstream of the rotor, caused by the blockage effects of the stalled blades themselves. Surge, on the other hand, is often recognized as a “system” phenomena. During this compression system instability, the flow over the blades of the compressor stalls and the pressure rise capability is reduced. When this occurs, the compressor cannot maintain the high-pressure downstream and a violent flow reversal occurs throughout the compression system.

Researchers have been examining the characteristics of stall and surge behavior of gas turbine engines for many years. Much research has been presented on the *characteristics* of stall and the *characteristics* of surge, but little has been discussed on the stall and surge differences inherent in various configurations of compressors. Different configurations of compression systems have different stall and recovery characteristics and interstage dynamics, although the basic physics of why a compressor stalls and the associated fluid mechanics are the same.

Over the past years, performance modeling, aerodynamic design modeling, and the design of basic performance-related parameters such as blade clearance, blade metal angles, and blade surface finish have improved to the

point that gas turbine performance is now limited primarily by the materials used. New materials that can withstand high stresses (due to high blade tip speeds) and high temperatures will help achieve greater performance. However, even with the development of new materials, engine performance can always be enhanced by operating the compression system closer to instability, to take advantage of the available higher pressure ratio.

There are basically three types of compression systems in present-day aircraft engines: axial compressors, centrifugal compressors, and axial-centrifugal compressors. (There is another design that uses what is called mixed-flow technology, which is part axial and part centrifugal, but these will not be addressed here.) Of course, whether an engine compression system is designed around a multi-stage centrifugal compressor, an axial compressor, or an axial-centrifugal compressor is a function of the size class of the engine. There is a range of compression system flow size where a multi-stage centrifugal compression system (shown in Figure 1-1) is clearly the best system to use in terms of efficiency, cost, weight and reliability. On the other end of the scale, at larger flows, there is a point at which centrifugal compressors become too heavy and the efficiency characteristics unacceptable for propulsion applications, and the axial compression system is the best choice. Between the appropriate size class for a multi-stage centrifugal compressor and the size class for which an all axial machine is appropriate, there lies a class of combined axial-centrifugal compression systems (Fig. 1-2) that can be designed to provide the best of both worlds. When a multi-stage centrifugal compressor is clearly not the correct choice, the decision often must be made whether to use an axial compressor or an axial-centrifugal compressor. In many engine applications that fall into about the 3,000 to 15,000 pound thrust class, such as many business, military and regional aircraft, the axial-centrifugal compression system is the system of preference. Figure 1-3 shows the TFE1042 engine (with the afterburner removed) containing a 5-stage axial-centrifugal compression system and a 3-stage axial

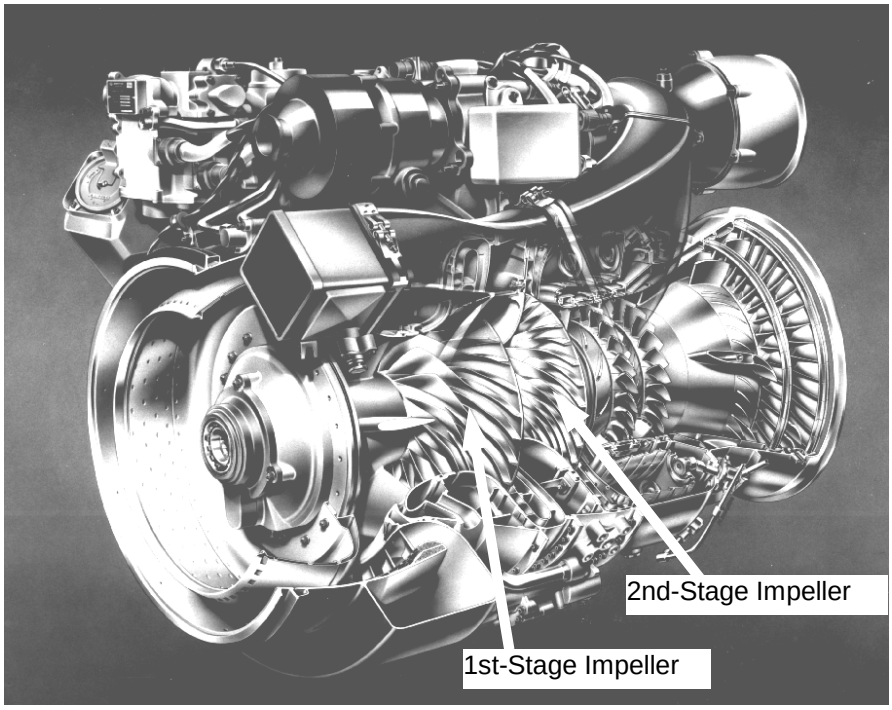

Figure 1-1 T800 Engine Containing a 2-Stage Centrifugal Compression System

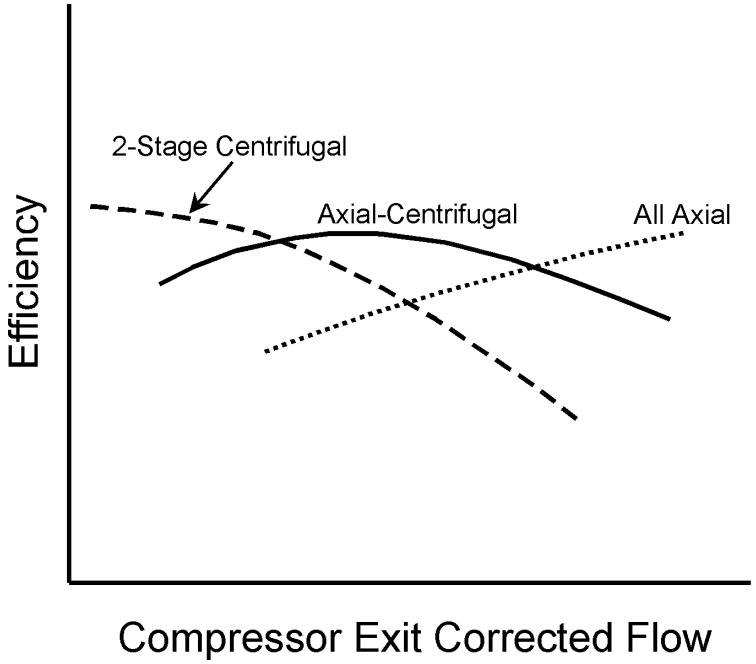

Figure 1-2 Typical Efficiency Characteristics for Several Compression Systems

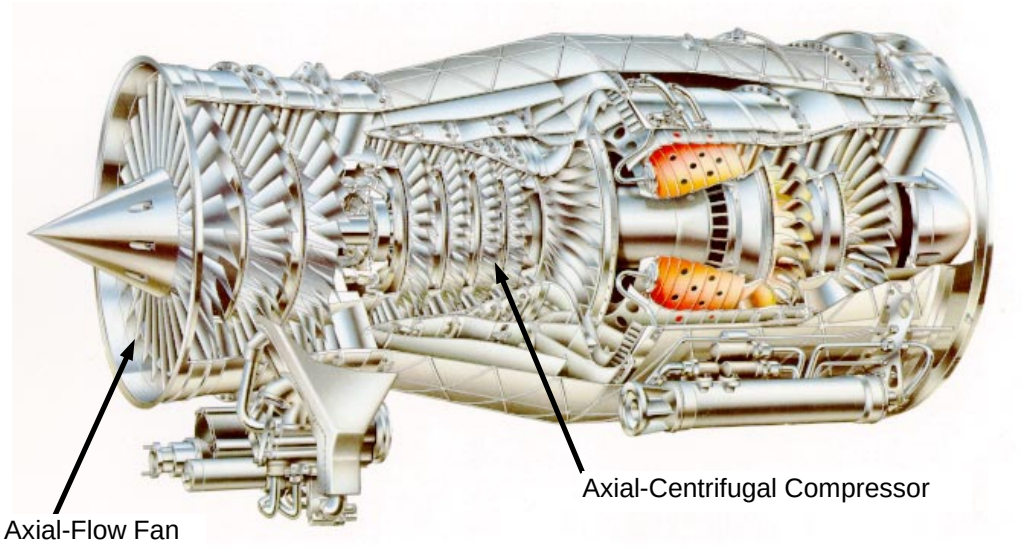

Figure 1-3 TFE1042 Engine w/o Afterburner Showing the 3-Stage Axial-Flow Fan and the 5-Stage Axial-Centrifugal Compressor

flow fan.

This dissertation is the first detailed investigation of the dynamic stage matching and the dynamic behavior that occurs in axial-centrifugal compression systems. Following a literature review of pertinent work, the design characteristics of axial and centrifugal blades are discussed. The special instrumentation that is necessary to perform a complete examination of the interstage dynamics that occur prior to and during compression system instability is then presented. Next, the compression systems that were examined and the detailed test results are shown. A dynamic model is evaluated and the model capability compared to the test data. Finally, a detailed discussion of the results is presented and conclusions are drawn.

2.0 LITERATURE REVIEW

Over the past 40 years, volumes of material have been written describing why stall and surge occur and what the characteristics look like. There have been many studies on the quasi-steady behavior of rotating stall, and surge (the behavior which may be exhibited once rotating stall is established), but examinations of the dynamic interactions (what occurs before rotating stall and surge) are few. The non-linear, unsteady behavior has historically been difficult to examine experimentally, due to the complexity of the instrumentation required. The general technique used to understand stall and surge has been to obtain whatever data possible, then to model the phenomena and draw conclusions. The majority of the work that has relevance to the dynamics of stall and surge has been performed on axial compressors. Work in the centrifugal compressor field generally attempts to follow the axial methodology.

The original work by Emmons, et al. (1955) is perhaps the first system modeling of incipient stall and surge. Model development and attempts at measuring stall and surge have continued for years. One of the early non-linear models that was created to attempt to examine the characteristics of rotating stall was that of Takata and Nagano (1972). While this model formed what looked like stall cell perturbations, the detailed formation of rotating stall through multiple stall cells was not possible. Other early work performed to measure and examine the dynamic response of a compressor stage was that by Adamczyk and Carta (1973). They worked in the area of distorted inflow and showed that the degradation of the stable operating range of a compressor stage was related to how the blade row attenuated the incoming distortion. The original work by Day (1976) examined the hysteresis behavior of rotating stall and showed that the more stages the axial compressor had, the greater the hysteresis behavior when trying to recover from rotating stall. While this work did not use high response measurements, and was performed on a low speed com-

pressor, the analysis of velocity diagrams during stall showed that the basic physics of flow velocity triangles were followed in the stalled regime. Later work by Greitzer (1978a, 1978b) showed a system interaction and a system dependence on the development of rotating stall and surge. Further work on the hysteresis behavior (Day, et al., 1978) showed that the blockage of the stall cell influenced the future performance of the compressor. Day and Cumpsty (1978) showed that in a multistage axial machine, the developed rotating stall cell was axial through the compressor and was not skewed as was previously thought. Later, Moore (1983) took a compressor map characteristic and defined an axisymmetric characteristic (on which the compressor would operate if it did not stall) as part of a system description of unstable operation. This work treated the whole compression system as a unit, providing pressure rise that could be affected by actions to the outside system. While this was probably one of the major works that examined a compressor as a system without regard to the inner workings, serious application was limited due to the difficulty of describing what was called the “axisymmetric characteristic,” that is, the flow and pressure ratio characteristic on which the compressor would run if it did not stall. Examinations of the pressure rise capability of an axial-flow compressor during instability by Koch (1981) found that energy input to the low-momentum fluid still gave some pressure rise capability to the axial stages. Detailed rotating stall measurements by Cheng, et al. (1984) showed that the time constants associated with blade stall and recovery were different. This was shown through measurements of the leading and trailing edge of a rotating stall cell in a single isolated rotor through hot wire measurements. Further work in the blade-row approach to the examination and modeling of stall and surge came about through the work by such individuals as Kimzey (1977), Sexton and O’Brien (1981), Cousins and O’Brien (1985), Boyer and O’Brien (1989), and Davis and O’Brien (1991). Through these works and others, it was shown that a blade-row-based model could be used to model overall unstable compressor operation. The

work by Sexton and O'Brien (1981) used a transfer function to describe the dynamics of the rotating blade row that do not exist in a stationary cascade. This first order dynamic response model was the first model developed from examinations of the differences between the stalling behavior of a cascade and that of a rotating blade row. Observations in all of these works showed how the balance of blade row operational loading conditions, loss increases, and flow stability determine the stall and surge behavior of a compressor.

Data obtained by Cousins (1985) showed surge and rotating stall beginning in the same manner, through local flow separation within the blade row. This local separation grew into either a full rotating stall or grew large enough to disturb the overall pressure balance of the machine, causing a surge. Day (1993) presented data showing this effect, and stated that it showed that surge is always preceded by rotating stall. Owen and Davis (1994) examined static pressure fluctuations during stall and surge in an axial-centrifugal compressor and matched a model to the data, showing the ability to model the overall system dynamics with a blade-row based model.

Throughout the literature search, even considering the work by Owen and Davis (1994), no in-depth investigation into the dynamics of stall and surge in axial-centrifugal compressors was found. The following work is intended to fill this gap, and is presented as a contribution to the understanding of stall and surge dynamics in axial-centrifugal compression systems.

3.0 THEME AND FOCUS OF THIS WORK

This work was performed to develop an understanding of the dynamics of stall and surge in axial-centrifugal compressors through experimental measurement and to examine the applicability of modeling these dynamics with a blade-row based analytical model.

There are four major contributions to the understanding of the dynamics of stall and surge that are addressed in this dissertation.

1. This work provides new information on interstage dynamics through a very detailed study of axial-centrifugal compression systems.
2. The modeling portion of this work shows that a contemporary, detailed, stage-by-stage model that is properly constructed can capture the main features of stall and surge, but some modifications are necessary to correctly simulate the reversed flow behavior.
3. The measurement results provide new insight into the development of stall and surge. These new insights can be extended to axial compressors and to compression systems of other configurations.
4. The measurement results provide new information on the probable limitations of both active and passive stability control systems, along with information necessary to be considered in the design of such systems.

4.0 CHARACTERISTICS OF AXIAL AND CENTRIFUGAL BLADES THAT RESULT IN DIFFERENCES IN DYNAMIC RESPONSE

4.1 The Pressure Rise Capability of Axial and Centrifugal Stages

Pressure rise in all compressors occurs by the conversion of shaft work to fluid pressure. However, there is a basic difference between the pressure rise capability of the axial blade and that of a centrifugal impeller. Close examination of a centrifugal impeller shows that the inducer section (the near-axial front portion) looks and acts in a way similar to the axial blade, but the rear of a centrifugal impeller is quite different. The rear of the centrifugal impeller obtains pressure rise not only from the diffusing passage but also from the radial flow vector. Figure 4-1 shows the h-s diagram for the centrifugal stage (impeller and diffuser).

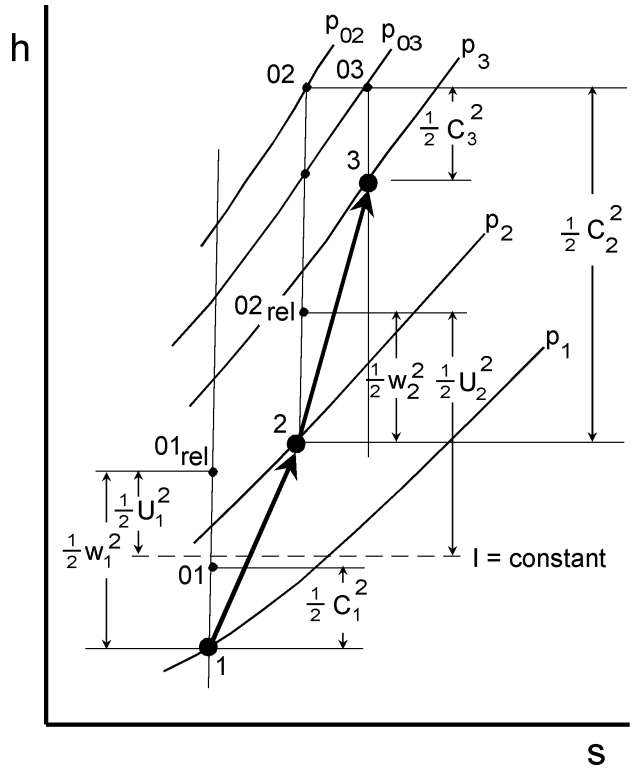

Figure 4-1 Enthalpy-Entropy Diagram for a Centrifugal Compressor Stage

The specific work done on the fluid is equal to the stagnation enthalpy rise in the rotor, or

$$w = U_2 c_{\theta 2} - U_1 c_{\theta 1} = h_{o2} - h_{o1} \qquad (4.1)$$

Substituting $h_o = h + 1/2\ c^2$, the equation becomes

$$h_1 + 1/2\ c_1^2 - U_1 c_{\theta 1} = h_2 + 1/2\ c_2^2 - U_2 c_{\theta 2} = I \qquad (4.2)$$

The function I is known as the rotational stagnation enthalpy, or *rothalpy.* The rothalpy is constant along a streamline from the inlet of the impeller to the exit. Since the velocity component c is made up of radial, tangential, and axial components (c_r, c_θ, and c_x), the rothalpy can be written as

$$I = h + 1/2\ (c_r^2 + c_\theta^2 + c_x^2 - 2Uc_\theta) \qquad (4.3)$$

Since $U - c_\theta = w_\theta$ and $w^2 = c_r^2 + w_\theta^2 + c_x^2$, the rothalpy can be expressed as

$$I = h + 1/2\ (w^2 - U^2) = h_{o\ rel} - 1/2\ U^2 \qquad (4.4)$$

Since the rothalpy is constant across the impeller, equation (4.4) gives

$$h_2 - h_1 = 1/2\ (U_2^2 - U_1^2) + 1/2\ (w_2^2 - w_1^2) \qquad (4.5)$$

The enthalpy rise due to the radial flow (and therefore the radial flow pressure rise), represented by the term $1/2\ (U_2^2 - U_1^2)$, makes the centrifugal impeller match so very important to the design of an axial-centrifugal compression system. As long as the system is rotating, pressure rise will be achieved by the $1/2\ (U_2^2 - U_1^2)$ term and flow will be pulled through the axial portion of the compression system. During surge, when the compressor backflows, this pressure rise must be overcome before backflow can occur. Figure 4-2 shows the h-s diagram for an axial stage. The enthalpy change across the rotor is rep-

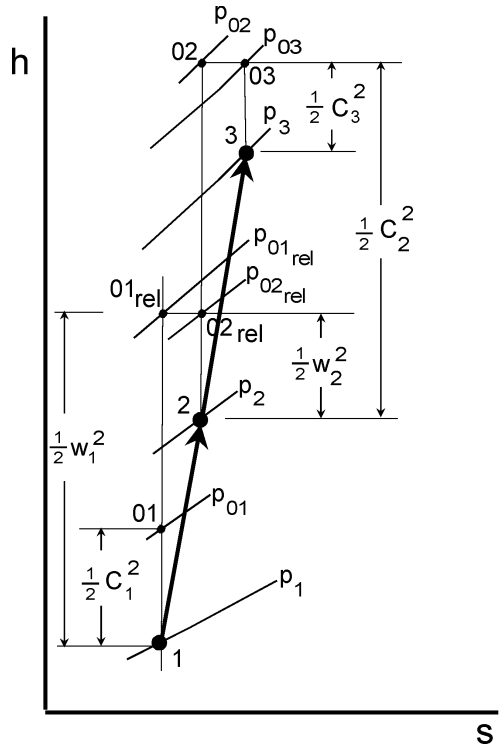

Figure 4-2 Enthalpy-Entropy Diagram for an Axial Compressor Stage

resented by

$$h_2 - h_1 = 1/2\ (w_2^2 - w_1^2) \qquad (4.6)$$

as long as there is no radial shift in the streamlines across the rotor. In reality, there is generally a very small radial shift, due only to the slight convergence of the flowpath. This convergence provides insignificant pressure rise when compared to the radial change in the centrifugal impeller. As will be seen in the following work, this is very important to the dynamics of the compressor operation during stall inception and recovery.

Centrifugal impellers also tend to have more tolerance to poor inlet flow conditions (conditions that vary in flow and pressure) than axial-flow compressor blades. The centrifugal impeller's tolerance to stall as a result of the radial pressure rise characteristic benefits the overall compression system into which

it is designed.

Figures 4-3 and 4-4 show a typical design loading diagram for a current technology compressor rotor and the associated Mach number distribution between the rotor blades. Examination of these figures shows that a slight diffusion occurs between the leading edge of the rotor and the throat, at approximately 35 percent of the meridional distance along the blade. In design, this slight diffusion is minimized, since turning the flow under high Mach number conditions generates excess losses. In effect, this causes most of the pressure rise in the rotor to occur between the throat and the trailing edge. The diffusion rate in this region is carefully controlled to minimize separation. Figures 4-5 and 4-6 show a typical loading diagram and the Mach number distribution for a stator in the same stage. In a typical axial compressor stage, the rotor is the component that limits the pressure rise of a stalled stage. It can be seen on a stage characteristic (Figure 4-7) that as the peak pressure is reached and rotor stall occurs, the work input to the flow continues until zero flow is reached. In current technology airfoils, it is generally more difficult to maintain the proper diffusion rate in the rotor than the stator, due to the Mach number control that must be maintained. Therefore, the interstage dynamic pressure measurements obtained for this work are taken at the rotor trailing edge wherever possible.

Figure 4-8 shows the loading diagram for a centrifugal impeller. The throat of the centrifugal impeller is typically very near the leading edge, in contrast to the axial rotor. The inducer section of the impeller provides rapid diffusion which lessens as the flow moves around the corner, into the radial portion of the impeller. In the radial portion of the impeller, the diffusion comes largely from the change in the flow cross-sectional area due to moving in the radial direction, rather than loading along the airfoil as in the inducer section and in an axial rotor. The loading diagram in Figure 4-8 also shows the loading on the splitter vanes, which have a leading edge starting about halfway through the flow transition to the radial direction. This is the radial portion of the impeller

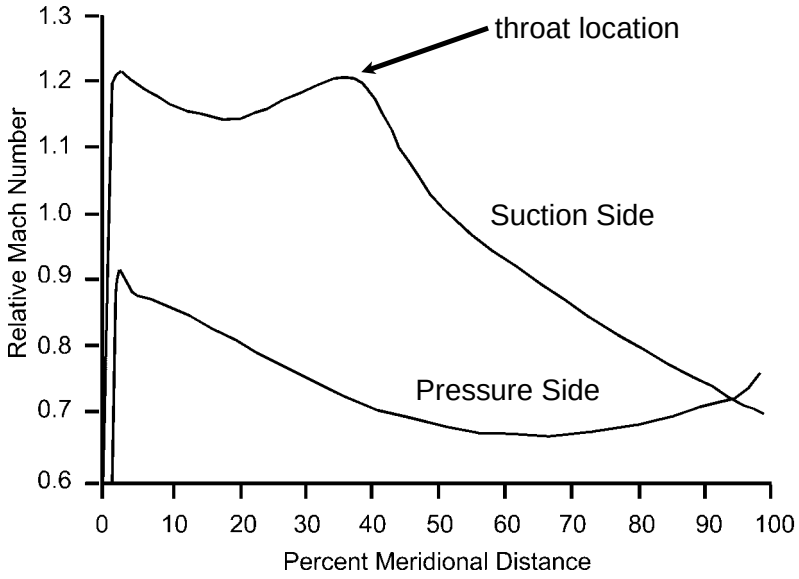

Figure 4-3 Typical Axial Rotor Loading Diagram

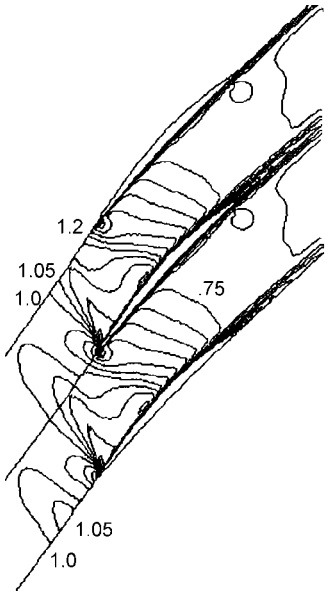

Figure 4-4 Typical Blade-to-Blade Rotor Mach Number Distribution

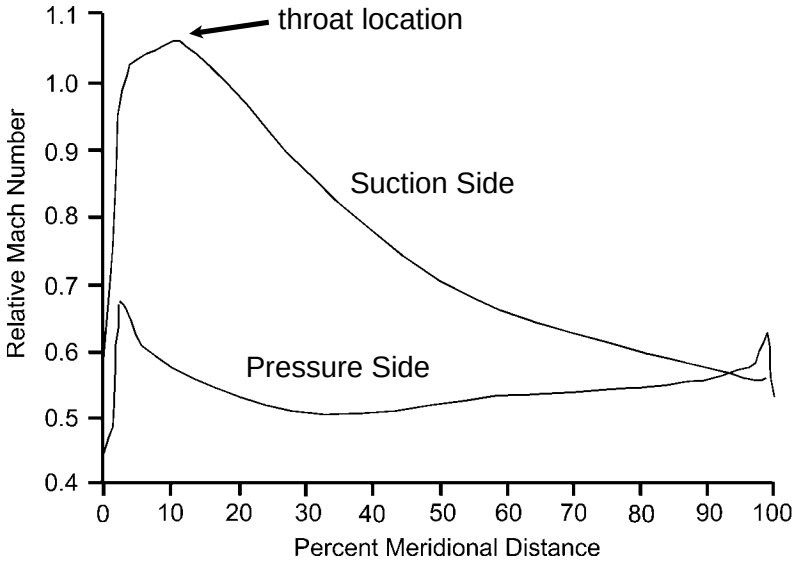

Figure 4-5 Typical Axial Stator Loading Diagram

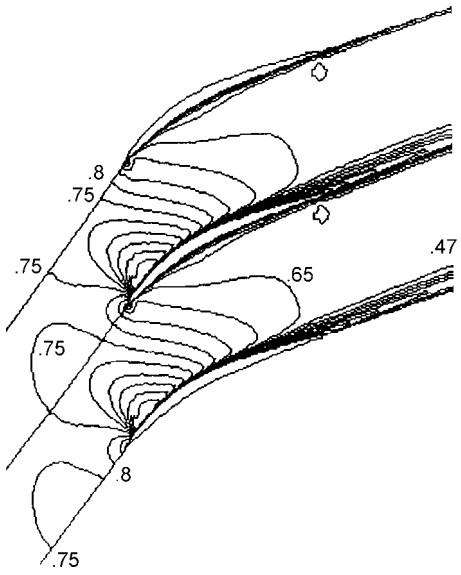

Figure 4-6 Typical Blade-to-Blade Stator Mach Number Distribution

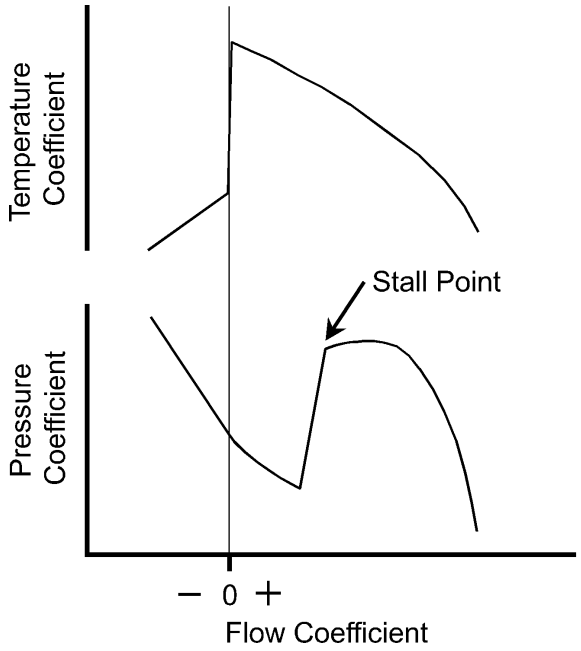

Figure 4-7 Shape of the Stage Characteristics for a Compressor

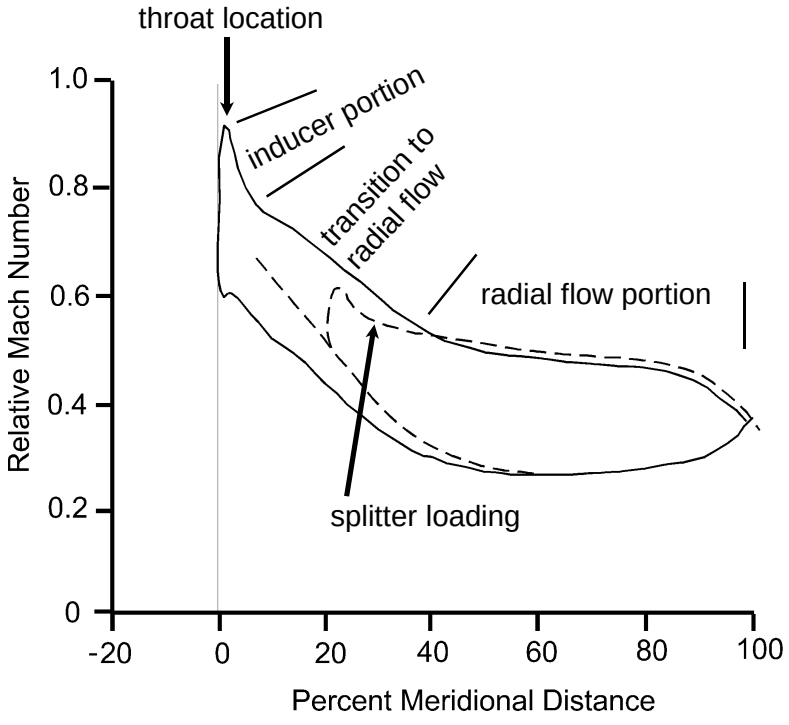

Figure 4-8 Loading Diagram for a Centrifugal Impeller

that causes the pressure rise shown as the 1/2 (U_2^2 - U_1^2) term presented earlier in Equation (4.5). It is this characteristic of the centrifugal impeller that is critical to the interstage dynamics of the axial-centrifugal compressor. Because the radial flow greatly increases the pressure rise and flow pumping capacity, the centrifugal impeller has a stabilizing effect on the axial portion of the compression system. This will be proven in the test data that follows. Another benefit of the radial portion of the centrifugal impeller is that it causes the impeller to be very tolerant to poor inlet flow conditions. This increased tolerance is an important reason for having the centrifugal impeller downstream of the axial compressor. During instability, which will be shown later to be often driven by the axial compressor, the centrifugal impeller must ingest highly turbulent, poorly distributed flow.

4.2 Axial and Centrifugal Blade Response to Changing Inlet Conditions

Sudden changes in inlet conditions affect axial and centrifugal rotors in different ways. Since the pressure rise of axial and centrifugal rotors is formulated in different ways (as discussed in Section 4.1), the time constants associated with changes in their pressure rise ability with varying inlet conditions must also be different. Careful examination of the axial rotor loading diagram (Figure 4-3) and the associated Mach number distribution (Figure 4-4) shows that most of the diffusion that occurs over the blade surface does so after about 35 percent of the meridional distance is reached. If a particle of fluid is traced as it enters into the blade passage, there is a time response associated with how long it takes the blade to “know” (or to respond) to the change that has occurred. The time response for the blade can be calculated by dividing the distance traveled to the throat of the passage (the start of the diffusion) by the relative velocity (either the average relative velocity or possibly even the integral along the path to account for the changing velocity with distance), as shown in Figure 4-9. If the blade rotates past a maldistribution in pressure (for example an ideal

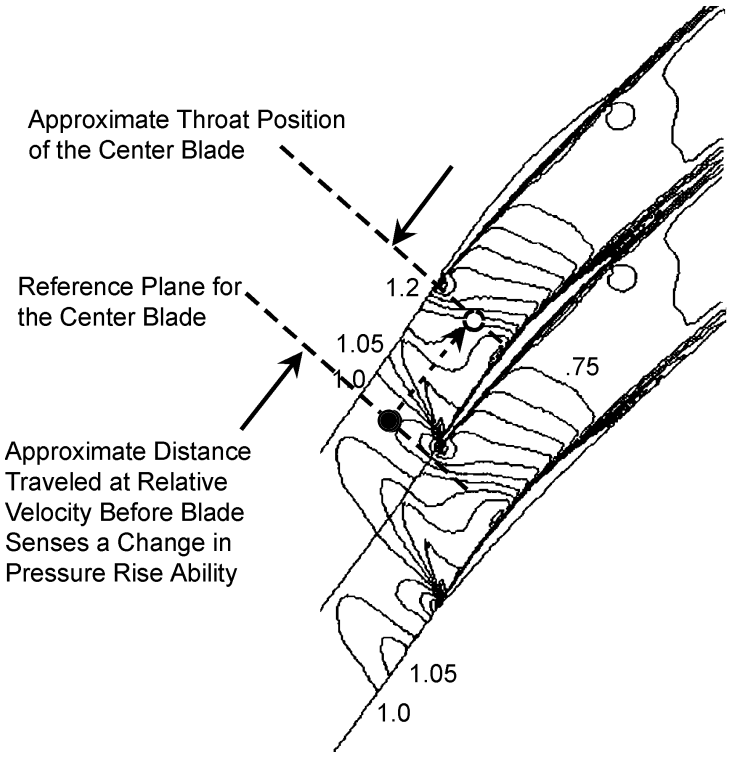

Figure 4-9 Distance a Particle of Fluid Must Travel to the Throat of the Blade Passage to Reach the Start of the Major Diffusion Process

square wave), the time the blade is resident in the low pressure region (low momentum fluid) can be compared to the time it takes for the particle of fluid to reach the throat of the blade. If the fluid particle transport time is less than the time the blade is resident in the low momentum fluid, the blade response will be maximized, as shown in Figure 4-10. This is because the blade has more time to respond to the low momentum fluid.

The time constant of a centrifugal impeller is significantly different than that for an axial blade. For the axial blade, once the blade senses the change in the inlet flow (the particle of fluid reaches the throat), there is a chance that the diffusion process along the remaining portion of the blade can be disrupted, causing flow separation. Once the flow is separated on an axial blade, the pressure rise capability is severely limited. In comparison, to have a similar ef-

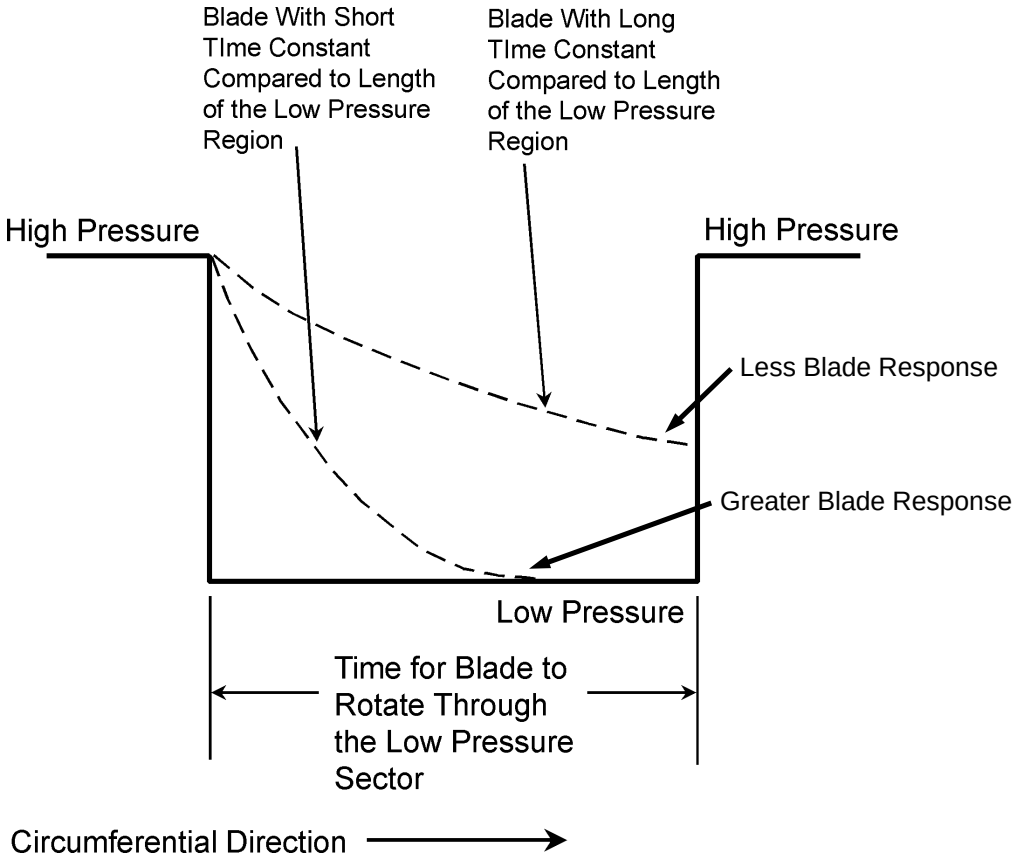

Figure 4-10 Blade Time Constant Comparison to a Distorted Inlet Flow Determines the Magnitude of the Blade Response

fect on the centrifugal rotor, the particle of fluid has to not only reach the throat (which it does very quickly since the throat is typically very near the leading edge, as shown in Figure 4-8) but has to travel far enough into the rotor to affect the radial flow component. In physical distance, this is much larger than the distance traveled in the axial blade and therefore requires significantly more time, giving the centrifugal rotor a greater tolerance to changes in inlet conditions. This can be seen by calculating the parameter known as the reduced frequency and defined as

$$k = \beta \omega / v \qquad (4.7)$$

where

β = 1/2 the rotor chord length (or the meridional distance for consistency),

ω = frequency of the disturbance in radians per second, and

v = the average relative velocity.

Careful examination of the reduced frequency indicates that increasing the reduced frequency of a blade row means increased tolerance to inlet disturbances and higher tolerance to unsteady flow effects. With the larger meridional chord length of centrifugal impellers, it is easy to see why there is an increased tolerance to poor inlet flow conditions. As the test data is presented in Section 7.0 of this document, it will be seen that this tolerance shows up as a benefit to the stall recovery capability of the axial-centrifugal compressor.

4.3 Axial and Centrifugal Stage Matching

In a well-designed axial compression system, the front stages of the compressor are designed to operate near their stability limit and the back of the compressor is designed to operate near choke when the machine is operating at low speed. At high speed, the reverse is true. The rear of the compressor operates near its stability limit while the front is matched near choke. In gen-

eral, this provides the most stable machine and is consistent with the physics of the flow as the compressor operating point moves toward high-speed operation. With an axial-centrifugal compression system, this general rule is the same, but if the centrifugal compressor is designed with enough flow range, it can be prevented from triggering the compression system instability. This will enhance the stability of the whole compression system since the centrifugal compressor stage then acts as a *stability enhancing device* to the axial compressor. Figure 4-11 shows the typical stage matching for an axial-centrifugal compression system where the stability is enhanced by the centrifugal stage. In a well-designed axial-centrifugal compressor, this surge trigger is controlled through the design configuration and the system operation such that the surge trigger remains in the axial portion of the compressor, under most conditions. The following measurements will show the effect of the centrifugal stage on the stall and surge behavior of an axial compressor.

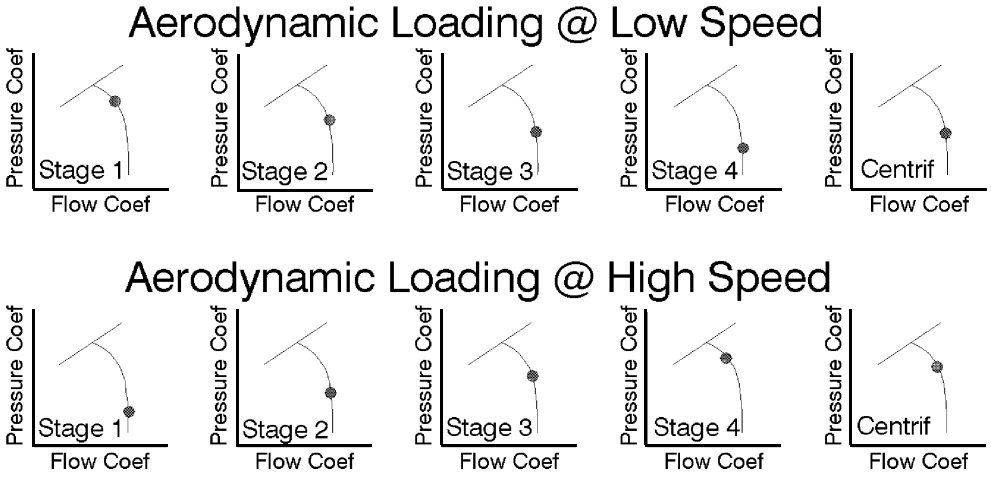

Figure 4-11 Preferred Axial-Centrifugal Loading Distribution

5.0 INSTRUMENTATION USED FOR DYNAMIC EVALUATION

Several configurations of axial-centrifugal compression systems were used to demonstrate the concepts presented in this work. These were a research compressor rig, the TFE1042 compressor rig, the TFE1042 engine, and the TFE731 engine. The TFE731 engine is of a split-core configuration, that is, the axial and the centrifugal compressors are on different spools. The other compression systems are designed with the axial and the centrifugal compressors on the same spool. These two configurations have some different characteristics, which will be discussed later.

While there are many ways to examine the unsteady flows in a compression system, one of the better methods is the monitoring of the pressure field with high response transducers. These can be used to measure both steady-state pressure levels and the rapid pressure changes that occur during the stall and surge process. To obtain good results, a high regard for the flow physics and an understanding of the flow in the compression system is necessary. Data signals from high-response transducers can be easily misinterpreted, if one is not familiar with the instrumentation frequency response, the effects of tape recording on data, and digital sampling theory. The results discussed here meet the criteria for good high-response data and are well within the accuracy and frequency requirements necessary for the analysis performed.

The measurement systems used to obtain the results of this work involve standard steady-state measurement systems normally used in compressor rigs and engines, and also high-response transducers designed to measure either total or static pressure, depending on the analysis requirements.

5.1 Measurement of Flow Through a Complete Surge Cycle

To examine the pressure/flow characteristics of a complete surge cycle, measurements capable of providing information through both forward and reverse flow in the compressor are necessary. Figure 5-1 shows a forward and

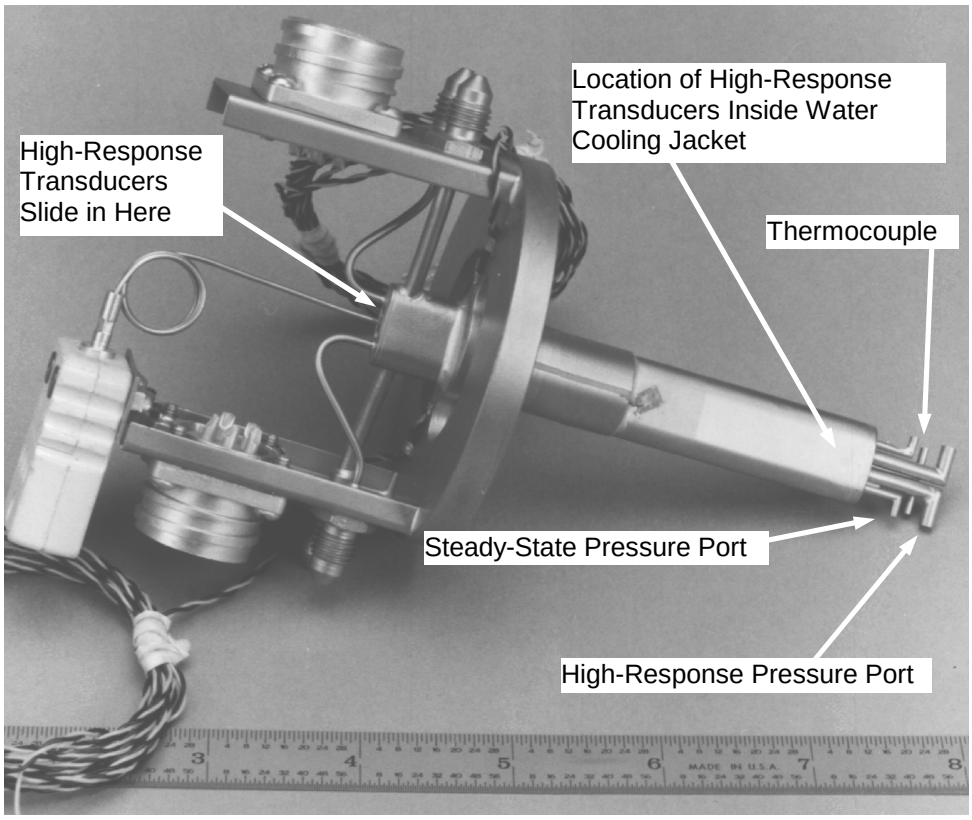

Figure 5-1 Fore-Aft Probe (Mach Probe) Used for High-Response Flow Measurements During Surge Behavior

aft facing probe that is used for this purpose. This special probe was designed to provide high-response data with a frequency response up to 5,000 Hz. The head of the probe contains two Kulite high-response pressure transducers, a high-response shielded thermocouple, and two steady state pressure measurements. The steady state pressure measurements were used as an in-place check of the pressure levels displayed by the high-response system. The probe is water cooled to keep the temperature of the transducers at a constant value, eliminating the worry of pushing the transducer past its compensated temperature range. While temperature is not a problem in the front of a compressor,

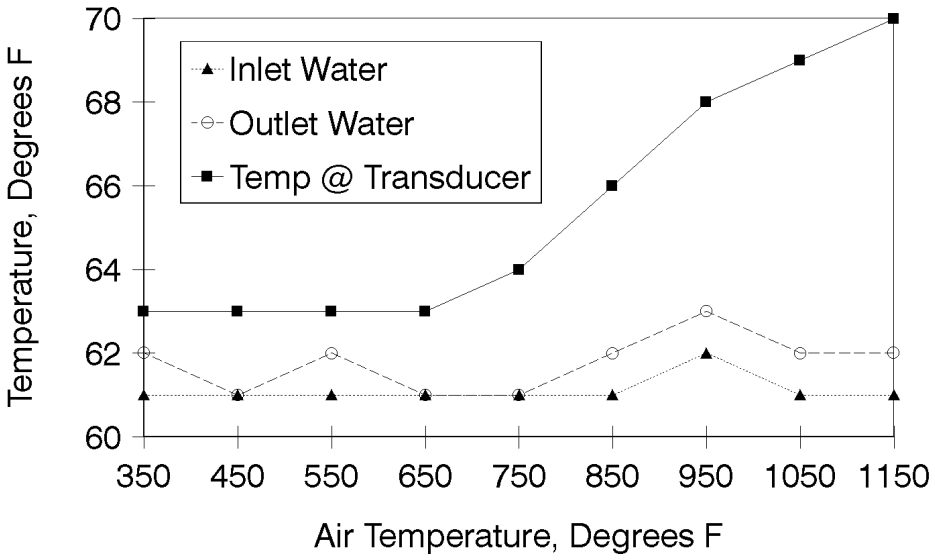

Figure 5-2 Cooling Effectiveness Test for Water-Cooled Fore-Aft Probe

use of a probe containing temperature-sensitive high-response transducers behind a compressor in the high-temperature environment or in an engine environment requires this special care. Figure 5-2 shows the results of a temperature test of the probe in a ceramic oven. Thermocouples specially built into the water passages of a development probe provided the temperature information near the transducer site, the inlet water temperature, and the exit water temperature. The water cooling passages in the probe were designed to pass volumes of water that could be easily obtained at a normal water faucet, eliminating the need for any special equipment.

Careful calibration of the fore-aft probe in a flow facility is required prior to use. While the forward-facing element reads total pressure during normal compressor operation, the aft-facing element reads a pressure value representative of the wake of the probe and is therefore neither total or static pressure, but is thought of as a “wake static.” Using the total pressure, temperature, and the wake static pressure, a “pseudo Mach number” can be calculated. Using

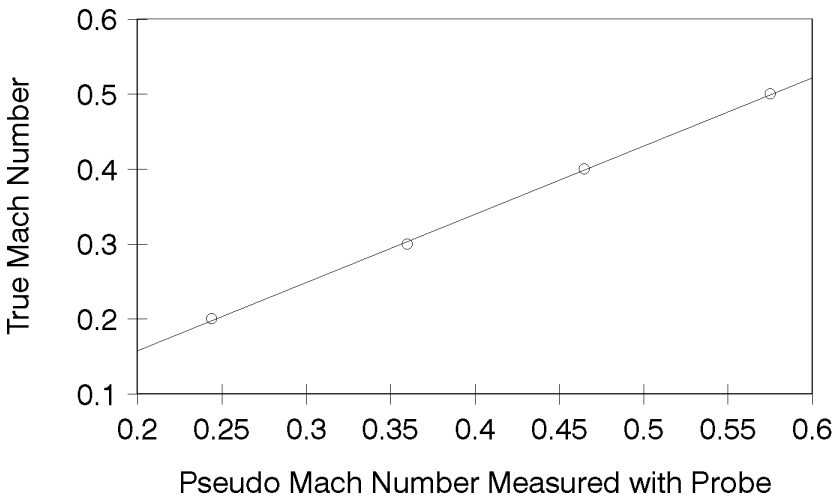

Figure 5-3 Calibration Curve for Fore-Aft Probe in Flow Facility

the true Mach number (calculated from the flow facility instrumentation) and the pseudo Mach number calculated from the probe values, a calibration curve can be drawn for forward flow over the probe. Figure 5-3 shows a typical calibration curve for the fore-aft probe. Also, knowing the flow values from the facility, a curve of Mach number versus flow per unit area can be developed. Once this information is obtained for the forward flow configuration of the probe, the probe must be turned around in the flow facility and the “reverse flow” configuration calibrated, developing the same information. During a compressor surge, the appropriate calibration curve must be applied depending upon the direction of flow at the probe. This is determined by a continuous comparison of the values of the two high-response pressure measurements. The element with the highest value is assumed to be facing into the flow.

For the probe described here, pitch and yaw calibrations were also performed in both the forward and reverse flow directions. It was found that the yaw acceptance of the probe was about 25 degrees for the forward-facing element and about 15 degrees for the aft (wake-static measuring) element. Pitch

angle acceptance of the probe was about 12 degrees, due to the large probe body that was necessary to provide the capability of a water-cooled probe. In many applications, water cooling is not necessary, depending upon the compensated characteristics of the high-response transducers. However, this probe was developed to run in both the engine and the rig during repeated surge tests; therefore, water cooling was desirable.

Obtaining correct data using the fore-aft probe therefore requires proper probe design, calibration, and placement in the flowfield. This must be based upon a thorough understanding of the characteristics of the probe, knowledge of the local flow swirl angle, slope of the compressor flowpath, and an understanding of the environmental conditions under which the probe will operate.

In a compressor where a good inlet flowrate measurement can be obtained by using a bellmouth or similar measuring device, using the probe allows a curve of true Mach number versus actual inlet corrected flow to be developed during steady state measurements. This avoids using the Mach number versus flow per unit area calibration curve, reducing the error that can be developed from not knowing the exact effective area in the flow measurement plane. Of course, the assumption of relatively planar flow is made when using this type of probe, unless one is willing to use several probes around the circumference of the compressor and then average the result. However, surge is a relatively planar event and for the type of time-dependent data being obtained, the increased accuracy achieved through the use of multiple probes often does not justify the extra effort and cost.

Figure 5-4 shows another fore-aft probe designed for use with higher temperature transducers or in inlet flows, where water cooling is not necessary. In addition, this probe does not contain any steady state pressure measurements. These are not absolutely necessary if the probe is calibrated in the compression system itself, by running at a series of steady state operating points and measuring the actual flow into the rig with a bellmouth or venturi.

Even when used in an engine environment, the flow can be diagnosed under steady state conditions through a diagnostic performance model matched to other engine performance measurements.

In addition to the fore-aft probe, high-response static pressure measurements located within the compression system stages are necessary to examine the dynamics of stage rematch and to determine the flow conditions just prior to compressor surge or stall.

One critical factor in the high-response instrumentation setup is the knowledge of the required frequency response for the analysis that will be performed. Since the static pressure measurements are used to examine the flow regime prior to stall, the phase angle and pressure levels measured are both critical. The best method of installing the high-response static pressure trans-

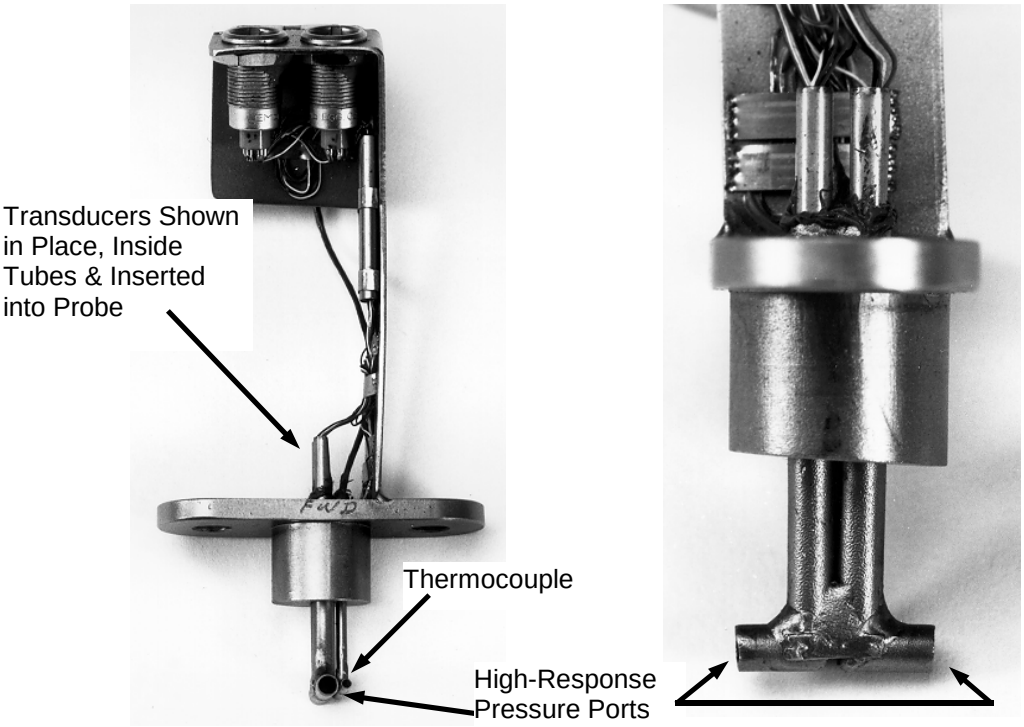

Figure 5-4 Fore-Aft Probe Designed Without Water Cooling

ducers is to flush mount the transducers with the shroud wall in the compression system. Not flush mounting the transducer results in a false pressure magnitude reading due to the acoustic behavior of the cavity between the shroud wall and the transducer face. For example, if a transducer (0.080 dia.) of a standard type is mounted in a shroud wall (under standard day temperature and pressure conditions) the frequency response is influenced if not flush mounted. Figure 5-5 shows the calculated response characteristics as a function of the distance from the shroud wall to the transducer face. In this type of measurement, not only is the offset depth important, but also the hole diameter. Whatever installation configuration is used, it is important to understand its effect on the measurement. High-response pressure transducers (for example, those manufactured by Kulite) typically have a frequency response of up to about 180 kHz. Interestingly enough, this response level is rarely available for the measure-

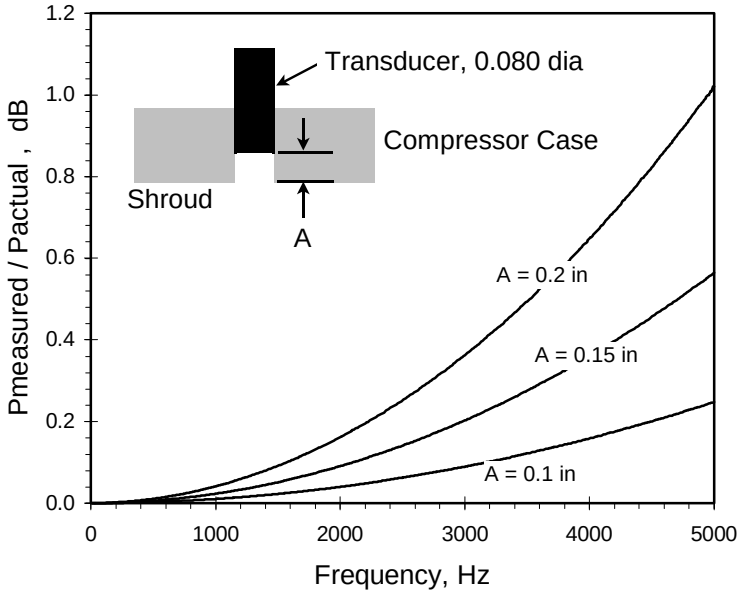

Figure 5-5 Frequency Response Characteristics of a Nonflush Mounted Transducer

ment, due to limitations of other equipment. A high quality bridge amplifier is used in conjunction with the transducer, but the amplifier frequency range may only extend up to 25 kHz. In addition to these limitations, if the data is recorded on FM magnetic tape (for example a Wide Band Group I instrumentation recorder), the tape speed limits the frequency response. A tape speed of 7.5 inches per second provides a frequency response of 5 kHz, 15 inches per second provides a frequency response of 10 kHz, 30 inches per second provides a frequency response of 20 kHz, and so on. Once the data is acquired, the digitizing rate then will also determine the frequency capability of the data. All of these factors must be considered when examining high-response data.

6.0 COMPRESSION SYSTEMS EXAMINED

Investigation into the stall and surge behavior of axial-centrifugal compression systems requires expensive testing in rigs and engines. While models are available, there must first be an understanding of the dynamics to be sure the models are providing the correct results. The measurement methods to examine the details of the dynamics of stage matching under near-instability conditions require great care to perform correctly, as has been discussed previously. The compression systems chosen in this work were chosen largely because other engine development program needs made them available. While the work presented here was important and the data acquisition for dynamic investigation intentional, it did not drive the overall program direction and therefore some decisions on what data to obtain were driven by other program concerns. In spite of this, the data obtained allows a complete and consistent examination of the interstage dynamics in axial-centrifugal compressors. Some of the data was acquired in compressor rigs and some was acquired in full engines. This was intentional and important to the conclusions of this work. There is often a question of whether a rig really represents what occurs in an engine. Some argue it does, some argue it does not. Both may be right. If discussing the dynamic conditions prior to engine instability, then the rig, if properly built, does operate the same as in an engine. However, under post-stall conditions, it is the system configuration that determines how the compression system will behave.

In this section, the compression systems used to capture the different dynamic effects are presented. Throughout the discussion and presentation of the systems examined and the presentation of the test data, reference is made to the parts of the engine systems such as the centrifugal impeller, the centrifugal diffuser, and the deswirl vanes. These parts and others are shown in Figure 6-1 for reference.

6.1 The Research Compressor

The research compressor was developed as a high-technology five-stage machine, with four axial stages and one centrifugal stage, as shown in Figure 6-2. Designed as a minimum-stage-count, maximum-performance machine, it has a design pressure ratio of about 15 at a corrected flow of 22 lbm/sec.

In addition to a full complement of steady-state instrumentation, flush-

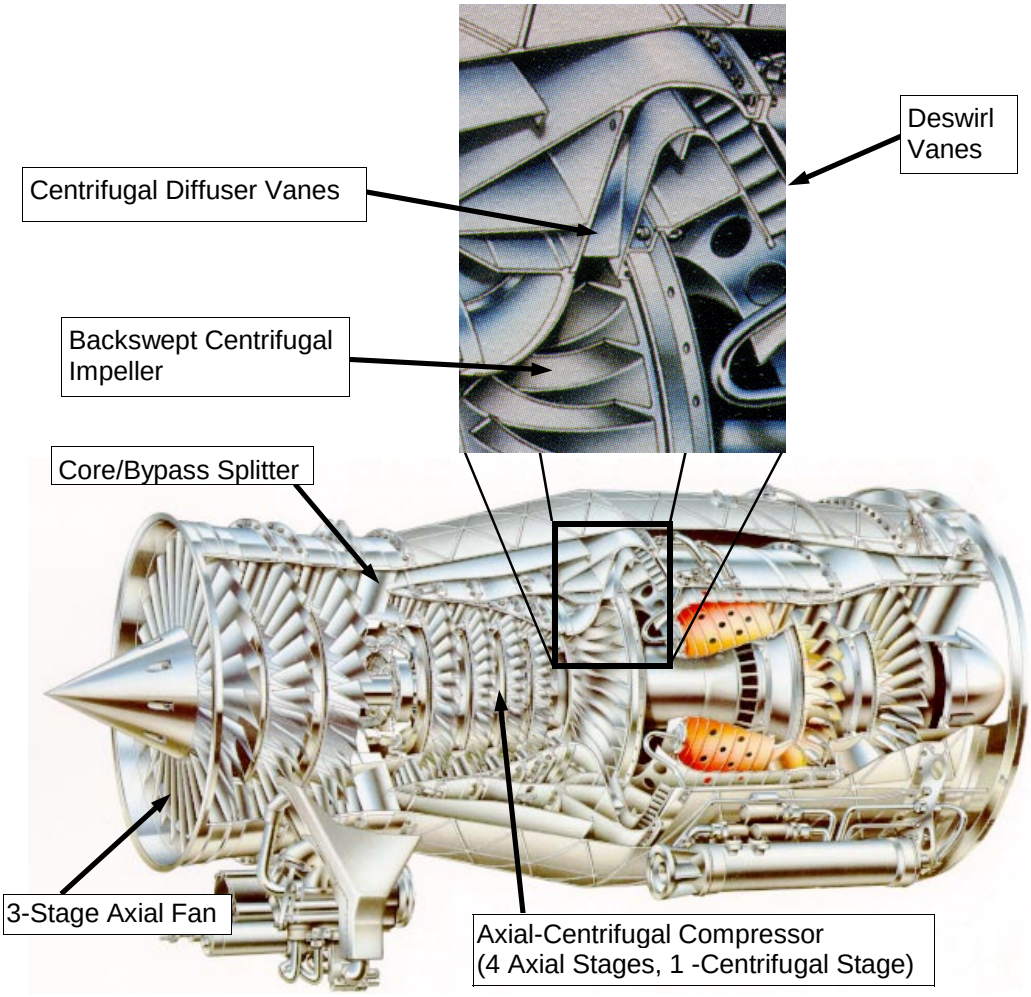

Figure 6-1 Detail Showing Parts of a Typical Axial-Centrifugal Compression System in an Engine, Here the TFE1042 w/o the Afterburner

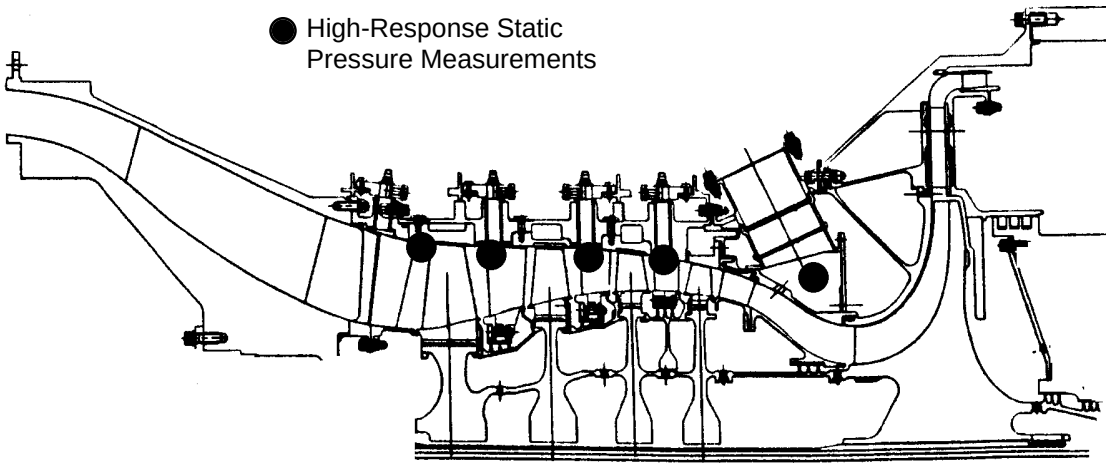

Figure 6-2 Research Compressor Layout Showing High-Response Measurement Locations

mounted high-response pressure transducers were located behind the inlet guide vane (IGV) and behind the first three axial rotors. A fourth transducer was located behind the fourth stator, just inside the bleed plenum. This compressor rig was run both with and without the centrifugal stage, allowing the examination of the effect of the centrifugal stage on the axial compressor.

6.2 The TFE1042 Compressor Rig

The TFE1042 compressor rig also consists of a four-stage axial compressor and a single-stage centrifugal compressor mounted on the same shaft, as shown in Figure 6-3. This particular configuration of the rig has a movable IGV and fixed vanes. This compressor is different from the research compressor in that its design pressure ratio is about 6.5 at a corrected flow of 25 lbm/sec.

In this compressor, in addition to the stage-based high-response static pressure transducers, two high-response fore-aft probes were installed. One was located at the inlet to the IGV at fifty percent span and the second was lo-

cated at the centrifugal compressor deswirl vane exit. Through the use of these two probes, the complete surge cycle was obtained. The configuration of the centrifugal diffuser and deswirl vane system was different in this rig than in the engine which is described in the next section. The difference affects the post-stall behavior of the rig, and this will be shown later in this dissertation.

6.3 The TFE1042 Engine

The TFE1042 is an afterburning turbofan engine in the 10,000 pound thrust class (during afterburner operation) with a bypass ratio of approximately 0.5. Since the overall stall and surge characteristics of an engine are a function of the fan and the core compressor match, some data will be presented to show the characteristics of both fan initiated and core compressor initiated surge behavior. The axial-centrifugal compressor in this engine (Figure 6-4) provides it

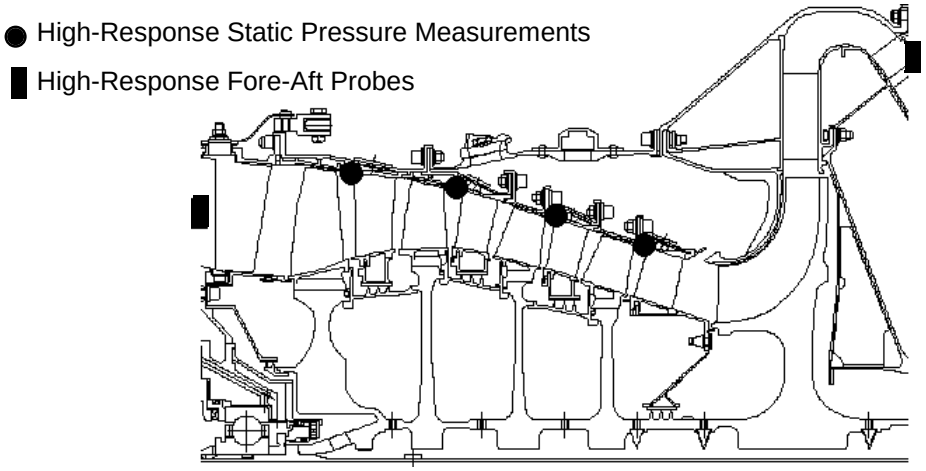

Figure 6-3 TFE1042 Compressor Rig Showing High-Response Instrumentation

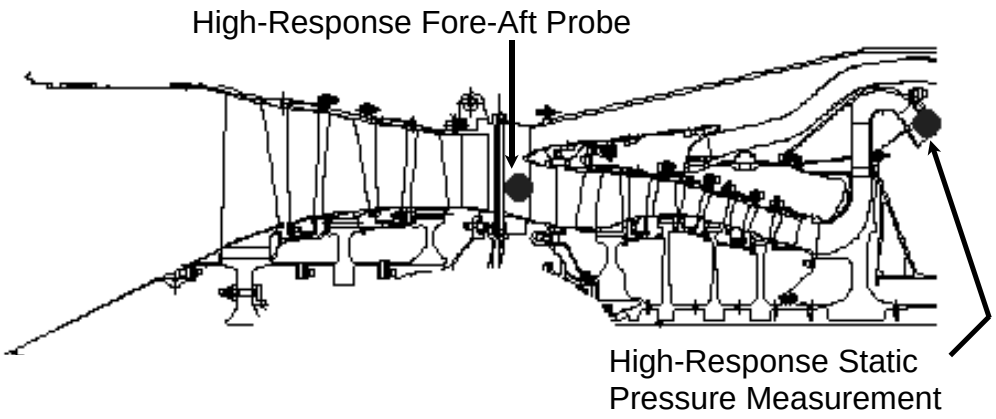

Figure 6-4 TFE1042 Engine Showing Location of High-Response Instrumentation

with a unique stall tolerance and enhanced recovery capabilities.

In the engine, a fore-aft probe was installed at the compressor inlet location just in front of the splitter, as shown in Figure 6-4. At the compressor exit, the expansion differences in the engine internal and external case parts prohibited the use of the second fore-aft probe without some case modification for the instrumentation. Since this was not desirable in this test due to the nature of the case hardware, a high-response static pressure was used at the compressor exit as though it were a total pressure, because the local flow velocity at the measurement station was approximately Mach 0.15 and compressibility effects are minimal. (The static-to-total pressure ratio is about 0.98.)

6.4 The TFE731 Engine

The TFE731 engine has a core compressor design that is slightly different from those already presented. This compressor is a split-core design, with the four-stage axial compressor and the single-stage centrifugal compressor on different spools, as shown in Figure 6-5. The spool shafts are concentric with the axial main shaft housed within the centrifugal spool. This compressor configuration, of which there are several variations, has been proven successful af-

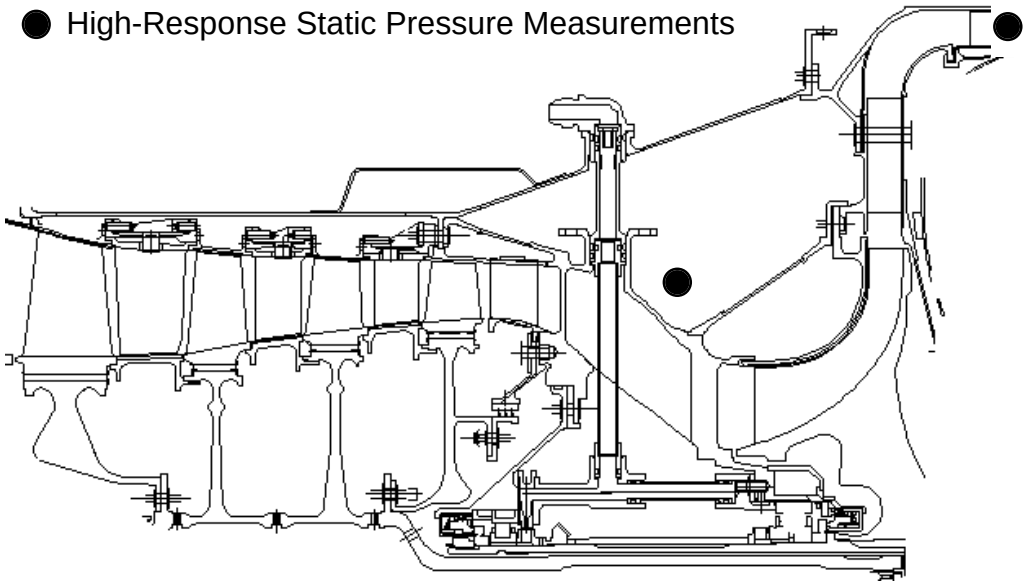

Figure 6-5 TFE731 Flight Test Engine Core Compressor Showing the Location of High-Response Static Pressure Measurements

ter many years of operation in the TFE731 engine line and demonstrates unique enhanced stability characteristics. The engine uses a geared fan that runs off the same shaft as the axial compressor. The centrifugal compressor stage is driven by another turbine. This configuration enhances the starting ability of the engine, allowing the two compression stages to match differently at full power than during starting. As with most axial-centrifugal compression systems, there is a bleed located between the axial and the centrifugal compressors.

Instrumentation was more difficult to locate in this engine, since data was obtained on it during flight testing and special provisions had to be made. Only high-response static pressure instrumentation was used. The transducers were located so examination of the axial and centrifugal compressor match could be obtained under various flight conditions and various bleed settings, with different actions on the engine throttle. The first of the transducers was located just

inside the bleed plenum behind the rear of the axial compressor. The other was located at the exit of the centrifugal compressor deswirl vanes, as shown in Figure 6-5.

7.0 TEST RESULTS AND DYNAMIC MATCHING ANALYSIS

7.1 Stall and Surge Inception in an Early Build of the TFE1042 Compressor Rig

Some of the early examinations of dynamic behavior of axial-centrifugal compressors were performed in the TFE1042 compressor rig. In this test, high-response transducers were located in the front two stages of the axial compressor to help define the characteristics of the stalling behavior at low speed where it was possible to measure a defined transition from a rotating stall to a surge condition. In addition, at high-speed the surge margin was not at the level desirable, so examinations of the dynamics of the front stages of the compressor were performed during various settings of the variable geometry. These early measurements of the interstage dynamics of stall and surge behavior were captured on an oscilloscope, then photographed with a Polaroid camera. The data presented here are the actual oscilloscope photographs. While not of the quality produced with the digital equipment available today, these photographs show the development of rotating stall and surge in this build of the compressor rig. The two transducers used in this test were located behind the first and second rotors. Being displayed on an oscilloscope, the vertical axis is not calibrated in these photographs, since the level changed continuously during the test and the two transducers were not only in different pressure fields, they were of different sensitivities. Figure 7-1 shows a data trace 102 ms long taken at 50% speed (9140 rpm). A rotating stall can clearly be seen in the second rotor. This stall frequency (89 Hz) corresponds to either one stall cell moving at 60% of the rotor speed or two cells moving at 30% of the rotor speed. The effect of the rotating stall in rotor two can be seen on rotor one. Note the static pressure decrease in rotor one where the flow accelerates around the leading edge of the passing stall cell in rotor two. Also note, there is a static pressure increase in the first rotor where the flow is blocked by the stall cell in rotor two.

This observation of the static pressure field is critical to determining the

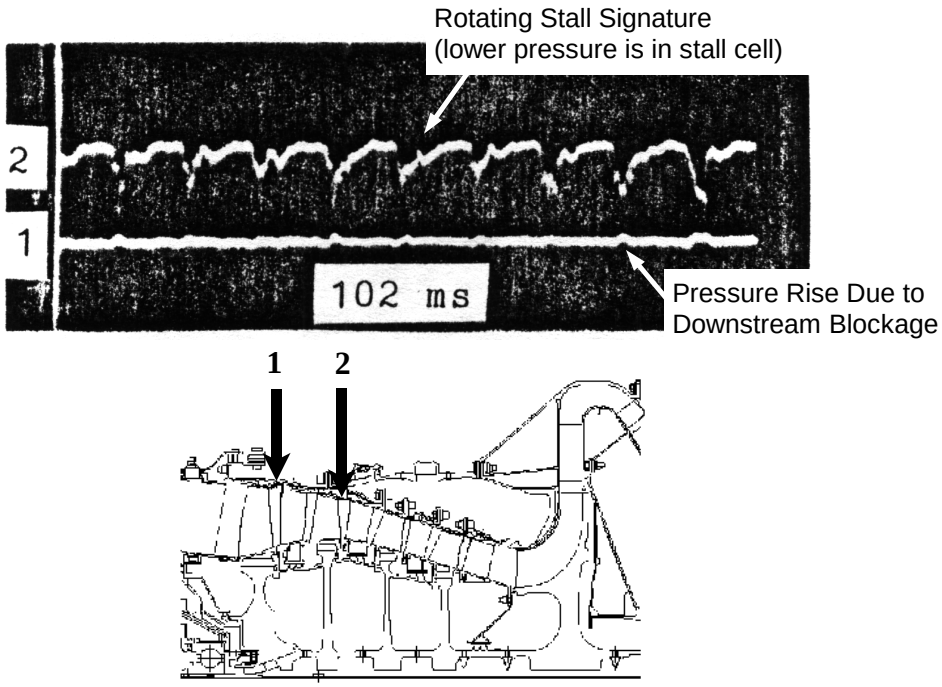

Figure 7-1 Rotating Stall in Rotor 2 of the TFE1042 Compressor Rig at 50% Corrected Speed

interstage stalling dynamics. When observing the pressure field at the exit of a rotor, the flow stability over the rotor blade surface can be examined. As the flow over a rotor blade begins to separate, the local static pressure downstream of the blockage (due to the separation) must drop since the local fluid has lower momentum. Upstream of the separated blade, the local static pressure rises. Using this as a guide, the blade row containing the separation prior to surge (the surge trigger) can be defined for a compressor operating at a particular speed. Figure 7-2 shows a typical surge trace obtained at 70% speed (12,800 rpm). In this particular build of the compressor rig, the boundary between rotating stall and surge was between 50% and 70% speed. The area of interest marked on the photograph is that area that must be examined just prior to the surge pulse to determine exactly what the matching dynamics are in the com-

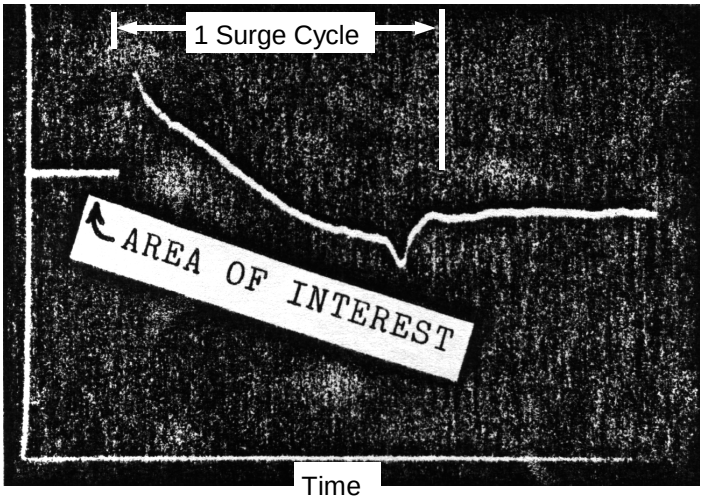

Figure 7-2 Pressure Trace of a Complete Surge Pulse Showing the Area to Examine for Pre-surge Dynamic Information (TFE1042 Compressor Rig, 70% Corrected Speed)

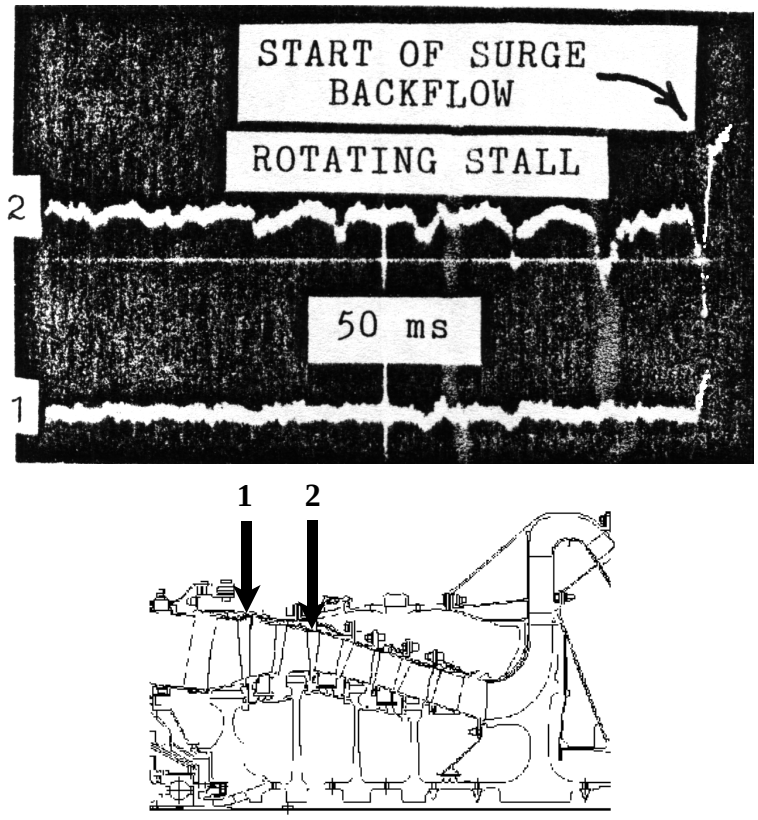

Figure 7-3 Data Trace Showing the Development of Rotating Stall Prior to Surge (TFE1042 Compressor Rig, 70% Corrected Speed)

pressor prior to surge. The dip at the end of the surge pulse is the centrifugal compressor “pulling” on the axial compressor, enhancing the recovery of the machine. This will be examined later in discussions of other data.

Examination of the data in the “area of interest” of Figure 7-2 is shown in Figure 7-3. This data is very significant in understanding the dynamics of the inception of compressor surge. It can clearly be seen that a rotating stall begins developing in the second rotor. At the start of the picture, it is very incipient in its behavior. About one-third of the way into the photograph, the stalled sector stabilizes into a recognizable rotating stall which then continues to grow in magnitude. As it grows in magnitude, it finally inhibits the overall pressure rise of the rotor enough so that the complete system breaks down and a surge results, which is the surge shown previously in Figure 7-2.

Data was taken at 100% speed (18,280 rpm) to investigate a surge line at high speed that was not satisfactory (the compressor did not have enough surge margin). Figure 7-4 shows one of the 100% speed traces. In this case, the first rotor is the stall trigger. This was not the design intent (the rear of the axial compressor should be the stall trigger at high speed) but since the stages were all relatively highly loaded, a slight mismatch in incidence angle was all that was necessary to cause the trigger to be in the wrong stage. The trace from rotor two shows a slight wavering instability. This is most likely due to a downstream stage nearing its stability limit. Just prior to the compressor surge, however, rotor one begins to get unstable and a large portion of the rotor row stalls (as can be seen when compared to the single revolution indicator on the picture). Next, the first stage stator was closed 2 degrees, in an attempt to unload the downstream and load the first stage rotor, to see if there was a difference in the stall trigger. As expected and shown in Figure 7-5, the stall trigger remained in the first stage rotor, although the wavering instability in the second rotor was reduced.

Next, to verify that the first stage rotor was the surge trigger under these

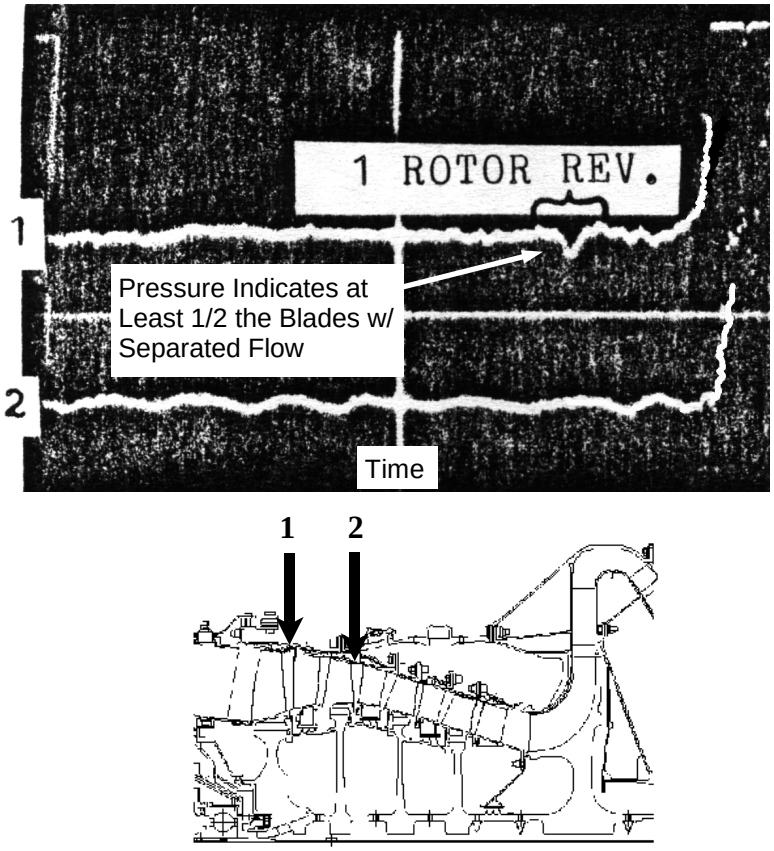

Figure 7-4 Data Trace Showing Improper Stage Dynamics at 100% Corrected Speed with the Surge Trigger in Rotor One in the TFE1042 Compressor Rig (Surge Trigger Should Be Down-stream)

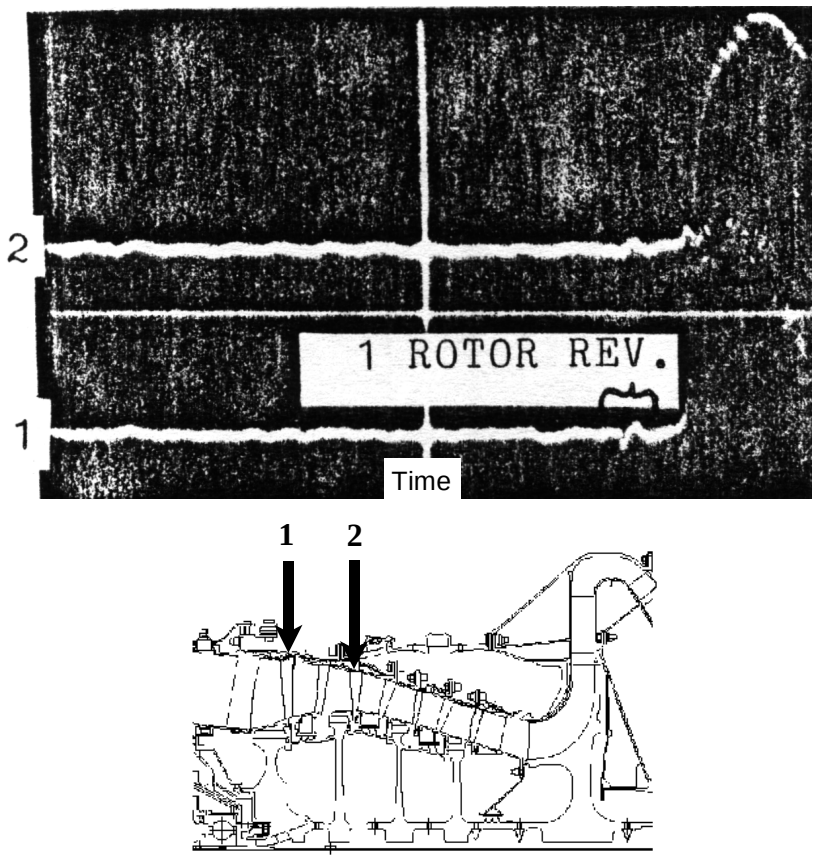

Figure 7-5 Data Showing the Surge Trigger Remaining in the First Rotor After Stator 2 Adjustment (TFE1042 Compressor Rig, 100% Corrected Speed)

conditions, the inlet guide vane was closed a full 10 degrees. This has the effect of unloading the first stage rotor by reducing the incidence angle. Figure 7-6 shows the data obtained under this configuration. As expected, the surge trigger moved out of the first rotor and into the back of the compressor, somewhere behind the second stage. This is shown by several characteristics in this data trace. First, the small pulses that can be seen growing prior to the surge are each representative of one rotor revolution (this can be calculated since the data trace is 102 ms long and the speed is 18,280 rpm). Since there were no high response static pressure measurements in the rear stages in the early days of this compressor rig, whether the surge trigger is the third or the fourth

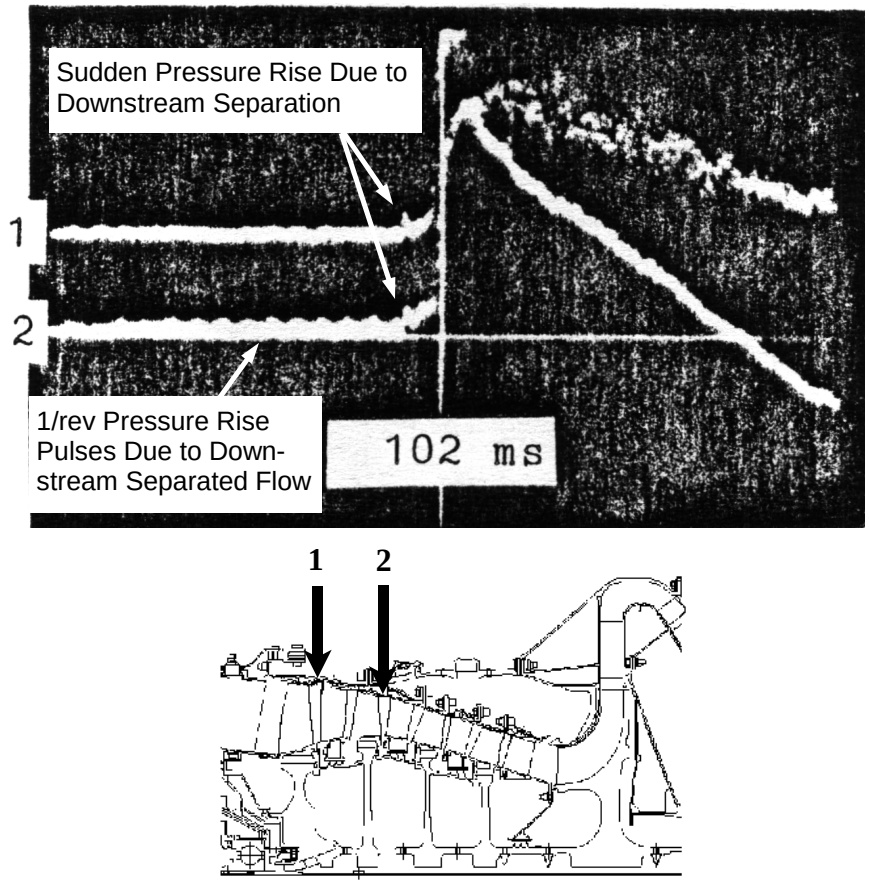

Figure 7-6 Data Trace Showing the First and Second Rotor Exit Static Pressures When the Surge Trigger is Behind the Second Stage (TFE1042 Compressor Rig, 100% Corrected Speed, IGV Closed 10 degrees)

stage cannot be determined from this data. Subsequent to this test, the first stage rotor was redesigned and the dynamic balance between the stages was changed. The other data shown in this document for the TFE1042 compressor rig is with the redesigned rotor and subsequently adjusted inlet guide vane and stator schedules.

Figure 7-7 shows a pressure trace and the start of the blade row blockage (the surge triggering stage) as determined through the use of the high-response transducers on the TFE1042 compressor rig during a portion of a de-

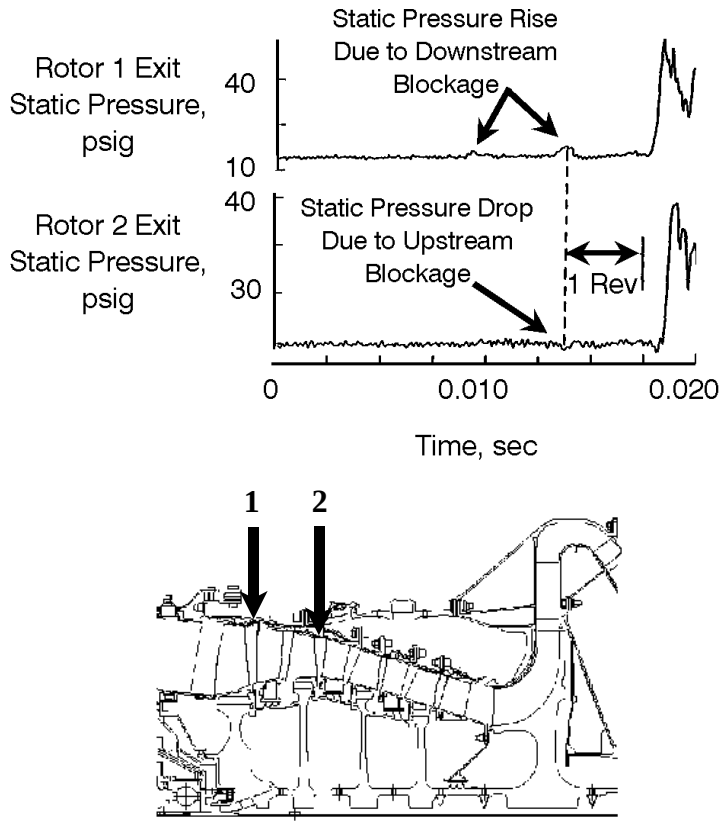

Figure 7-7 Static Pressure Indication of Blockage in the Second Compressor Stage

velopment test several years later. Here the magnitude of the pressure change can be seen, as better equipment was available for use in the analysis. The static pressure rise at the exit of the first stage rotor is about 6 psi. The pressure behind the second stage rotor drops at the same time the static pressure behind the first stage rotor rises. This is due to the blockage (separated rotor) being between the two measurements, in other words, rotor two is the surge trigger. Therefore, if more surge margin were desirable at this speed, the place to work would be rotor two.

With the data reviewed so far, it can be seen that it is important to understand the dynamics of instability prior to full surge or rotating stall before attempting to design any active control system. It is the position of this author

that if an active surge control is ever to be built, it will have to control both the interstage dynamics and the overall system response. In a well-designed axial-centrifugal compressor, the design configuration and the system operation ensure that the surge trigger remains in the axial portion of the compressor. The following results show the characteristics and the stability enhancing properties of a well-matched, well-designed system.

7.2 The Effects of the Centrifugal Impeller on Surge and Stall Dynamics - Research Compressor Results

The research compressor was run with and without the centrifugal compressor to examine the effect on the behavior of the axial portion of the machine. This test series provided a unique opportunity to examine the enhancement to surge recovery that the centrifugal impeller provides.

Figures 7-8 and 7-9 show the differences in the surge characteristic with and without the centrifugal compressor. The points that are labeled on the figure are as follows:

A Surge initiation at the stability limit of the compressor

B Point of maximum surge overpressure due to backflow of the compressor

C Point of minimum flow (seen as the maximum static pressure behind the IGV after the backflow)

D Point of minimum pressure, where the compressor starts to pump again

E Point at which the compressor has reached a steady-state condition again

During this test, the compressor was operating at 97.5 percent corrected speed. In Figure 7-8 at point D, the effect of the centrifugal stage's early pumping capability (due to the radial flow which was previously discussed) can be seen as the pressure throughout the axial stages drops due to the enhanced recovery effects of the centrifugal stage. In Figure 7-9, as the rear stages of the axial begins to pump again, the static pressure upstream drops. Detailed ex-

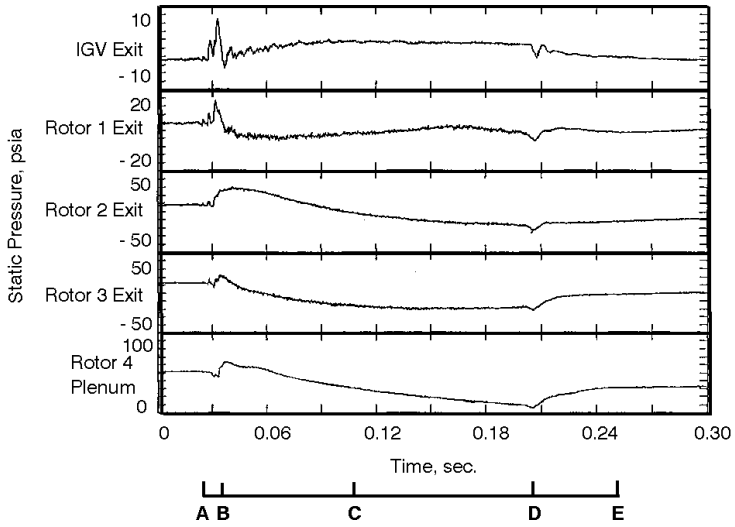

Figure 7-8 Surge in the Research Compressor at 97.5% Corrected Speed with Centrifugal Stage

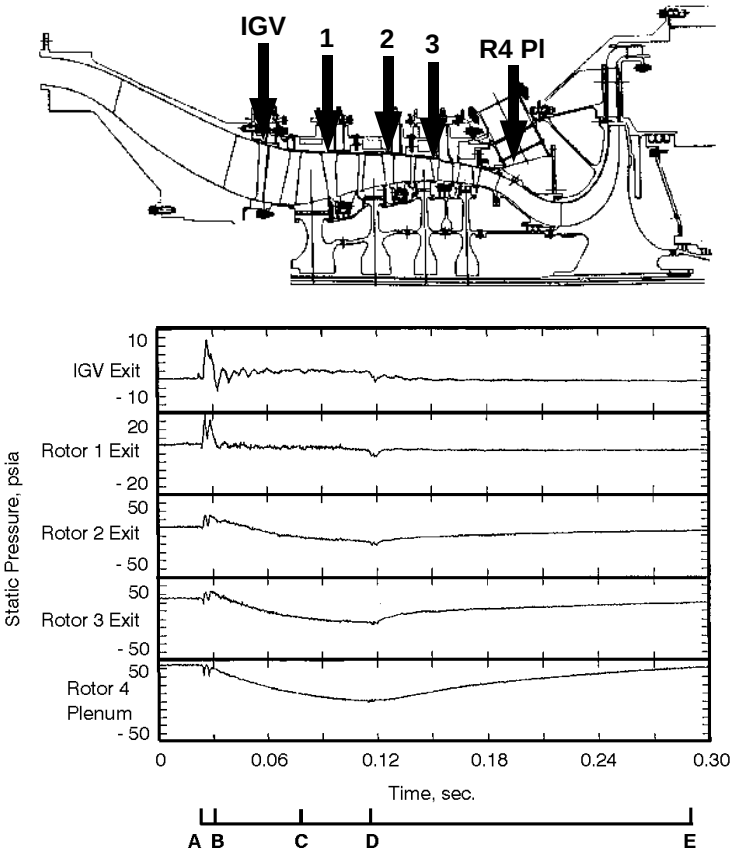

Figure 7-9 Surge in the Research Compressor at 97.5% Corrected Speed without Centrifugal Stage

POINT	TIME WITH CENTRIFUGAL STAGE	TIME WITHOUT CENTRIFUGAL STAGE
A - B	11 ms	5 ms
B - C	70 ms	52 ms
C - D	99 ms	46 ms
D - E	38 ms	175 ms

Table 7-1 Summary of the Effect of the Centrifugal Stage in the Research Compressor on Stalling and Recovery Time

amination of the time required to complete the surge cycle is presented in Table 7-1.

The time required to move from the stability limit of the compressor to the point of maximum backpressure (point A to B) is longer in the axial-centrifugal compressor than in the axial only compressor. This is to be expected because the centrifugal compressor chokes on backflow, limiting how fast the blowdown can occur. The same is true from B to C and from C to D, since this is part of the backflow portion of the surge cycle. However, the recovery portion of the cycle (from point D to E), is almost five times faster with the centrifugal stage in place. The centrifugal compressor stage recovers very quickly from a stalled condition because most of the pressure rise in the centrifugal stage comes from the radial flow. As long as the stage is rotating, it will try to pump. The inception and blowdown portion of the surge cycle (from A to D) takes 180 ms with the centrifugal stage present and 103 ms without the centrifugal stage. One might reason that the axial compressor alone might be better in terms of system stability, because the inception and blowdown portion of the surge cycle is faster and recovery can begin sooner. However, the recovery time is so much longer in the axial compressor by itself that the total surge cycle occurs faster with the centrifugal stage in place (218 ms with the stage and 278 ms without the centrifugal stage).

There is another benefit to the centrifugal stage choking during the surge cycle, and while it cannot be seen in Figures 7-8 and 7-9 it is important to mention here. When the centrifugal compressor chokes on backflow and the compressor is designed such that the surge trigger is in the axial portion of the machine, the surge overpressure in front of the compressor is significantly reduced. This cannot be seen in the research rig results since the two sets of data are at a different pressure ratio. This does not affect the time data already presented, but it does affect the surge overpressure level. This overpressure level dependence on the surge trigger will be shown later in the TFE731 results, where the surge trigger is intentionally changed from the axial to the centrifugal stage in the same compressor configuration.

7.3 Measurement of the Dynamics of a Complete Surge Cycle - TFE1042 Rig Results

Data obtained in the TFE1042 compressor rig using the fore-aft probes previously discussed, allowed examination of the detailed surge behavior of the compressor rig through the complete surge cycle. Figures 7-10 through 7-13 show the individual data signatures from the inlet and exit high-response fore-aft probes, as the compressor goes through three surge cycles at 80 percent corrected speed. Figures 7-14 and 7-15 are calculated traces obtained by using the traces in Figures 7-10 through 7-13. The traces in Figures 7-10 through 7-13 are actually a display of the analog data traces that have been digitized at a rate of 5000 Hz. During the pressure ratio calculation (shown in Figure 7-14), the pressure difference across the individual probes is monitored to ensure that the elements that are measuring total pressure (rather than wake static pressure) are being used. Of course, this is critical to the calculation as the compressor goes into full reverse flow during the surge cycle. Figure 7-15 shows the compressor inlet corrected flow during the same three surge cycles. To obtain this trace, the calibration curve of pseudo-Mach number versus inlet cor-

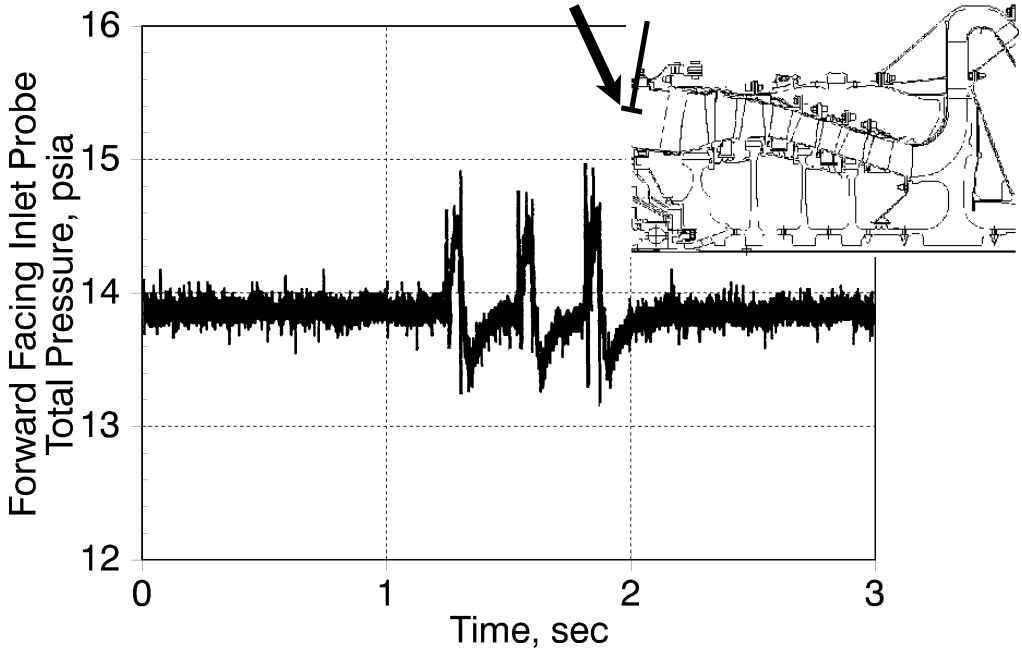

Figure 7-10 Inlet Fore-Aft Probe Total Pressure During 3 Surge Cycles on the TFE1042 Compressor Rig, 80% Corrected Speed

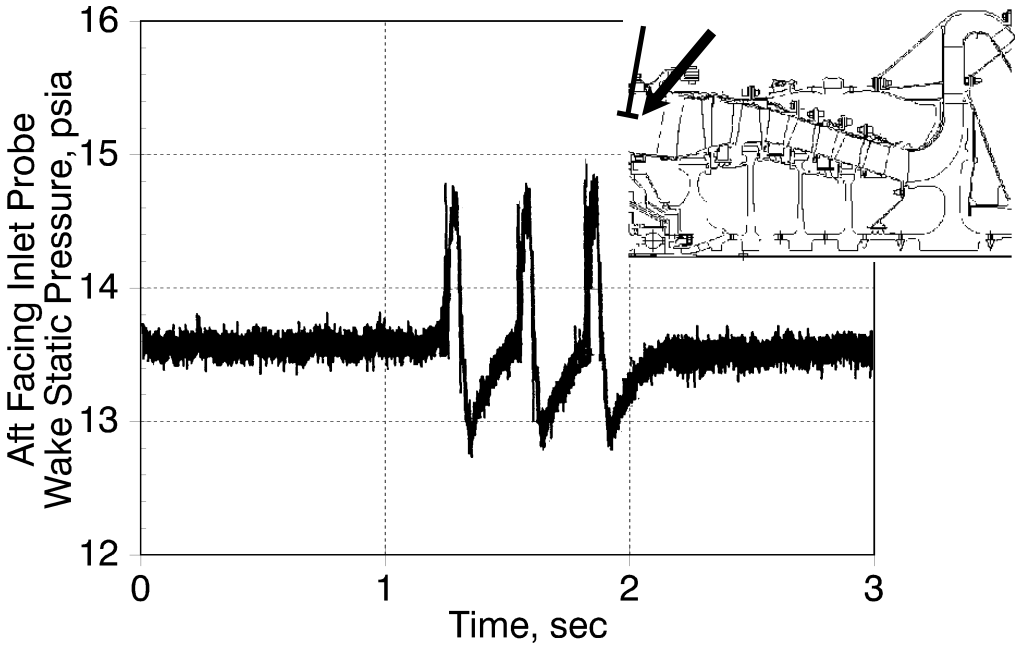

Figure 7-11 Inlet Fore-Aft Probe Wake Static Pressure During 3 Surge Cycles on the TFE1042 Compressor Rig, 80% Corrected Speed

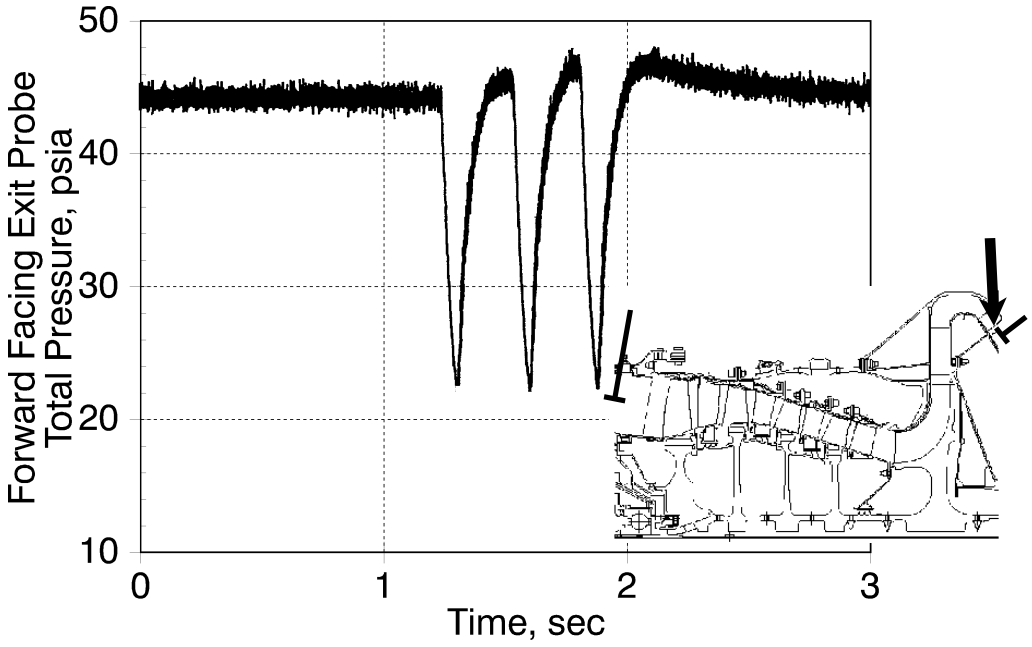

Figure 7-12 Exit Fore-Aft Probe Total Pressure During 3 Surge Cycles on the TFE1042 Compressor Rig, 80% Corrected Speed

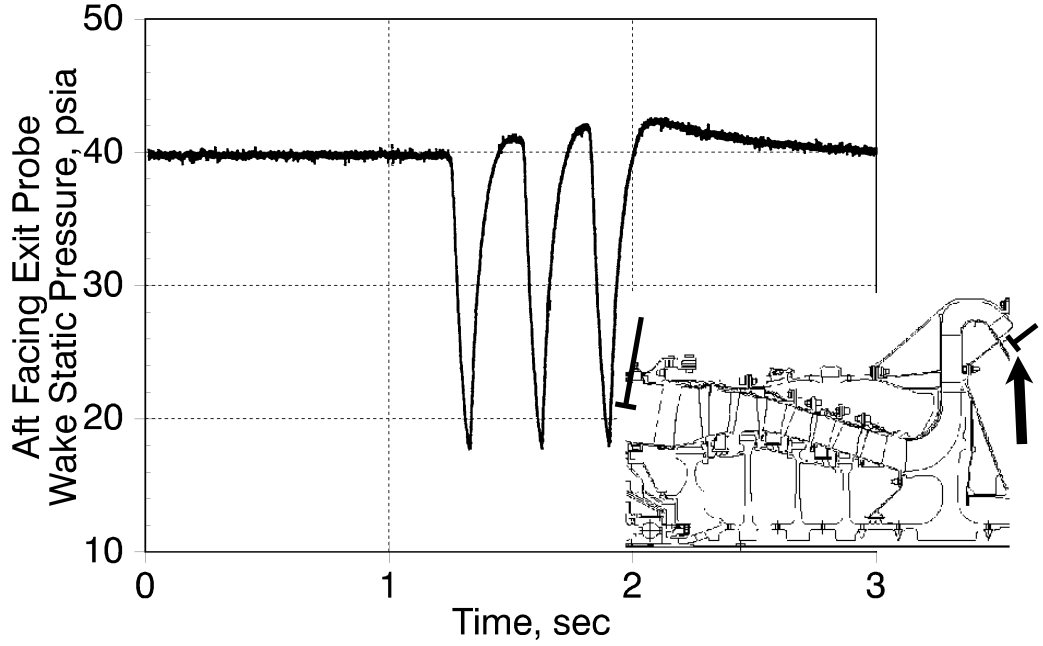

Figure 7-13 Exit Fore-Aft Probe Wake Static Pressure During 3 Surge Cycles on the TFE1042 Compressor Rig, 80% Corrected Speed

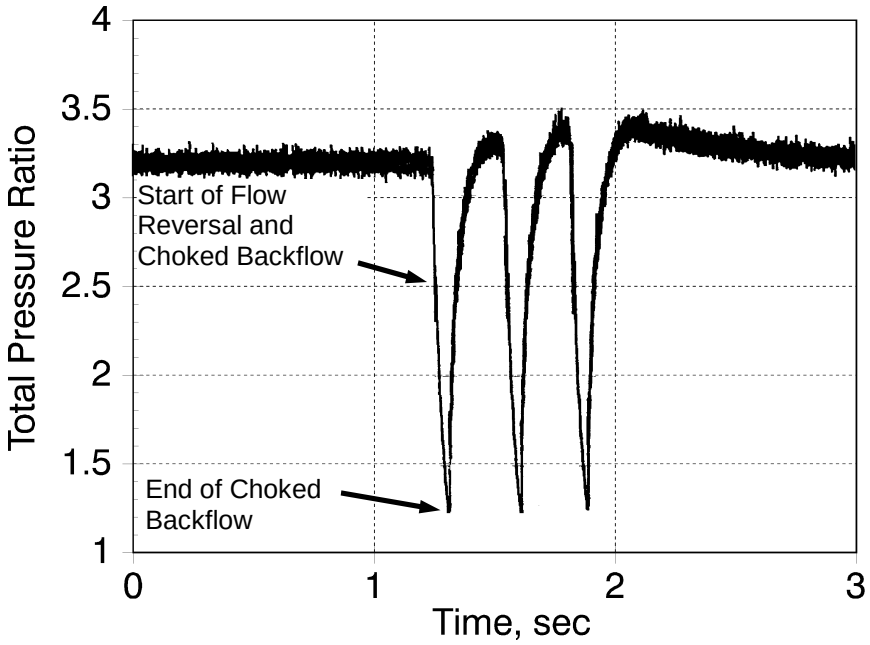

Figure 7-14 Total Pressure Ratio Measured with Fore-Aft Probes During 3 Surge Cycles on the TFE1042 Compressor Rig, 80% Corrected Speed

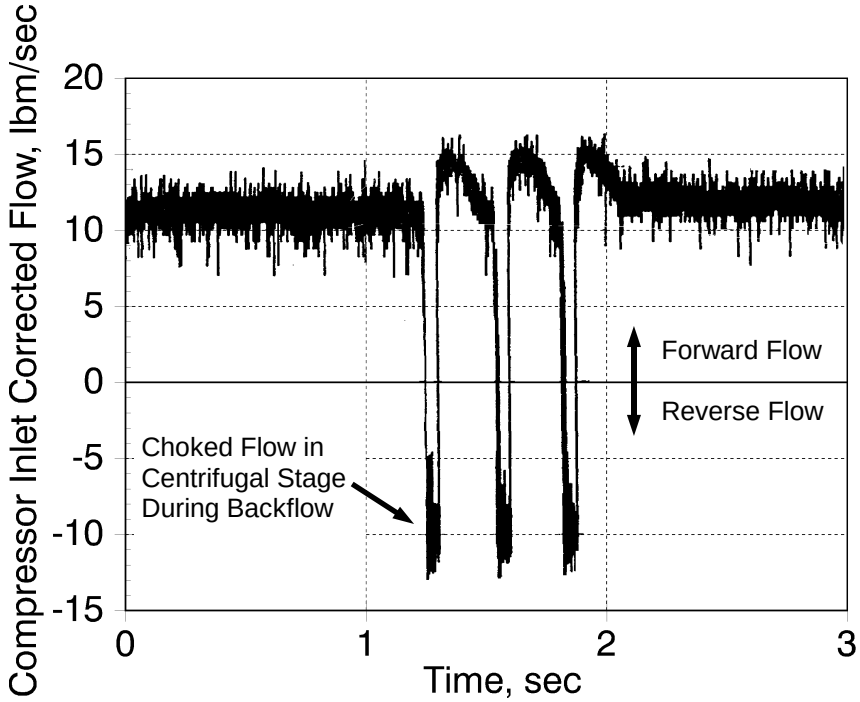

Figure 7-15 Compressor Inlet Corrected Flow Measured with the Inlet Fore-Aft Probe During 3 Surge Cycles on the TFE1042 Compressor Rig, 80% Corrected Speed

rected flow was used. As with the total pressure ratio, the Mach number calculation must be performed while monitoring which of the elements of the inlet probe is measuring total pressure (and therefore proper flow direction).

Examining only the first surge cycle and plotting the total pressure ratio and the compressor inlet corrected flow gives the surge cycle on a compressor map, as shown in Figure 7-16.

There are several observations about this surge cycle that need to be pointed out. First, the compressor pressure ratio is close to a value of 1.2, that is, the exit pressure gets very close to the inlet pressure at the end of the blowdown cycle. Second, the actual flow reversal (going through zero flow) happens between the top of the total pressure trace (Figure 7-14) and the minimum on the total pressure trace. This is observed because whenever the aft element pressure is higher than the forward element pressure, the flow is reversed.

The time required to move through the surge cycle can also be observed. Since the digitizing rate of this data was 5000 Hz, the time between data points is 0.2 milliseconds. The points that correspond to the points in the research compressor discussion have been placed on Figure 7-16. The time required to move from the stability limit to the start of the choked portion of the blowdown cycle is 1.6 milliseconds. The time required to move from the bottom of the choked portion of the blowdown cycle across the bottom of the surge cycle to the start of the pressure recovery is 0.8 milliseconds. As was the case in the research compressor, the recovery occurs quite quickly, due to the centrifugal compressor enhancing the recovery characteristics. These times cannot be directly compared to the research compressor times because the research compressor times include some of the unsteady inception time seen in Figure 7-16 at the stability limit where the surge starts. Also included is some of the repressurization time seen on the right side of the surge cycle. Exact comparison of the surge cycles of the two compression systems could only be performed if there was a fore-aft probe in the research compressor, but the probe was devel-

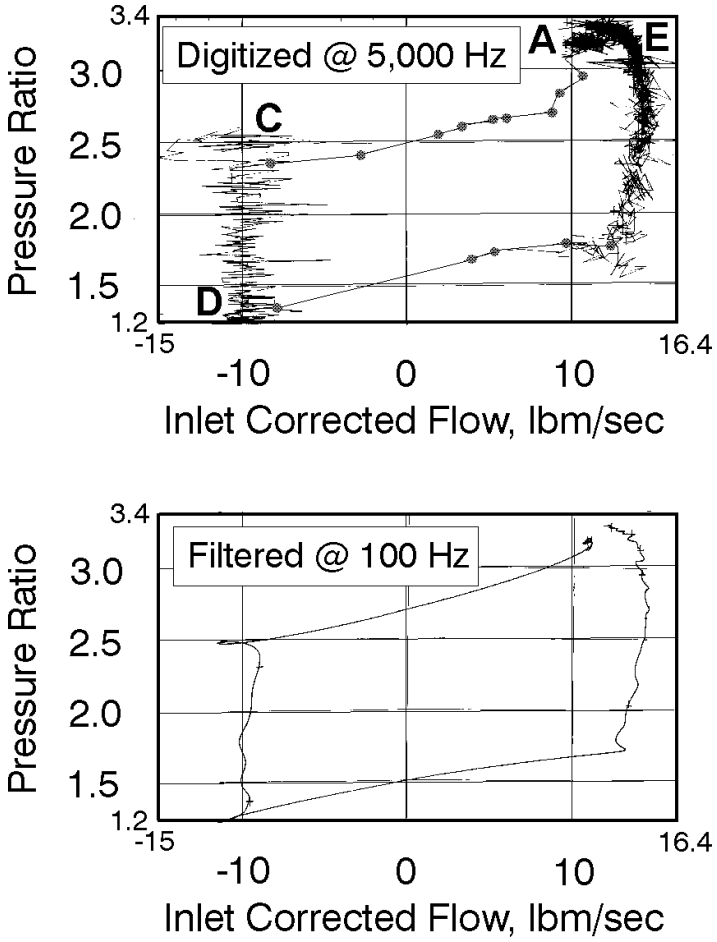

A: Inception Point
C: Start of Choked Blowdown
D: End of Blowdown, Start of Recovery
E: End of Surge Cycle

Note: These points correspond with those on the research compressor traces shown in Figures 7-8 and 7-9.

Figure 7-16 Full Surge Cycle Measured on the TFE1042 Compressor Rig at 80% Corrected Speed

oped only after the research compressor data was obtained.

The last item of importance to note in the rig high-response surge cycle measurement is that the high-response data falls exactly on the steady-state measured stability limit. This was the case even if the downstream discharge valve on the compressor rig was closed as rapidly as possible. Although not as fast as the effect of a fuel pulse in the engine, this test did provide some assurance that the core compressor on the engine (on which data was to be obtained after this rig test) could be mapped using high-response measurements in the core compressor.

7.4 Fan and Compressor Interactions - TFE1042 Engine Results

This turbofan engine, as with any turbofan, can have an engine surge initiated in the core compressor or in the fan. It is really quite easy to determine if an engine surge is triggered by either the fan or the core compressor, through the use of a high-response transducer behind the fan. Figure 7-17 shows an engine surge initiated by a stall in the fan section of the engine. The static pressure behind the fan falls off rapidly as the fan stalls. Once that happens, the core compressor experiences a drop in inlet pressure, and therefore suddenly sees a higher pressure ratio than it can sustain. The operating point on the core compressor is forced up the compressor characteristic to the stability limit of the compressor and a compressor surge occurs, driving the peak static pres-

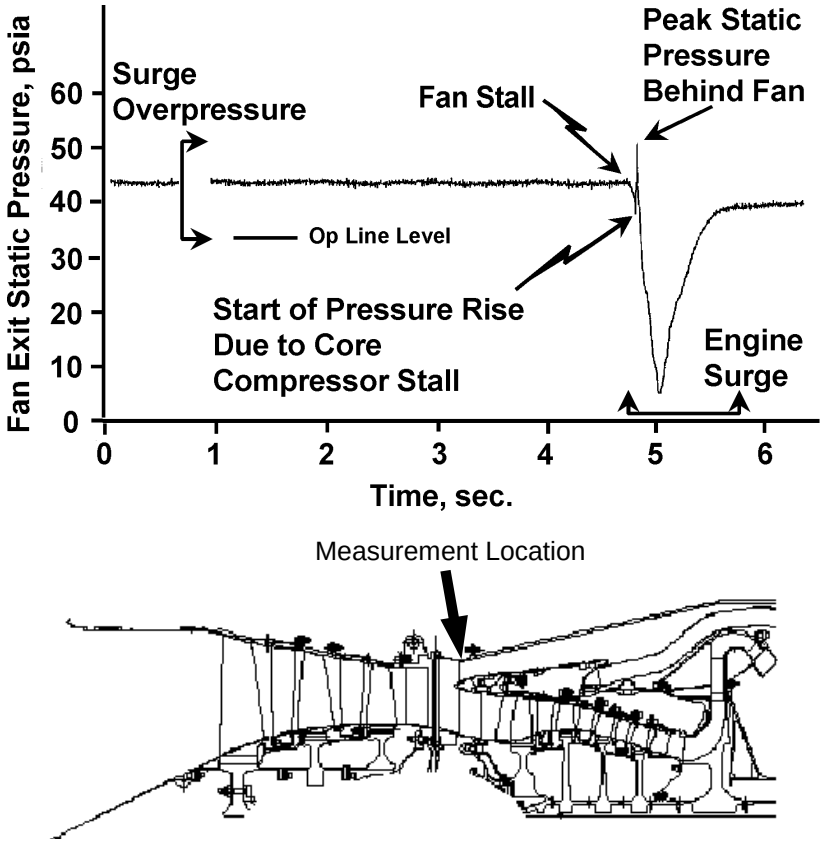

Figure 7-17 Pressure Trace from TFE1042 Engine when Engine Surge is Initiated by a Fan Stall

sure behind the fan up to a level higher than it was at the fan stall point. The backflow continues in both components as the engine surge progresses. On high bypass engines, it is possible to see the fan stall and undergo a backflow from the bypass only, while the core compressor keeps pumping. In this case, the spike seen in Figure 7-17 that is caused by the core compressor does not exist. If the core compressor initiates the engine surge, the fan stall indicated in Figure 7-17 does not occur. Instead, the compressor overpressure spike occurs as the first disturbance in time. This same behavior and general trace interpretation can be used in an axial-centrifugal compressor to identify a surge trigger as existing in the axial or in the centrifugal stage. This will be discussed to a greater extent in the next section.

Figures 7-18, 7-19, and 7-20 show a series of three surge cycles measured on the TFE1042 engine. These surge cycles were initiated by a fuel pulse at 80 percent compressor inlet corrected speed so they could be compared to those measured in the compressor rig. Many surges (over 80, with distorted and undistorted inlet conditions) were obtained and the data used to verify that the compressor rig was providing the same stability characteristics as the compressor in the engine. This was accomplished and the core compressor was “mapped” in the engine, proving that the compressor in the engine was responding in the same manner as the compressor rig. This technique was used to validate that the rig-generated compressor maps that were being used in the performance computer model for the engine were in fact correct. The rig and the engine had the same stability limit (since that is governed by the blade row loading and the compressor match), while the post-stall behavior is slightly different. Examination of the post-stall behavior shows that the engine surge cycle has a “flatter” appearance and does not drop off in pressure as much as the rig (Figure 7-16). This could be caused by the change in the upstream and downstream effective volume between the rig and the engine and the effect of the fan and the bypass on the compressor inlet. Also of note is the difference in

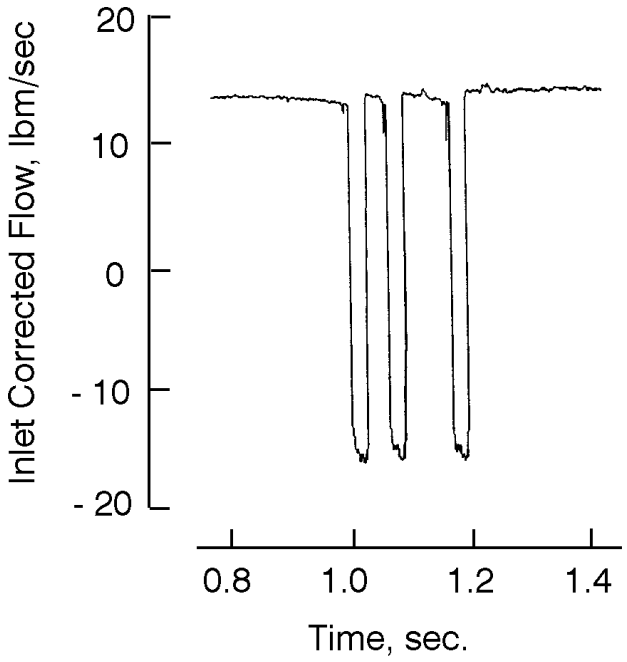

Figure 7-18 Fluctuation in Flowrate for Three Surge Cycles on the TFE1042 Engine

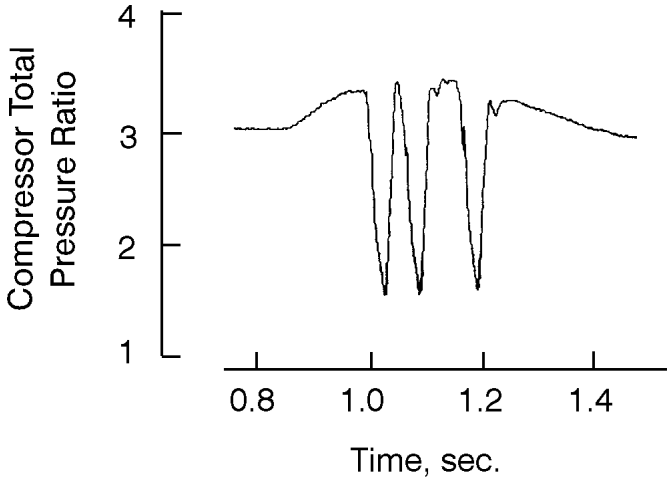

Figure 7-19 Fluctuation in Pressure Ratio for Three Surge Cycles on the TFE1042 Engine

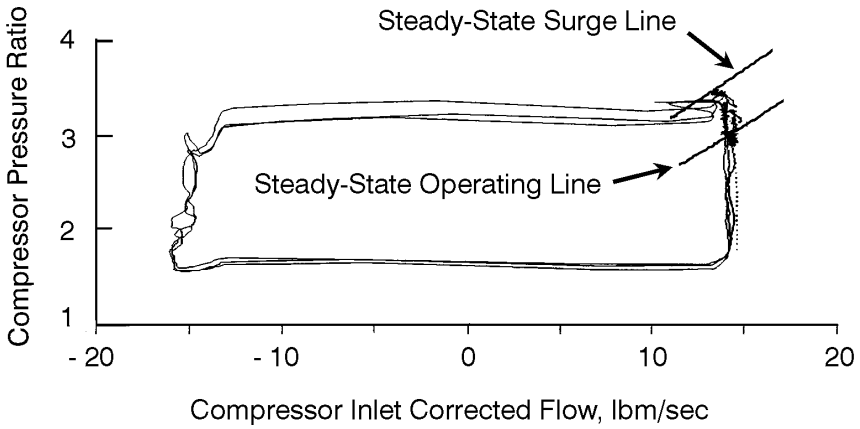

Figure 7-20 Three Full Surge Cycles Measured on the TFE1042 Engine at 80% Corrected Speed (Filtered @ 100 Hz)

the post-stall choked blowdown portion of the cycle. The engine shows a choked blowdown at a larger reverse flowrate than the rig (Figure 7-20 vs. Figure 7-16). This is due to the difference in the centrifugal stage diffusion system in the two machines. Figure 7-20 also shows the steady-state surge line measured in the rig. The high-response pressure and flow measurements in the engine reflect the same compressor surge line as in the rig.

7.5 Interactions Within a Split Spool Compression System - TFE731 Engine Results

The TFE731 engine was tested in the base level test cell and at altitude on the AlliedSignal Boeing 720 test aircraft. As mentioned previously, the design of this engine compressor is unique in that it is a split spool machine, with the axial compressor on one spool and the centrifugal compressor on another. Several different tests were performed to determine the characteristics of the split spool configuration. These tests involved moving the surge trigger into the centrifugal stage using bleed, turbine temperature change, or speed mismatch. Many base-level tests were performed with different fuel and turbine temperature schedules, while performing snap accelerations. Figures 7-21 and 7-22

show two different surge triggers. Figure 7-21 shows the pressure trace when the surge trigger is in the centrifugal stage. The first indication that the surge trigger is in the centrifugal stage is the rapid rise in pressure between the axial and the centrifugal stages. Figure 7-22 shows an engine surge that is initiated in the axial compressor, the preferred location for axial-centrifugal compressors because of the inherent recoverability. The beginning of the centrifugal stage backflow can be seen in the trace. It is important to note that the surge over-pressure (at the rear of the axial compressor) is higher when the centrifugal compressor is the surge trigger. When the axial compressor is the surge trigger, the local axial discharge pressure is reduced before the centrifugal compressor backflows, providing a buffer for the backflow of the high-pressure downstream air.

During the flight test, surge behavior in the engine was initiated by fuel pulsing. The fuel pulse was performed during two different types of transients, as shown in Figures 7-23 and 7-24. The first technique was to heat soak the engine at 31,000 RPM on the centrifugal compressor (the speed consistent with the maximum climb power), and perform a snap deceleration, executing the fuel pulse when the engine speed reached the desired value. (The speeds of the centrifugal compressor are corrected to the engine inlet.) The second technique was to again heat soak the engine at 31,000 RPM on the centrifugal compressor and perform a snap deceleration. This time, the engine was allowed to decelerate to a speed point lower than the intended fuel pulse point. The engine was then accelerated and the fuel pulse executed when the desired speed was reached. This forced a speed mismatch between the axial and the centrifugal compressors.

Figure 7-25 shows the results of performing a rapid deceleration and fuel pulsing to cause a surge, with and without bleed. This test was performed at 20,000 ft. altitude with the fuel pulse executed at 26,000 RPM on the centrifugal compressor. Without bleed between the axial and the centrifugal compressors,

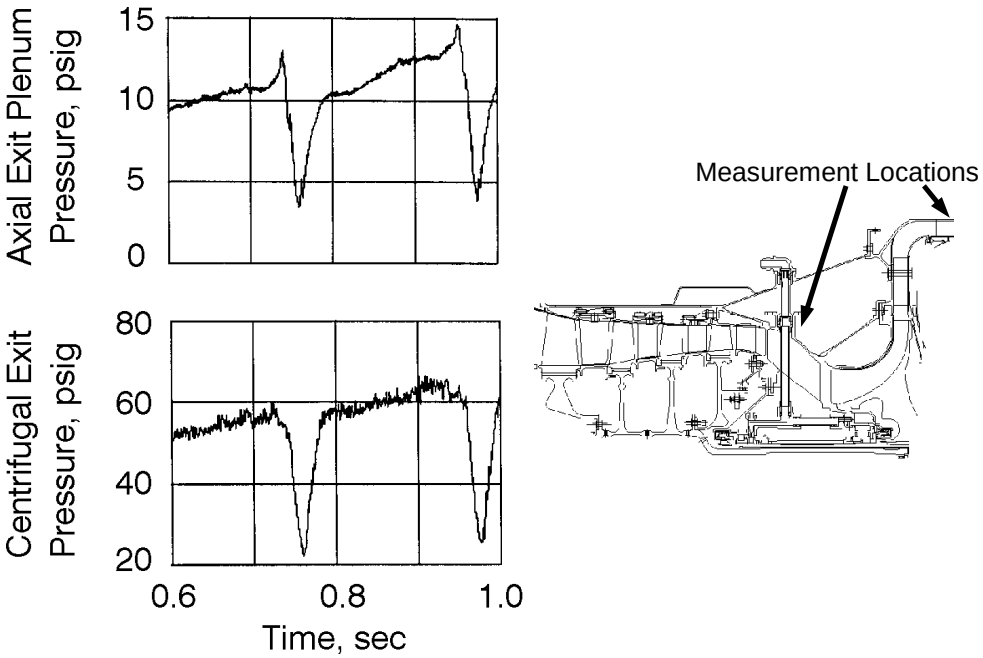

Figure 7-21 Surge Pulse from the TFE731 at Sea Level with Centrifugal Compressor as the Surge Trigger

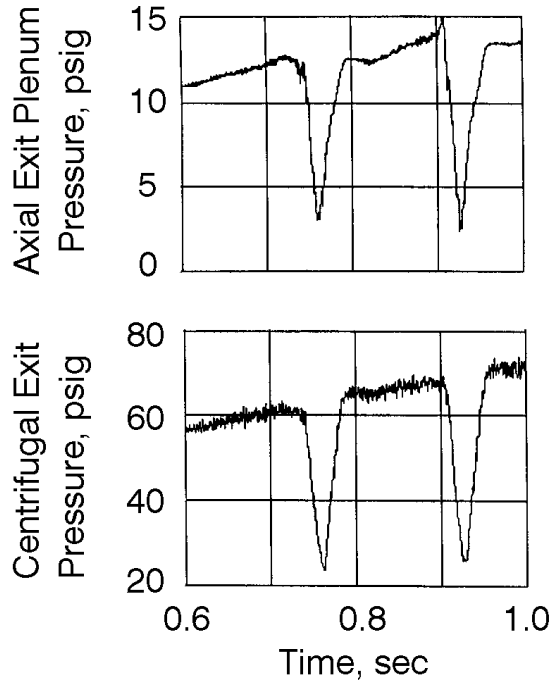

Figure 7-22 Surge Pulse from the TFE731 at Sea Level with Axial Compressor as the Surge Trigger

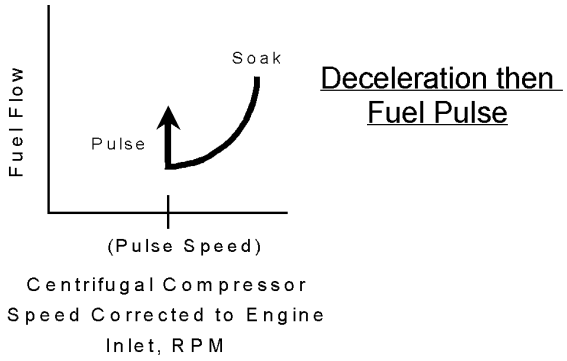

Figure 7-23 First Method of Surging the TFE731 Engine During Testing - Deceleration then Fuel Pulse

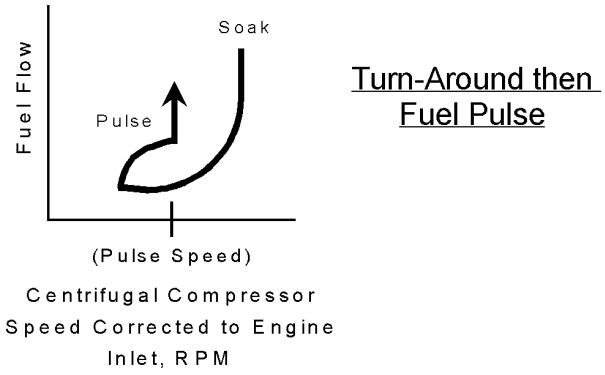

Figure 7-24 Second Method of Surging the TFE731 Engine During Testing - Decel / Accel then Fuel Pulse

the axial compressor stalls, dropping the inlet pressure to the centrifugal compressor stage, forcing it to reach the stability limit and then stall. The pressure trace is similar to that shown in Figure 7-17 for the core compressor and the fan, since the flowfield responds in the same manner. Opening the bleed causes the operating line on the axial compressor to drop so low that the surge trigger moves to the centrifugal stage. As the centrifugal stage begins to stall, it does not initiate surge right away, but as the stalling behavior of the centrifugal impeller gets more severe, the engine surges. The disturbances in the centrifugal impeller are picked up by the probe in the bleed plenum between the axial and the centrifugal compressors.

Figure 7-26 shows the effect of the speed mismatch on the surge trigger of the engine. This test was performed at 20,000 ft. altitude with the fuel pulse executed at a speed of 28,000 RPM on the centrifugal compressor. In the deceleration/fuel pulse test, the surge trigger is in the axial compressor. For this case, the axial speed is 16,681 RPM and the centrifugal speed is 28,160 RPM at surge. When performing a hot turn-around pulse (decelerate to below fuel pulse speed, then accelerate and fuel pulse), the centrifugal compressor stalls first (is the surge trigger). This time, the surge trigger moved into the centrifugal stage because the axial compressor, having more inertia, accelerated slower from the minimum speed point, and the centrifugal compressor picked up the load faster by accelerating faster. The axial compressor speed was 14,358 RPM and the centrifugal compressor speed was 28,848 RPM at surge. Therefore, when the centrifugal compressor was forced to become the stability limiting component of the compression system, the axial compressor was running 2,323 RPM slower and the centrifugal compressor was running 688 RPM faster than in the previous case, where the hot turn-around was not performed and the axial compressor was the surge trigger.

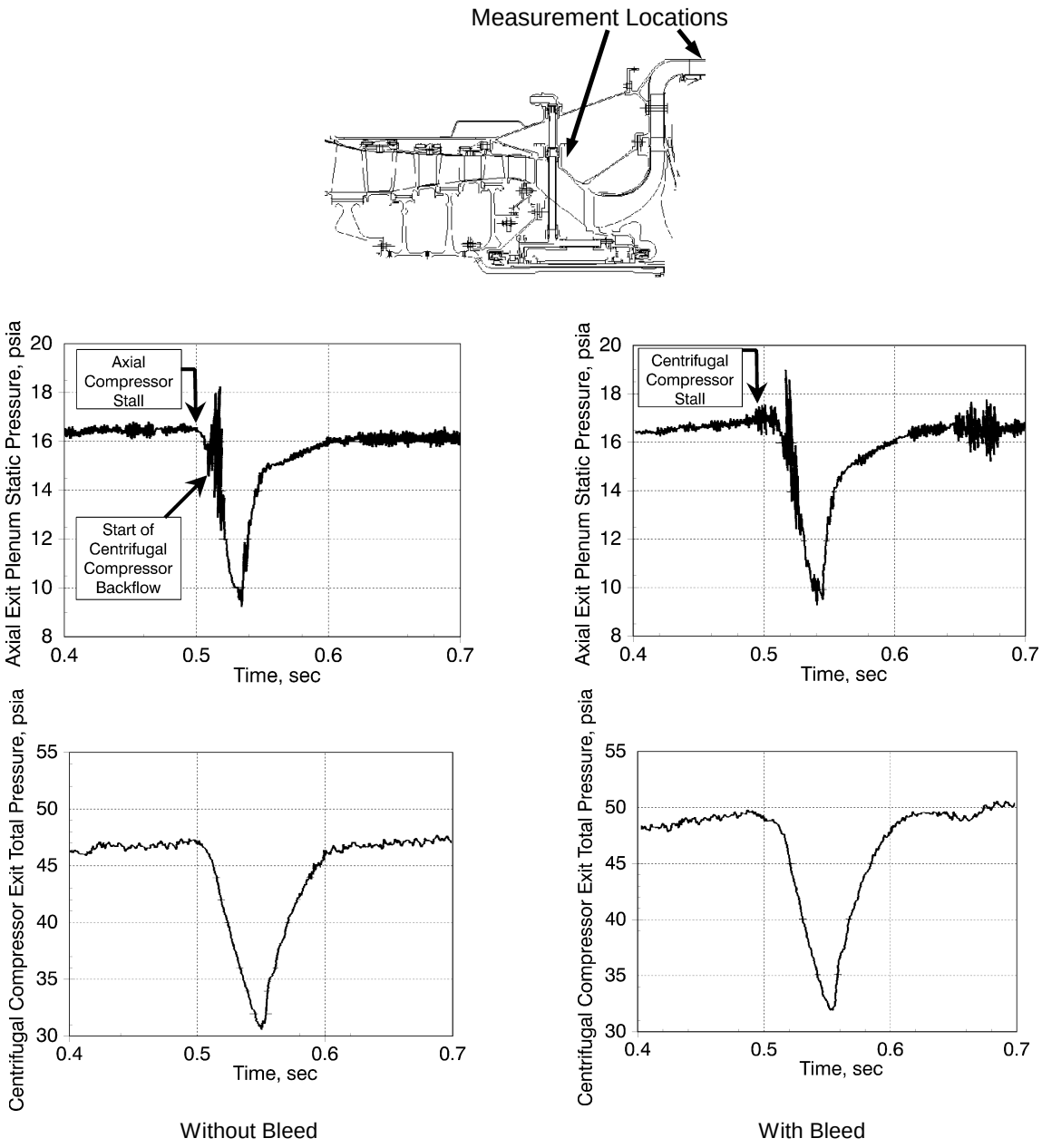

Figure 7-25 Effect of Bleed on Surge Trigger After Deceleration

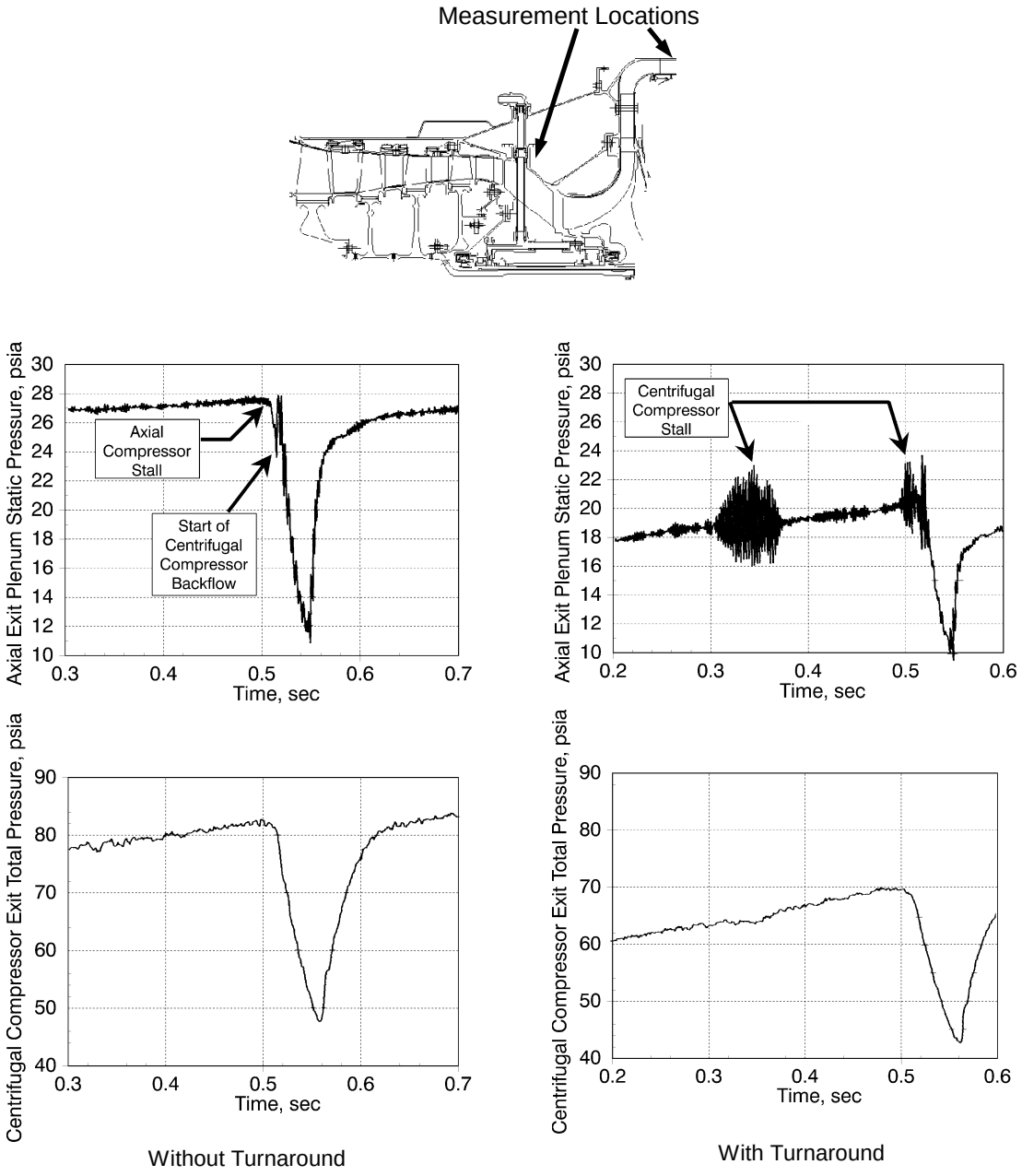

Figure 7-26 Effect of Speed Mismatch on Surge Trigger Caused by Rapid Compressor Speed Turnaround

7.6 Measurement and Test Data Accuracy

Detailed analytical evaluation of the measurements in this work is not documented here due to the complexity of the measurement systems. Rather, the individual components of the measurement systems were verified in calibration and in proper working order through the Metrology Department at AlliedSignal Engines.

All of the high-response pressure measurements were obtained using "Kulite" brand transducers. These transducers were all verified by calibration to be within the manufacturers specifications. Temperature compensation was used in all measurements, as specified by the transducer manufacturer. Bridge amplifiers manufactured by Vishay Corporation and good up to 25 kHz were used with the transducers. With these amplifiers, bridge balance and system validation was obtained prior to every test run. Data was recorded on 28-channel instrumentation recorders at tape speeds of 15 inches per second or higher, resulting in a minimum acquisition frequency of 10 kHz. Experience with these systems has shown the data to be accurate to approximately +/- 0.1 psi. For the measurements obtained and the results provided here, this is adequate for the analysis performed.

8.0 EVALUATION OF A DYNAMIC MODEL

In this work, the dynamic compression system modeling technique chosen for investigation is the Dynamic Turbine Engine Compressor Code (DYNTECC) model developed at Arnold Engineering Development Center (AEDC). This model was chosen because of its successful application to previous compression system simulations (Owen and Davis, 1994; Gorrell and Davis, 1993; Davis and O'Brien, 1991; Davis, 1991; Hale and Davis, 1992). All of the other simulations developed in the history of the model have been compared to the static pressure distributions in the compression systems. Overall, the model has proven to be a useful tool for investigating pre-stall and post-stall events, in addition to simulating effects of inlet flow distortion, compressor geometry changes, and overall system effects on compressor performance. The model's capability to simulate the correct frequency of compressor surge, the interstage static pressure rise and fall prior to surge, and the change on pre-stall conditions has been shown in the aforementioned works. However, none of these model evaluations have validated the calculation of the dynamic flow behavior during stall and surge events, due to the lack of measured high-response flow data. The following examination of the model's capability to properly represent dynamic flow in an axial-centrifugal compression system was performed using detailed measurements of high-response flow obtained from the TFE1042 compressor rig.

8.1 The DYNTECC Compressor Modeling Technique

The following description of the formation of the DYNTECC model is taken from the paper by Owen and Davis (1994).

> "DYNTECC is a one-dimensional, stage-by-stage, axial compression system mathematical model which is able to analyze any generic compression system. DYNTECC uses a finite difference numerical technique to simultaneously solve the mass, momentum, and energy equations with turboma-

chinery source terms (mass bleed, blade forces, heat transfer and shaft work). The source terms are determined from a complete set of stage pressure and temperature characteristics. A brief summary of the theory behind DYNTECC is presented below. A more detailed explanation of the theory and capabilities of DYNTECC is presented in Hale and Davis (1992).

Illustrated in Figure 8-1 is a representative, single-spool, multi-stage compressor and ducting system. The compressor and ducting system are modeled by an overall control volume. Acting on the control volume is an axial-force distribution, FX, attributable to the effects of the compressor blading and the walls of the system. Energy supplied to the control volume include the rate of heat added to the fluid (Q) and the shaft work (SW). Mass transfer rates across bound-

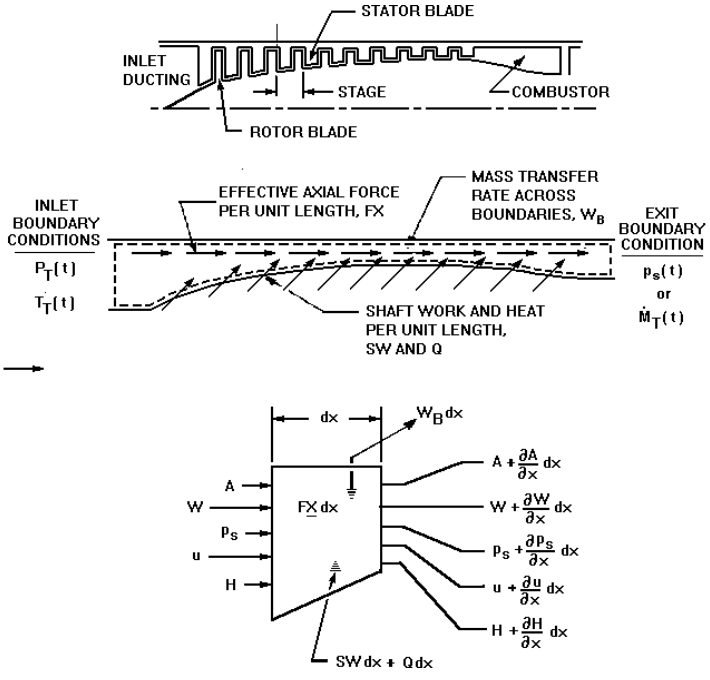

Figure 8-1 DYNTECC Control Volume Modeling Technique

aries other than the inlet or exit (such as the case of inter-stage bleeds) are represented by the distribution, W_B.

The overall control volume is subdivided into a set of elemental control volumes. Typically, the compressor section is subdivided by stages either as a rotor-stator or vice versa depending on the way experimental stage characteristics may have been obtained. All other duct control volumes are divided to ensure an appropriate frequency response. The governing equations are derived from the application of mass, momentum, and energy conservation principles to each elemental control volume.

Continuity

$$\partial (\rho A) / \partial t = - \partial W / \partial x - W_B \qquad (8.1)$$

Momentum

$$\partial W / \partial t = - \partial (IMP) / \partial x + FX \qquad (8.2)$$

where

$W = \rho u A$,

$IMP = Wu + P_S A$ is a momentum impulse term,

and

$FX = F_b + P_S \partial A / \partial x$ is an axial-force distribution consisting of blade force and the force produced by the walls of the system.

Energy

$$\partial (EA) / \partial t = - \partial H / \partial x + SW + Q - H_B \qquad (8.3)$$

where

$E = \rho (e + u^2 / 2)$,

$H = C_P W (T_T - T_{REF})$; $T_{REF} = 0$, and

H_B is the enthalpy associated with bleed flows.

To provide stage force and shaft work inputs to the momentum and energy equations, a set of quasi-steady stage characteristics (Figure 8-2) must be available for closure. The stage characteristics provide the pressure and temperature rise across each stage as a function of steady airflow. Using pressure rise, temperature rise, and airflow, a calculation can be made for stage steady-state forces and shaft work.

The above discussion centers on the steady characteristics. During transition to surge and development of rotating stall, the steady stage forces derived from the steady characteristics are modified for dynamic behavior via a first-order lag equation of the form

$$\tau \; d(FX) / dt \; + \; FX \; = \; FX_{ss} \qquad (8.4)$$

The time constant, τ, is used to calibrate the model to provide the correct post-stall behavior.

The inflow boundary during normal forward flow is the specification of total pressure and temperature. The exit boundary condition is the specification of exit Mach number or static pressure. During reverse flow the inlet is converted to an exit boundary with the specification of the ambient static pressure. Therefore, both the inlet and exit boundary function as exit boundaries during a surge cycle."

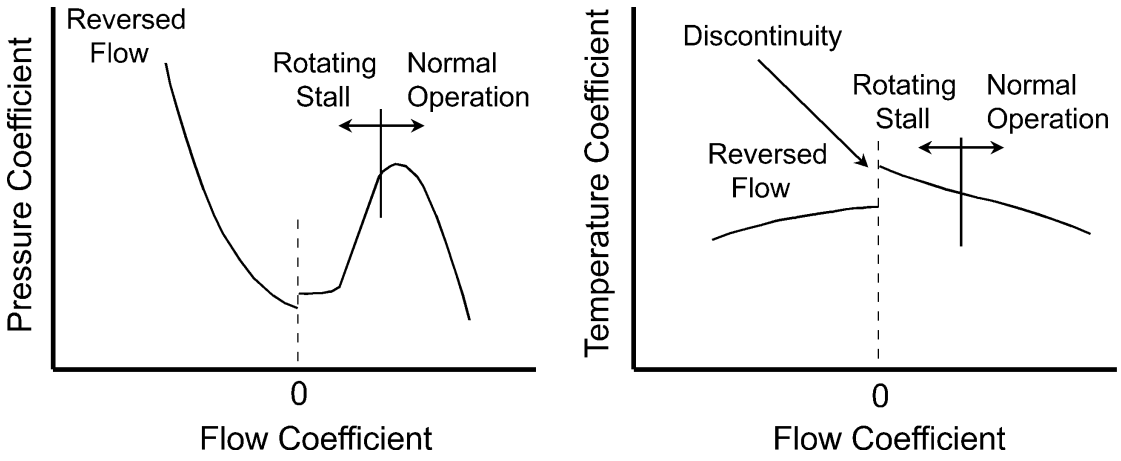

Figure 8-2 General Regions of the Typical Stage Characteristic

8.2 The TFE1042 Geometry Input to the DYNTECC Model

The geometry input for the DYNTECC model was developed from the TFE1042 compressor rig, as was depicted earlier in this document. Figure 8-3 shows the geometry input for the TFE1042 compressor. The compressor was modeled from the bellmouth through the discharge plenum, up to the valve in the discharge plenum. Upstream of the bellmouth, there was an inlet settling chamber that contained flow straightening screens. Previous work with the model showed that the same result was achieved whether or not the settling chamber was included. This conclusion was expected, since the settling chamber is large enough not to have an effect on either the normal operation of the compressor or the post-stall behavior. Based on this earlier conclusion, the settling chamber was not included in the model, which allowed faster turn-around times on the model runs.

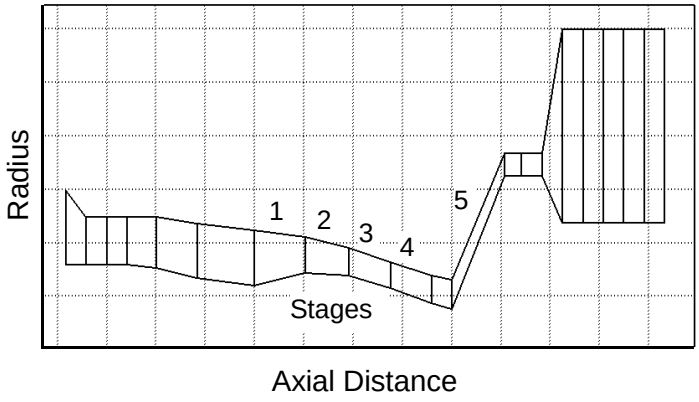

Figure 8-3 Geometry Input for the TFE1042 Compressor

8.3 Results of the DYNTECC Model of the TFE1042 Compressor Rig

To provide the system of stage characteristics for inclusion into the DYNTECC model, a data match to the test data taken with vane-mounted instrumentation was performed with an AlliedSignal off-design computer program. This allowed detailing the stage characteristics in the form of rotor-stator characteristics rather than stator-rotor characteristics. This form was preferred because it was not desirable to model the fourth stage stator by itself, or include it with the centrifugal stage. Figures 8-4 and 8-5 show the TFE1042 stage characteristics for 80, 90, and 100 percent corrected speed. The points on the temperature characteristics are there to facilitate creating the curve fit which is used in the DYNTECC model. The pre-stall pressure and the temperature characteristics are based on the test data while the post-stall characteristics are synthesized based on low-speed rig tests and typical characteristics for compressors of this type.

For reference, the DYNTECC model results will be compared to Figures 7-14, 7-15, and 7-16 presented earlier in this dissertation for surge behavior at 80 percent corrected speed.

The DYNTECC model was set up and configured with the time constants which matched the surge data as closely as possible. Figure 8-6 shows a surge cycle comparison of the model results to the rig test data. The pre-stall steady state side of the compressor map is very similar. The peak pressure ratio at surge is modeled very well, as is the flowrate at the point where the surge cycle meets the steady-state speed line (at a pressure ratio of about 2.5). The obvious difference in the two surge cycles is in the post-stall behavior. The data shows a constant-flow blowdown at about -10 lbm/sec. Although the model does reach the -10 lbm/sec flow, it does not show the constant-flow blowdown. Another similarity of the surge cycles is the downward slope of the inception of the surge cycle and the upward slope of the right side of the recovery portion. Comparison of the pressure stage characteristics (Figure 8-4) to the model

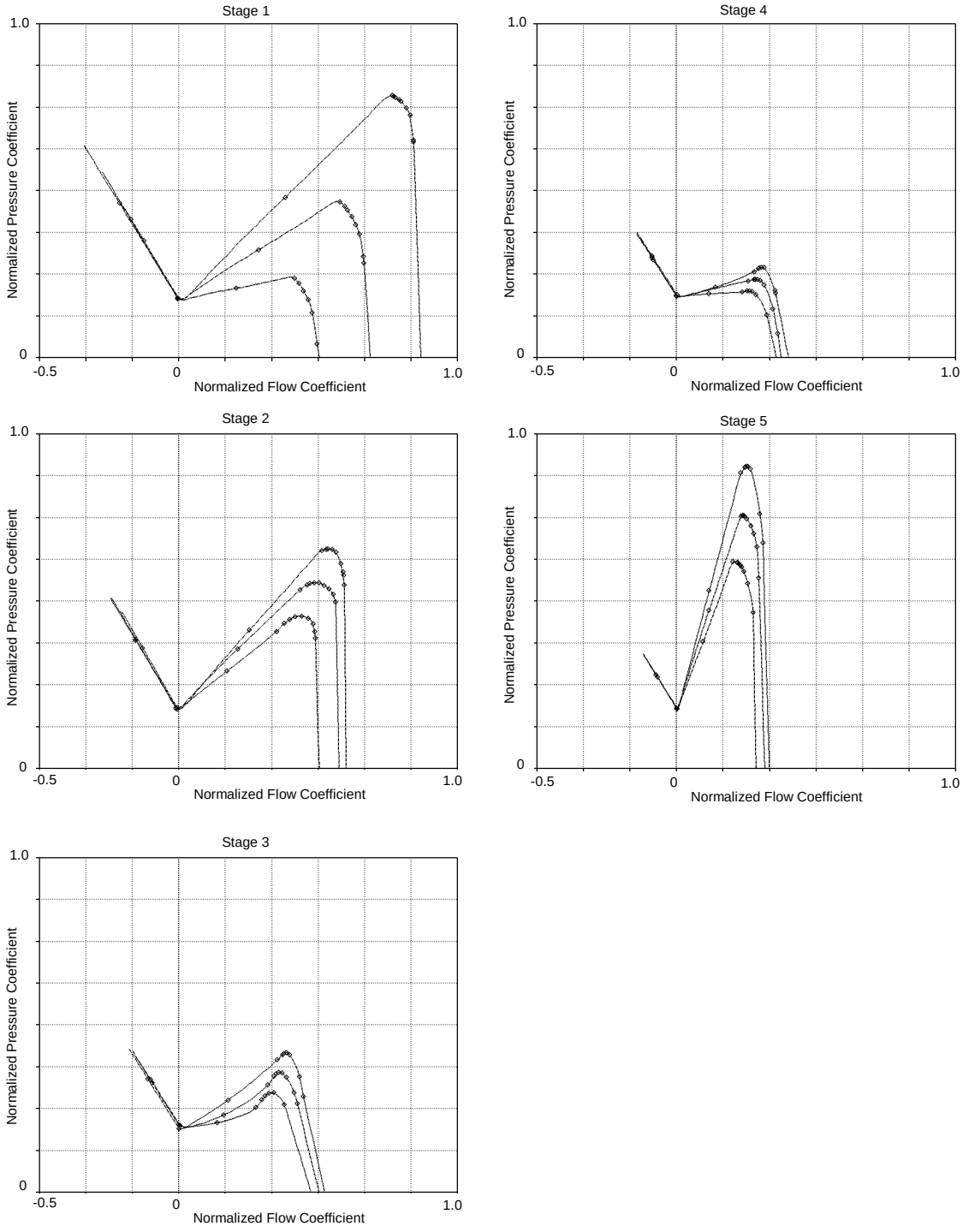

Figure 8-4 TFE1042 Rig Stage Pressure Characteristics for 80, 90, and 100% Corrected Speed

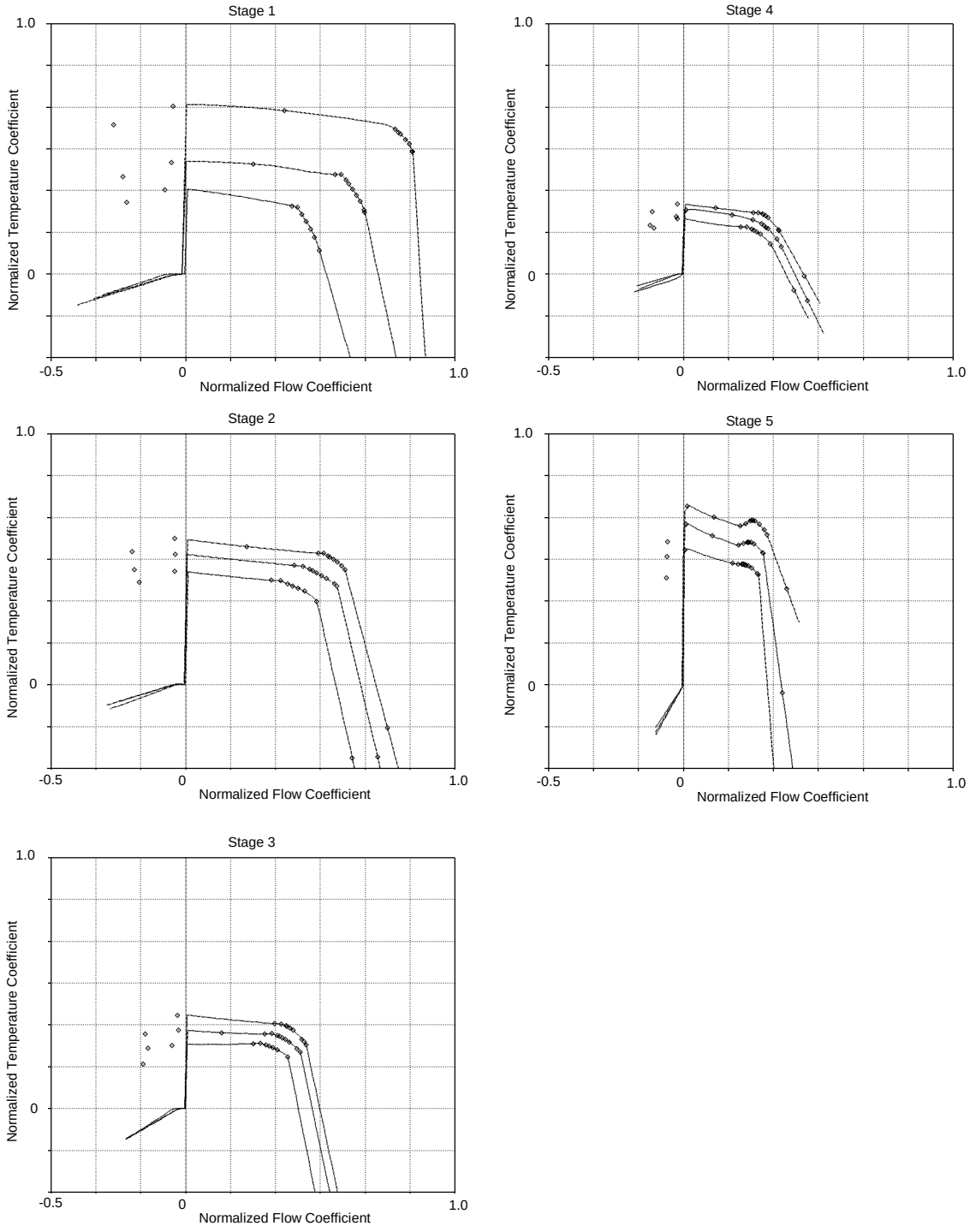

Figure 8-5 TFE1042 Rig Stage Temperature Characteristics for 80, 90, and 100% Corrected Speed

DYNTECC Model Result

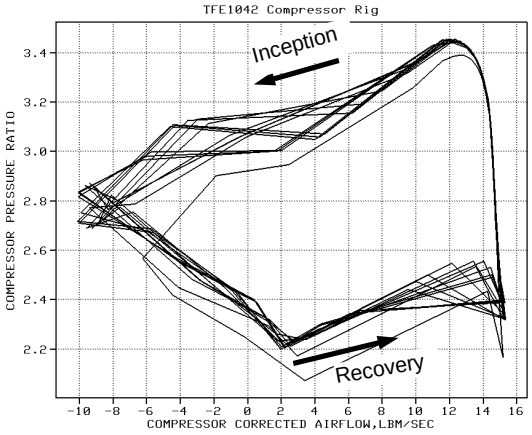

Rig Data

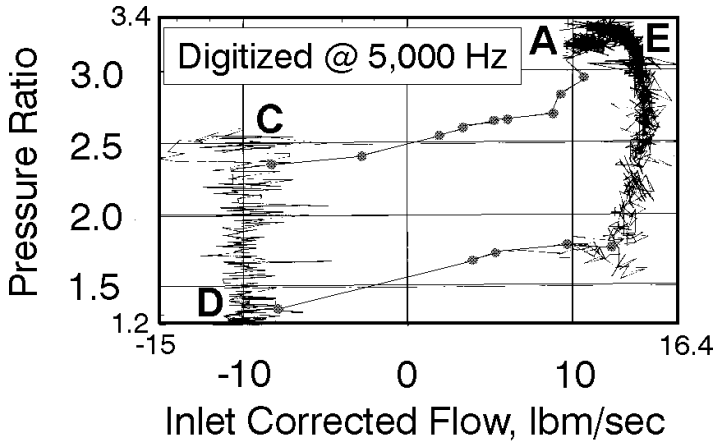

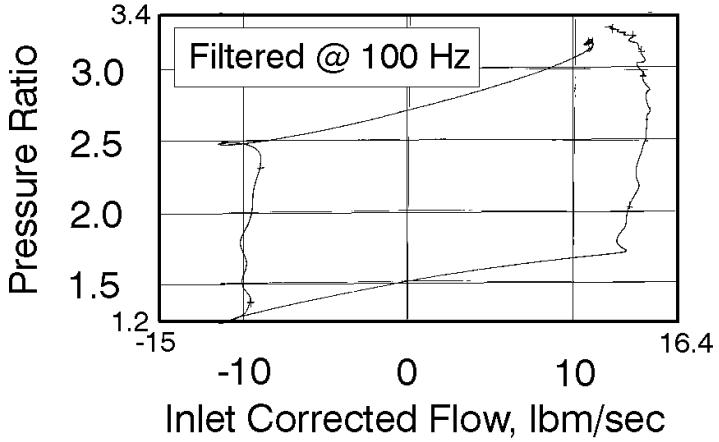

Figure 8-6 Surge Cycle Comparison of the DYNTECC Model Results to the TFE1042 Measured Data

surge result (Figure 8-6) indicates that the left side of the recovery portion of the surge cycle is following the upward-slanting reverse-flow pressure characteristic. No matter what time lagging factors were applied to the model, this characteristic could not be changed.

The comparisons shown in Figures 8-7 and 8-8 were obtained by breaking apart the surge cycle into its basic characteristics of total pressure ratio and corrected flow. Examination of the time scale shows that the blowdown portion of the surge cycle alone takes about 75 ms. (Referring back to Table 7-1, the research compressor surge cycle blowdown was 99 ms with that compressor running at 97.5% corrected speed.) From Figure 8-7, the complete surge cycle for the TFE1042 compressor rig takes about 300 ms. This represents a surge cycle frequency of 3.3 Hz. However, the dynamic model shows a surge cycle frequency of 25 Hz because the blowdown portion of the surge cycle is not adequately represented. (The model shows about three surge cycles during the time period of the rig blowdown.) No matter what time constants were applied to the model, the surge cycle frequency and blowdown could not be affected.

Since the time constants in the dynamic model could not change the characteristics of the surge behavior and the geometry was correctly represented, the next step was to make a modification to the pressure stage characteristics to examine the effect on the blowdown and recovery portion of the surge cycle. The pressure characteristics were modified (Modification A) by increasing the slope of the reverse flow characteristic as shown in Figure 8-9. It was hoped that with a more vertical reverse flow characteristic and long lagging time constants, the actual model path would overshoot the characteristic and remain more vertical in nature. Figure 8-10 shows the result of “Modification A.” While the characteristic is more vertical on the blowdown side, it is quite unstable and never reaches a flow of -10 lbm/sec, as indicated in the data.

Since the flow characteristic did have the tendency to be more vertical, a second modification was made. It was thought that the model might respond to

DYNTECC

Model Result

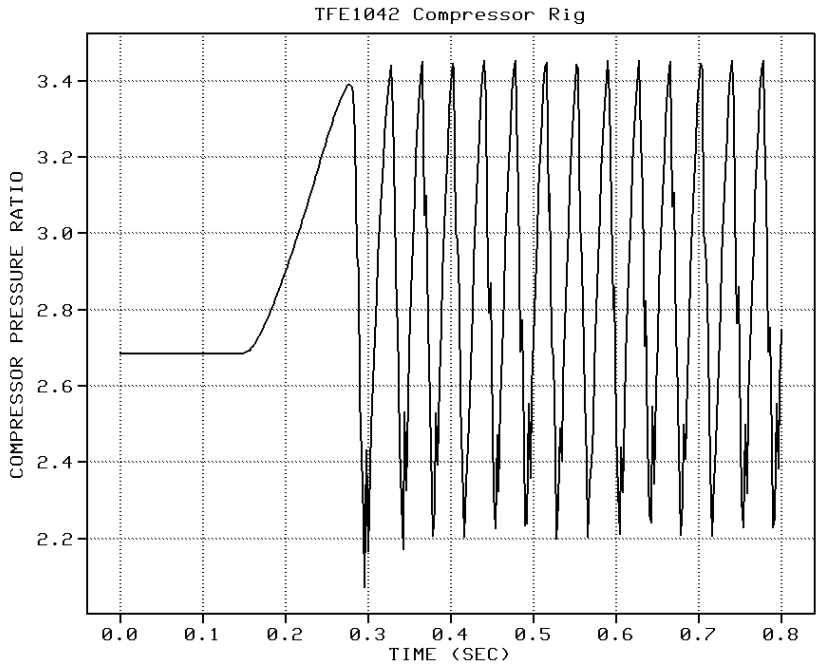

Rig Data

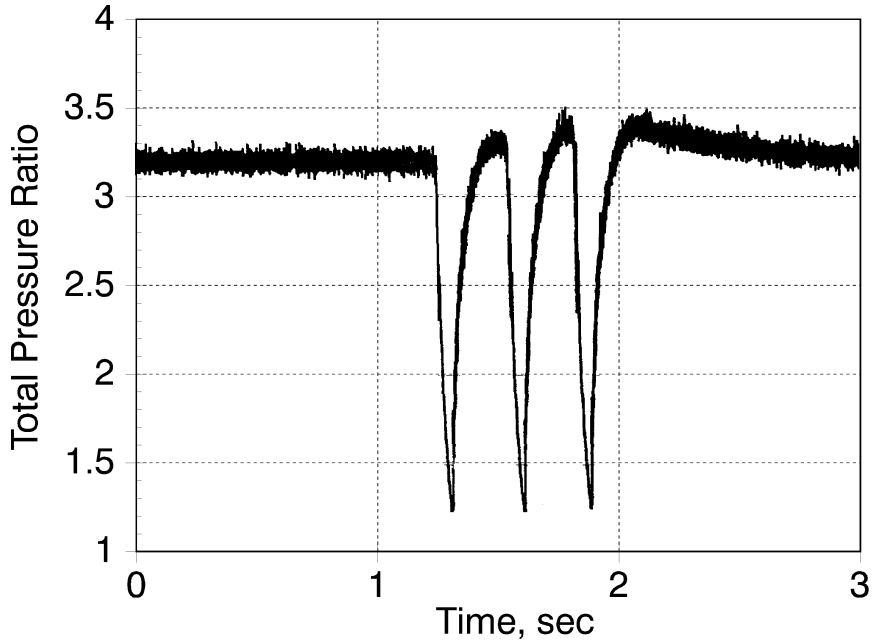

Figure 8-7 Total Pressure Ratio Comparison of the DYNTECC Model Results to the TFE1042 Measured Data

DYNTECC

Model Result

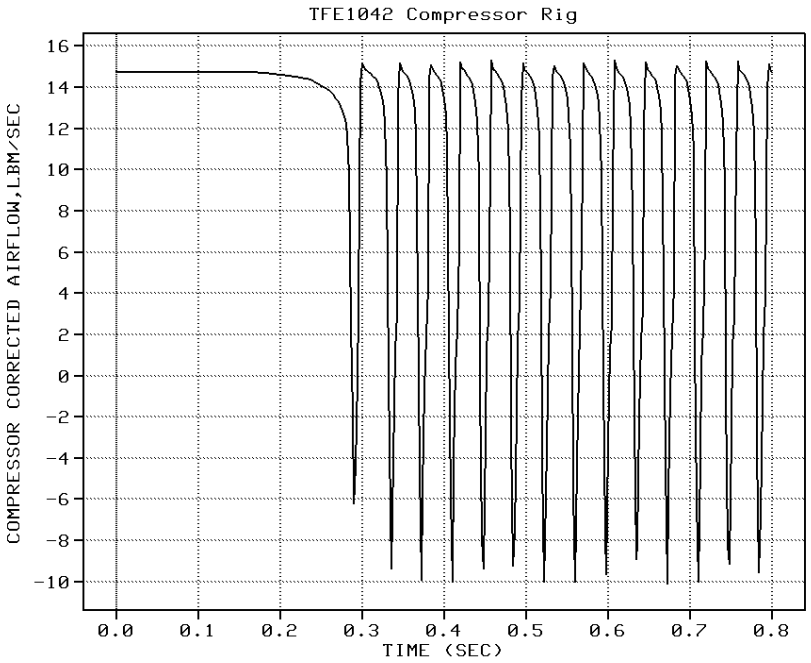

Rig Data

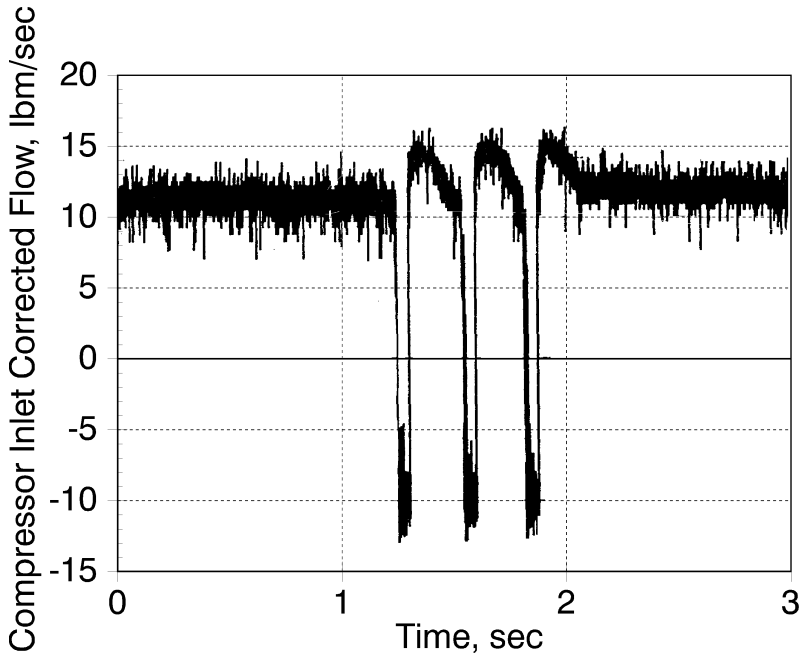

Figure 8-8 Inlet Corrected Flow Comparison of the DYNTECC Model Results to the TFE1042 Measured Data

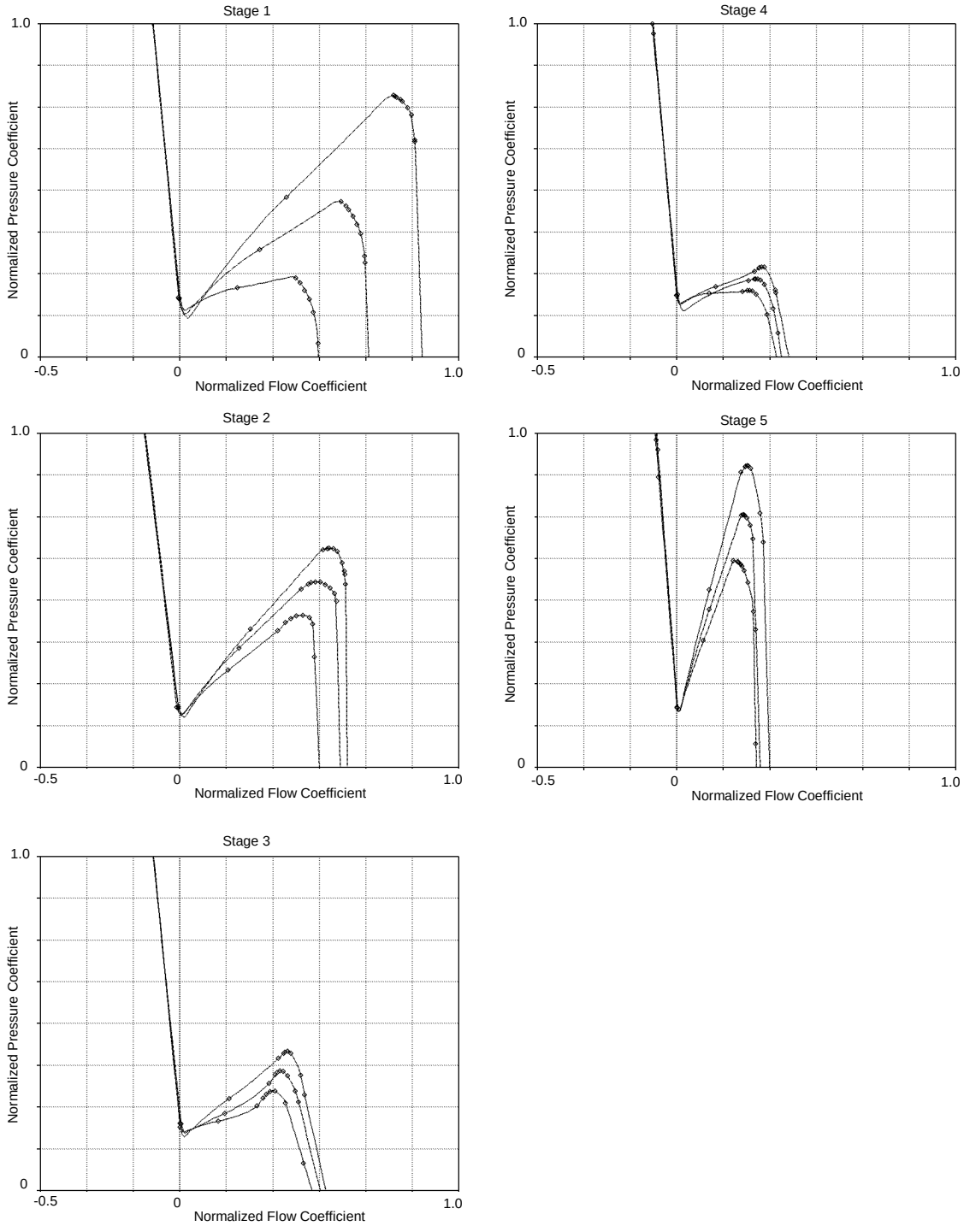

Figure 8-9 Modification A: Change to the Slope of the Reverse Flow Pressure Characteristic for the TFE1042 Compressor Rig

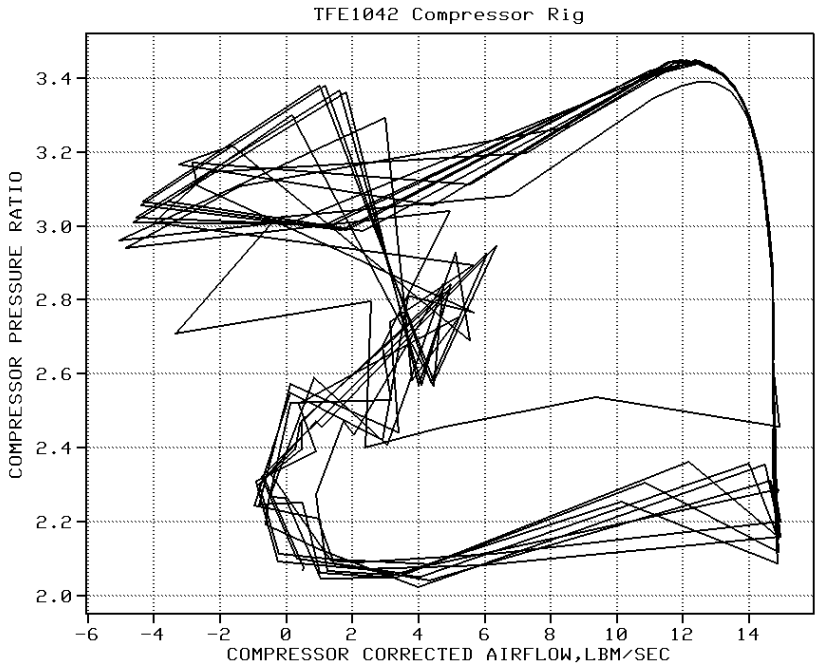

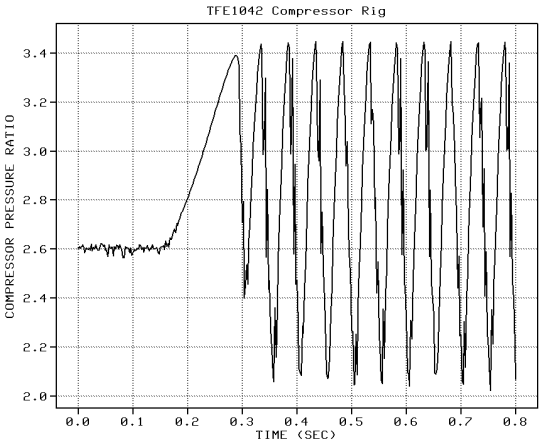

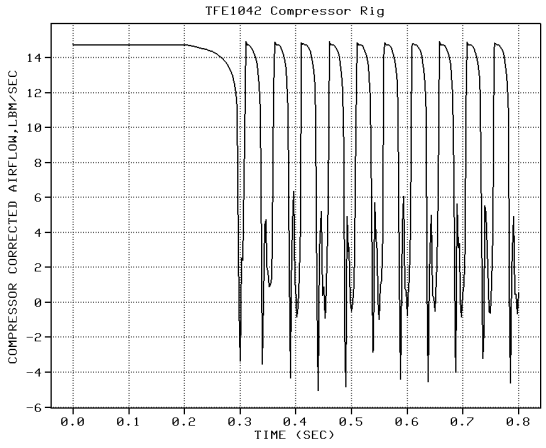

Figure 8-10 DYNTECC Model Result for the Surge Cycle Using Modification A

somewhat shorter time constants and might track the nearly vertical reverse flow characteristic if the characteristic was shifted to a flow coefficient that represented approximately -10 lbm/sec. Figure 8-11 shows “Modification B,” which was made with the intent of forcing nearly constant flow at -10 lbm/sec. The initial attempt at matching the data was made with little change to the time constant associated with the inception side of the surge cycle. Results of this are shown in Figure 8-12. While the modification did force the reverse flow closer to -10 lbm/sec, it resulted in some very unstable behavior of the model. Examination of the corrected flow versus time trace shows that the model also took longer to traverse the reverse flow region.

An attempt was made to minimize the apparent model instability on the reverse flow side of the surge cycle by adjusting the time constants for the inception, blowdown, and recovery characteristics. With the nearly vertical slope of the stage characteristics, the model was very sensitive to changes in the time constants. Figure 8-13 shows the best match that could be achieved with the “Modification B” stage characteristics. Once model stability was achieved, the maximum reverse flow reached about -10 lbm/sec, but the model would not maintain a constant reverse flow. This indicated that there was something missing from the model capability. There are some physics not modeled correctly or there are some physical processes during reverse flow that are not modeled. The next section discusses the physics of the reverse flow region.

Since it is known that the volume dynamics have an effect on the frequency of the surge cycle, the inlet settling chamber was added to the geometry as shown in Figure 8-14. Running the model again with the same time constants as in the previous run (Modification B stage characteristics with the time constants adjusted to achieve model stability) produced the results shown in Figure 8-15. The frequency of the surge cycle was not affected by the inlet settling chamber. This in itself is somewhat satisfying since the utility of an inlet settling chamber is to provide uniform flow to the compressor rig without having

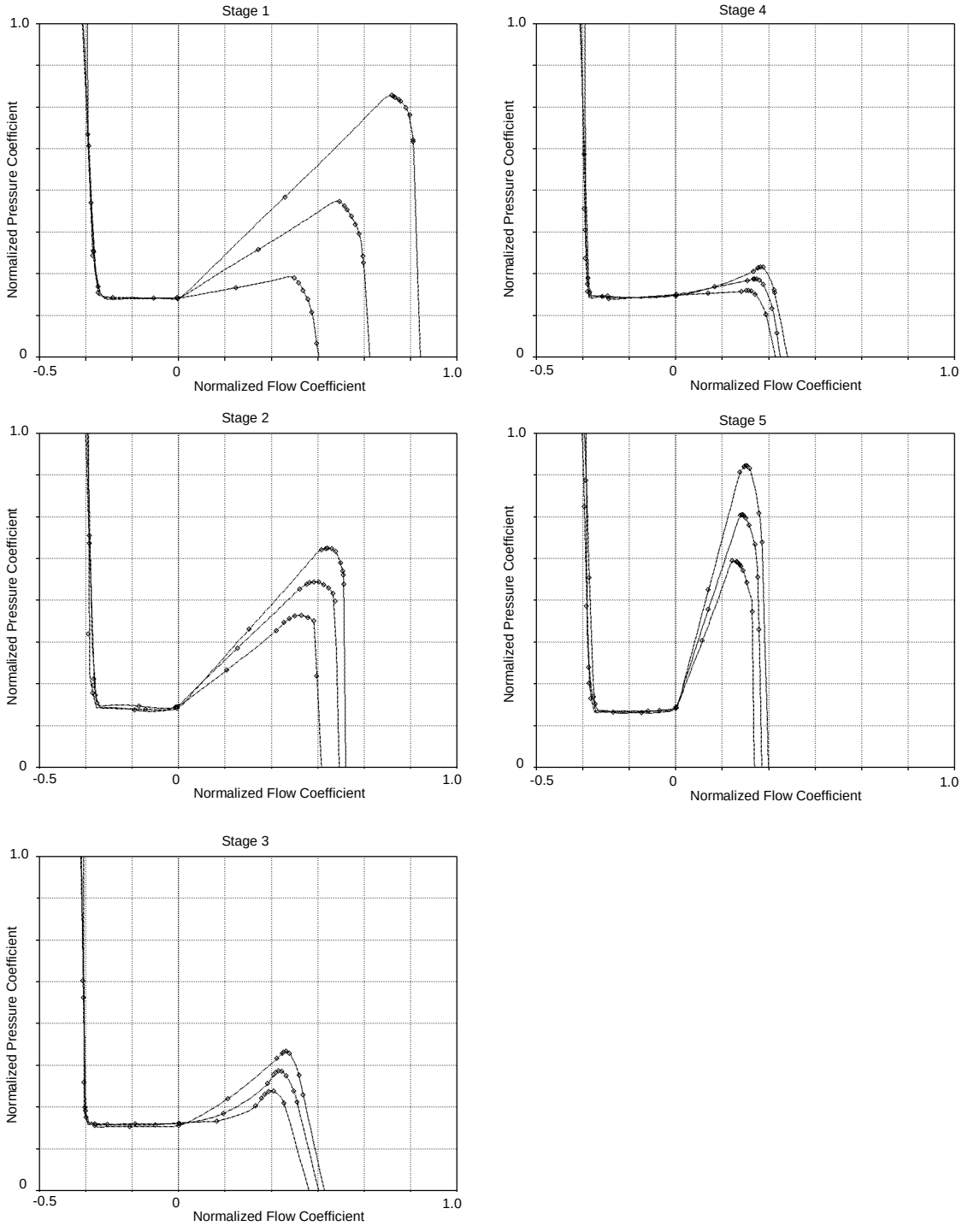

Figure 8-11 Modification B: Shift of the Reverse Flow Pressure Characteristic to a Negative Flow Coefficient

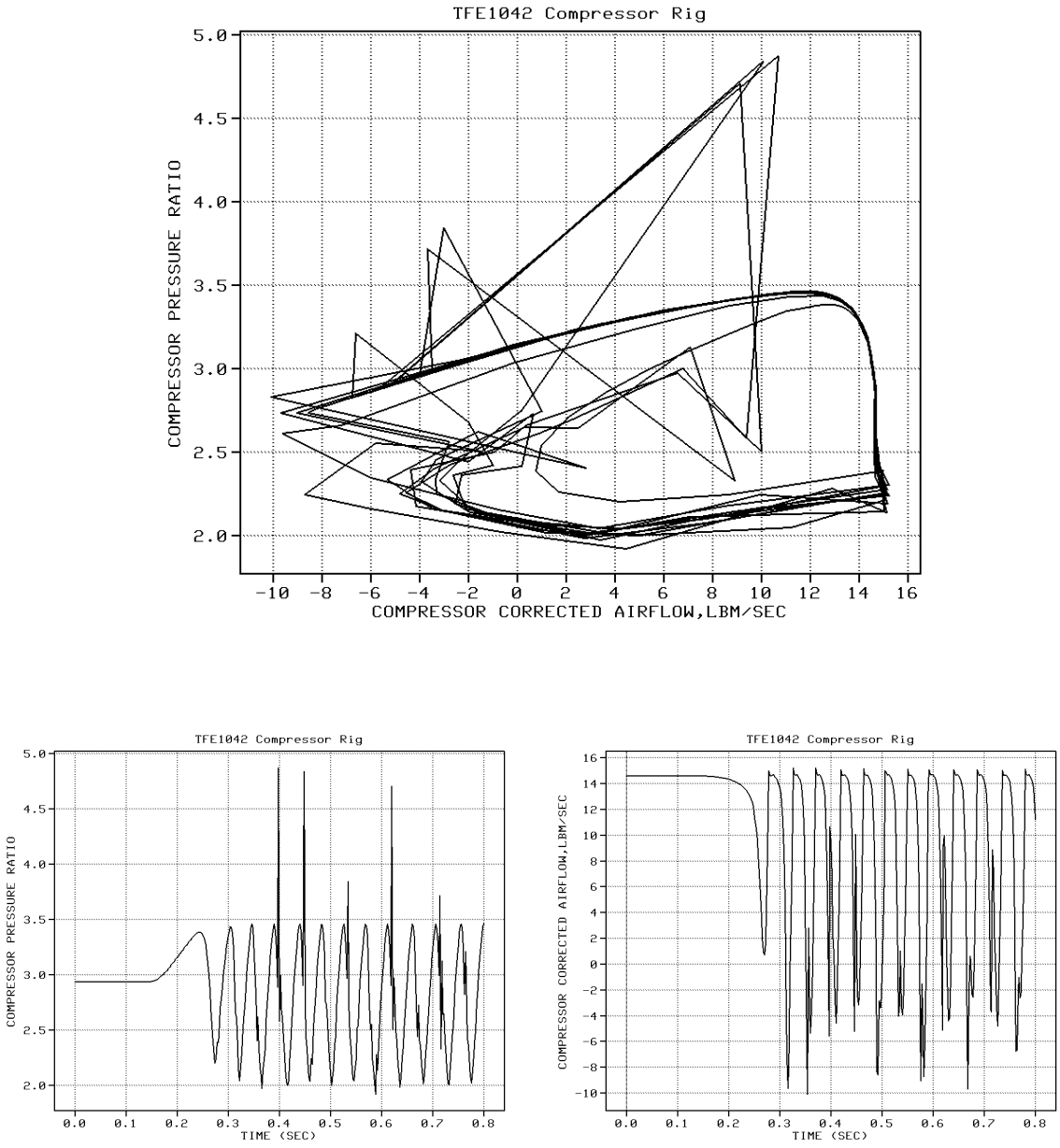

Figure 8-12 DYNTECC Model Result for the Surge Cycle Using Modification B Stage Characteristics, Without Time Constant Adjustment

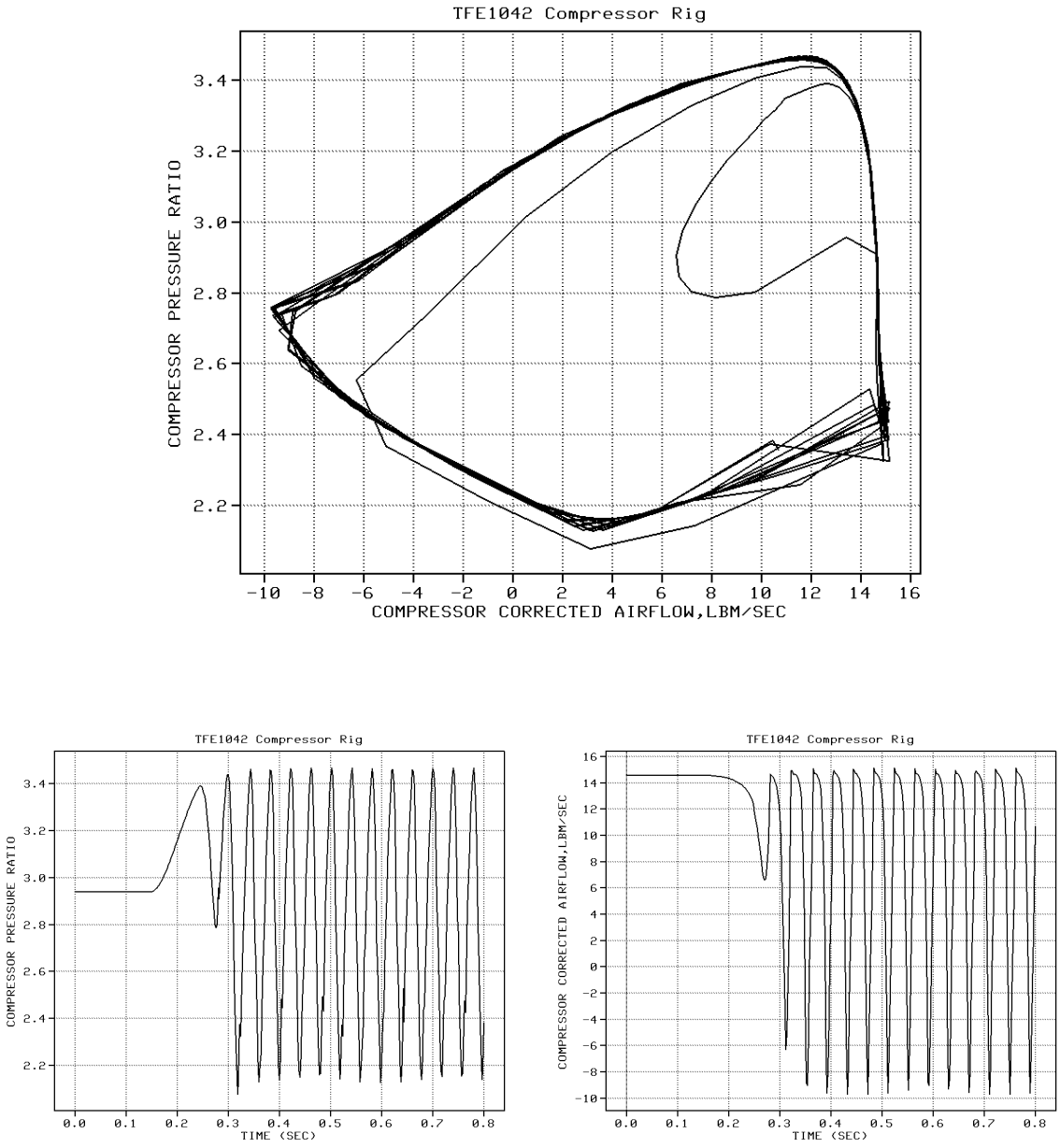

Figure 8-13 DYNTECC Model Result for the Surge Cycle Using Modification B Stage Characteristics and Adjusting the Time Constants to Achieve Model Stability

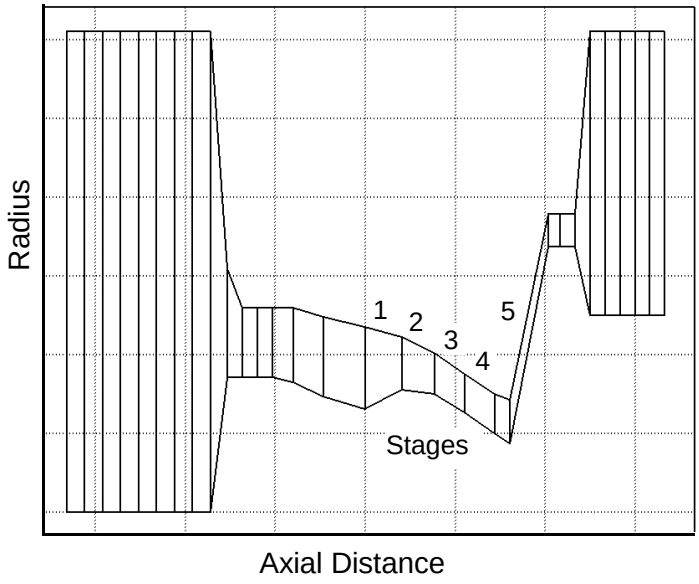

Figure 8-14 Geometry Input for the TFE1042 Compressor, Modified to Include the Inlet Settling Chamber

any effect on the rig performance.

8.4 The Missing Physics of the DYNTECC Model

Examination of the DYNTECC model results and comparison to the TFE1042 surge data showed that there are some physics not being modeled properly in the reverse flow region. Figure 8-16 depicts the rotor exit velocity diagram for a highly backswept impeller and a vaned diffuser. Under normal forward flow operation, the flow leaves the diffuser at a relatively low Mach number. This low Mach number allows the final flow leaving the deswirl vanes (not shown) and entering the combustor to have a Mach number of about 0.15. During surge behavior, the pressure in front of the impeller drops to near ambient (this can be seen in Figure 7-8 for the research compressor) as the flow breaks down in the axial portion of the compressor. This reduction in pressure (and therefore inlet Mach number and flowrate) results in a severe reduction in the

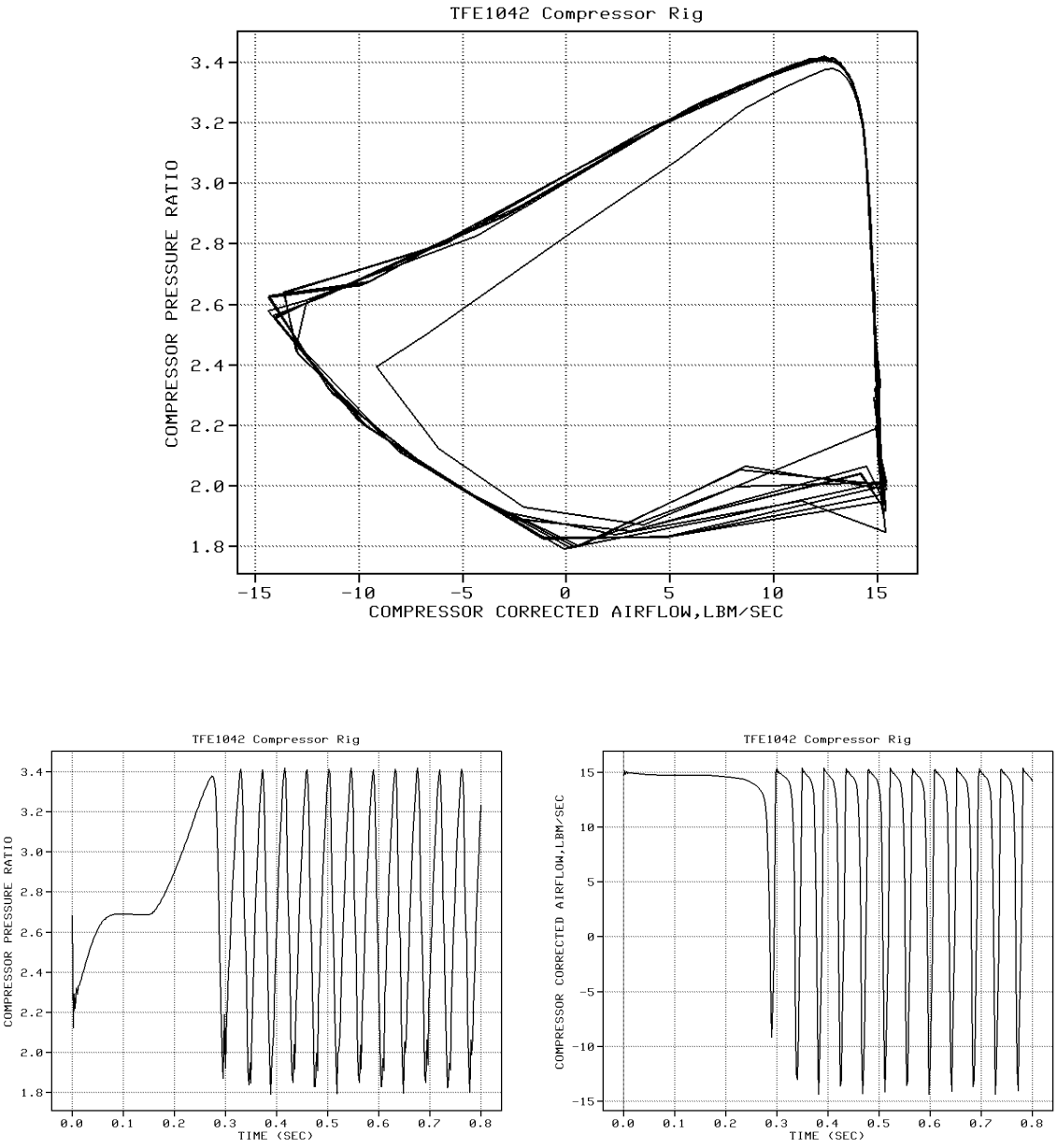

Figure 8-15 DYNTECC Model Result for the Surge Cycle Using Modification B Stage Characteristics and Adjusting the Time Constants to Achieve Model Stability - With Addition of Inlet Settling Chamber

pressure rise capability of about the first forty percent of the centrifugal impeller (Figure 4-8). With only the radial portion of the centrifugal impeller providing the pressure rise (the 1/2 (U_2^2 - U_1^2) term of equation 4.5), the pressure across the impeller is greater than can be sustained and backflow occurs. Figure 8-17 shows the velocity diagram during the centrifugal backflow. Depending upon the impeller-diffuser match, choking occurs either in the diffuser throat (most likely) or in the impeller exit, depending upon the "b" width of the impeller. It is this choking that causes the backflow to be held at -10 lbm/sec during the surge cycle shown in the TFE1042 data plot in Figure 8-6. This behavior makes the surge frequency lower than if choking did not occur. In the DYNTECC model, there is no mechanism to simulate the choking and constant flow of the back-flow portion of the surge cycle. If the model did simulate this correctly, then the frequency of surge would be lower and the lowest flow portion of the flow-time trace in Figure 8-13 would look more like that of the data trace in Figure 8-8.

In other work by Owen and Davis (1994) the compressor rig for the T55-L-712 axial-centrifugal compressor (hereafter called the T55) was matched with the DYNTECC model. In this match, high-response flow data was not available and static pressures were matched with the model. The surge frequency pre-

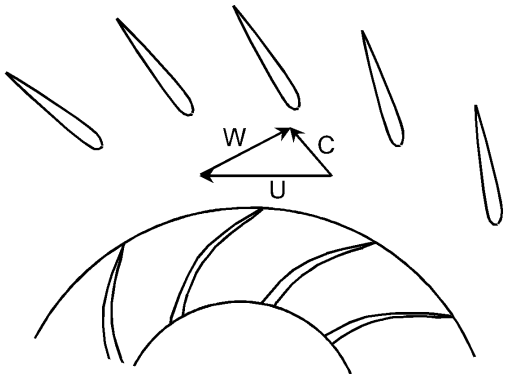

Figure 8-16 Velocity Diagram for Flow Leaving the Impeller Under Normal Forward Flow Conditions (impeller and vanes not to scale)

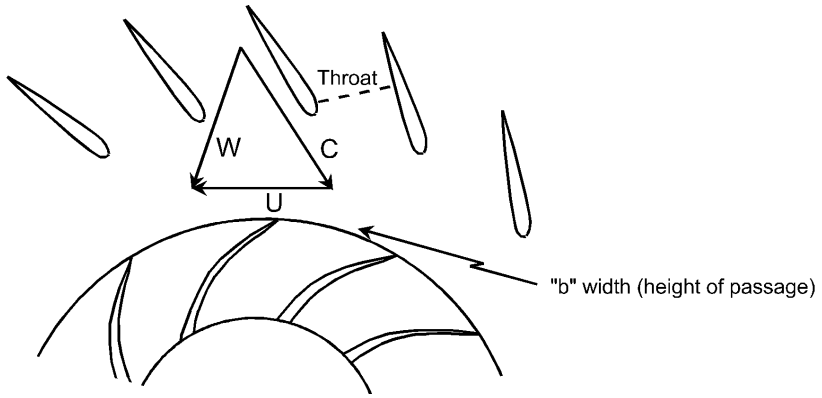

Figure 8-17 Velocity Diagram for Flow Entering the Impeller Under Reverse Flow Conditions During Surge (impeller and vanes not to scale)

dicted by the model was the same as that observed in the compressor as measured by static pressure transducers in the shroud of the machine. Without high-response flow measurements, whether or not the post-stall flow behavior is correct is not known, since it is probably possible to obtain the correct frequency without the correct flow distribution. There is a major difference between the T55 compression system and the TFE1042. The T55 has a straight radial impeller (rather than a highly backswept impeller) and the match to the diffuser is significantly different. In the T55, the centrifugal impeller is the surge trigger under standard conditions along the high end of the map. In addition, the rig diffuser was somewhat unstable at high flows (this can be seen in the data presented in the paper). Figure 8-18 shows a reproduction of Figure 8 from Owen and Davis (1994). In the figure, the unsteadiness of the centrifugal stage can be seen. It is the opinion of this author that this unsteadiness is caused by the rig diffuser, just downstream of the centrifugal stage. This diffuser had a half angle that approached 30 degrees. This can also be seen in the geometry input representation of the rig exit ducting in the Owen and Davis paper. In effect, the T55 rig has a compressor not matched as discussed and shown in Fig-

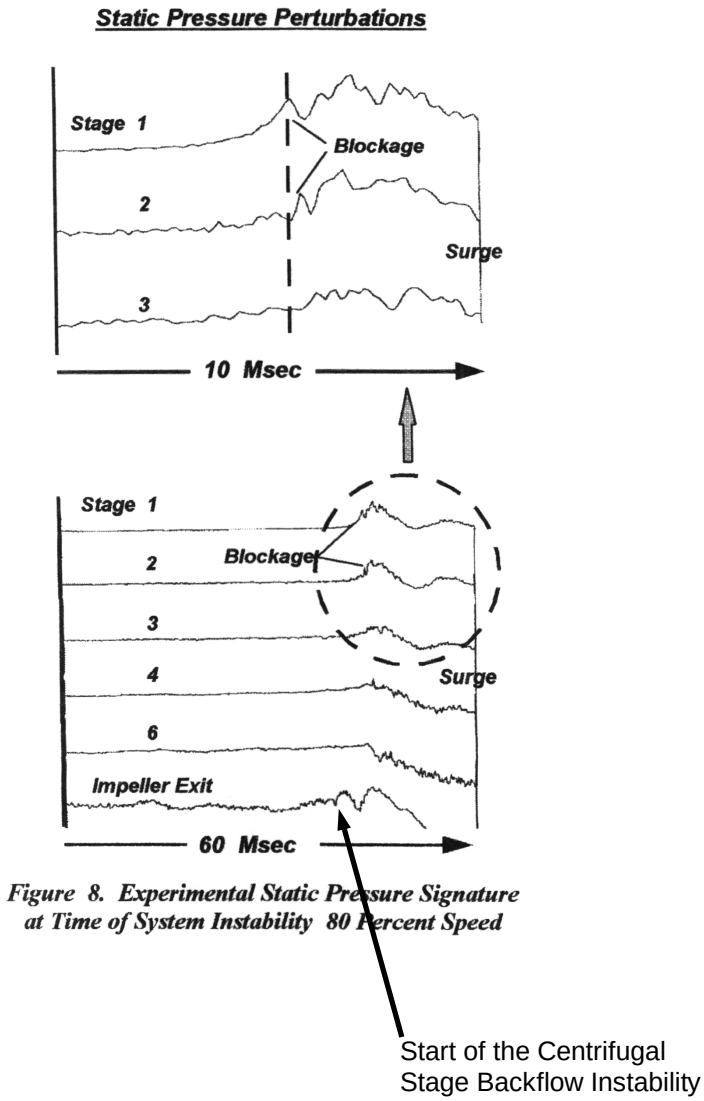

Figure 8. Experimental Static Pressure Signature at Time of System Instability 80 Percent Speed

Figure 8-18 Reproduction of Figure 8 from Owen and Davis (1994) (Arrow indicating the start of the centrifugal stage backflow added by Cousins)

ure 4-11 of this dissertation. Matching the centrifugal stage so that it is not the stall trigger at high speed is not possible without a backswept impeller. Having a radial impeller, the centrifugal stage in the T55 is the surge trigger at high speed. In this particular rig, the centrifugal compressor stability is further reduced by the fact that the downstream diffuser is not optimum. The authors state in the paper that at speeds higher than 80%, it was difficult to fully understand the data due to the centrifugal unsteadiness. The authors also state that in all the results, the first stage appeared to be the stall trigger. In fact, with further investigation, the authors may have realized that what was being observed as a first rotor phenomena was in fact a second order result being triggered by the centrifugal stage causing the axial to mismatch, aggravated by the poor downstream diffuser. If Owen and Davis had the details of the flow provided by high-response flow measurements (a fore-aft probe), they probably would have arrived at a different conclusion. At the time Owen and Davis obtained this data, much of what has been discussed here was not known. This author has had the benefit of more study of the rig and the overall performance of the T55 compressor than Owen and Davis had at the time their work was performed, due to the acquisition of the Lycoming Company by AlliedSignal Engines, and the availability of more detailed performance models of the compression system.

9.0 DISCUSSION OF RESULTS

Although the stall and surge phenomena in compression systems has been investigated in many ways over the years, the interstage dynamics have never been investigated and documented to this extent. Therefore, the analysis, data, and model results presented herein provide a significant advance to the understanding of the dynamics of the unsteady behavior in compressors. The characteristic differences in axial rotors and centrifugal impellers that has been presented supports the measured data and the interstage effects that are observed. The differences in the sensitivity of axial and centrifugal rotors to changes in inlet conditions and the benefit of the pressure rise capability of centrifugal impellers under adverse flow conditions can be seen in the calculation of the reduced frequency for the blades. The reason for the tolerance of the centrifugal impeller to adverse flow conditions is the enthalpy rise that is generated from the change in radius in the flow passage.

The dynamics of flow change in the axial compressor has been shown to be important to understanding the overall physics of stall and surge. The unique high-response fore-aft probe provides flow information that cannot be gleaned out of the pressure data, especially during the post-stall portion of the surge cycle. The data presented has provided a new insight into the interstage dynamic interactions that occur prior to and during stall and surge. The TFE1042 data showed that the static pressure effects can be felt both upstream and downstream of the stalling airfoils. In addition, the inception of rotating stall and the inception of surge are the same phenomena. In the paper by Day (1993) it is stated that rotating stall always precedes surge. This is not the case if rotating stall is defined as a self-sustaining quasi-steady blade-row based phenomenon that starts with a few blades experiencing flow separation, which grows in magnitude and extent until a quasi-stable condition is reached. The exact same flow separation starts the surge process, as shown by the TFE1042

data. The difference is that before the stalled sector can grow in magnitude and extent to become quasi-stable rotating stall, the lack of available pressure rise from the stage (and therefore the compressor) is recognized by the system (there is enough energy storage downstream that the compressor cannot pump against the high pressure with degraded pressure rise ability) and surge occurs. When the compressor is operating at high speed, there is a greater amount of energy stored downstream and the surge occurs very soon after the formation of a few locally stalled blades. This can happen within two or more rotor rotations. At lower speed, not as much energy is stored downstream, so the tendency is to develop a larger defect in the rotor row (larger separation) prior to surge, over a longer time period. If the energy stored downstream is not significant enough to cause a surge, a rotating stall results.

Axial-centrifugal compressors afford a unique enhancement to recoverability, especially if they are not the stall trigger stage. Designing the centrifugal compressor stage to enhance the compression system stability requires that the centrifugal rotor have the proper flow capacity and be matched correctly to its diffuser and to the axial machine. The data taken on the research compressor shows that the recovery time is almost five times faster with a centrifugal stage designed to operate as a stability enhancing device. On the inception side of the surge cycle, the centrifugal stage retarded surge inception, increasing the inception time by 30 percent. This matching technique takes full advantage of the radial pressure rise available in the centrifugal impeller by not having it as the stall trigger and provides the axial-centrifugal compressor a great advantage in recoverability.

The engine data that was taken on both the TFE1042 and the TFE731 shows that during surge, the location of stall initiation determines what the surge overpressure in the front of the compression system will be. Fan-initiated surges cause less overpressure in the inlet than core compressor-initiated surges. In the unique case of a split-spool axial-centrifugal compressor, the

phenomenon is similar. When the centrifugal stage is the stall trigger, the overpressure in front of the compressor is higher than when an axial stage is the stall trigger. The split-spool compression system also provides other unique characteristics. It is easier to start the engine because the allowed speed mismatch lets the centrifugal stage tolerate the off-design condition of density mismatch during starting; however, it is possible to pull so much bleed from between the axial and the centrifugal compressors that the surge trigger is forced from the axial system to the centrifugal stage. This occurs because the flowrate into the centrifugal stage is reduced, thereby increasing its loading. At the same time, the axial compressor is unloaded because of the increased flowrate at constant compressor corrected speed. Care must be taken therefore, because the answer to a surge margin issue may not be to pull a greater amount of bleed, as might be expected.

This investigation has also shown that models that simulate the proper blade row details can capture the main features of stall and surge. The model that has been examined, DYNTECC, requires some additional internal physics to properly simulate the reverse flow effects of downstream choking. This has not been apparent before, since the model has not been used to simulate an axial-centrifugal compressor that is matched in the manner of those investigated. In the referenced paper by Owen and Davis (1994), some misconceptions about the surge trigger stage are presented for the T55 compressor rig, due to the dynamics of the rig diffuser interacting with the centrifugal stage and rematching the axial compressor. This was aggravated by the fact that the centrifugal stage is the stall trigger at high speed. The conclusions reached in the paper might have been different if the investigators had the capability to observe the high-response flow during the stall and surge behavior. In spite of this, the paper is still very useful because it shows the capability of the DYNTECC model to simulate the global details of stall and surge. Since the centrifugal stage is not designed like those presented in this dissertation, this au-

thor believes that there is no choking present during the surge backflow behavior as was seen in the data presented here. For this reason, the model correctly simulated the surge frequency of the T55 compressor rig.

The data that have been examined and the model that has been presented also provide some new insights into the issues of both passive and active control of stall and surge. Passive stall and surge control includes the effects of such variables as bleed, tip casing treatment, inducer venting systems, inlet guide vanes and scheduled, moveable stators. Examination of these passive devices shows that each affects the internal stage dynamics that have been discussed here. They affect the static pressure distribution, the flow capacity, and the match between the stages. They are also designed to be effective in a particular area of the compression system, known to be “weak” in terms of stability margin. This then poses an interesting question for the technology area of active control of stall and surge. Investigators have proposed the existence of “precursor waves” that occur prior to surge in the compressor. The present results and data show that the “precursors” are probably nothing more than the inception of stall over one or more of the blade rows. It has been shown here that such disturbances can be sensed through the static pressure signature both upstream and downstream of the stalling blade row. Therefore, the precursors are probably not functions of the system properties, but rather an observation of the upstream flowfield disturbance caused by the same local blade row separation that initiates rotating stall and surge. While investigators have measured these precursors in low speed machines and in high-speed machines run at low speed, it is questionable whether this pressure disturbance would be sensed upstream of a properly designed high-speed compressor where the stage initiating compressor instability is in the rear, and the front of the compressor is operating near choke.

Some of the recent attempts by investigators to apply active control techniques to compressors are based on the theory that overall compression sys-

tem control is possible through global techniques involving blowing air into the inlet, or “wiggling” inlet guide vanes at some predetermined frequency, without knowledge of the interstage dynamics of the stall and surge behavior. Some of the success shown by blowing air into the inlet has been on compressors with the surge trigger stage in the front of the compressor, or on low speed compressors that do not experience the choking behavior observed in high-speed machines. It is the belief of the present author, based on the data presented, that designing a high-quality and reliable active surge control to manage the overall compression system stability is not possible without understanding and controlling the interstage dynamics and flow breakdown prior to stall and surge. System parameters (such as energy storage downstream) are important, but the interstage dynamics are equally as important. In addition, the data presented shows that at high speed, the local blade row separation exists only for a few rotor revolutions at best, prior to the surge backflow condition. It is certainly possible that this is why sensing the “precursor” to stall and surge has been difficult on high speed compressors. Eventually, active stability controls surely will be a reality, but unless the interstage dynamics of stall and surge are further defined and controlled, control of surge through interactions with the overall system does not seem plausible. What seems to be a greater possibility is that there is some proper mix of total system control and interstage control that is necessary to form a true active stability control.

With all the measurements and analysis presented and examined in this work, it is somewhat satisfying to note that everything observed can be explained by the thermodynamics and the physics associated with the design of the compression system, the known physics of unsteady flows, or the interactions that occur within the compression system and between the compression system and the surrounding components.

10.0 CONCLUSIONS

There are four primary conclusions that can be drawn from this work.

1. A new understanding of the interstage dynamics of stall and surge in axial-centrifugal compressors has been developed, through the examination of detailed interstage high-response pressure and flow data.

2. It has been shown that blade-row based analytical models are capable of modeling the global features of stall and surge, but not without an understanding of the interstage dynamics that occur during the unstable processes. The DYNTECC model used in this investigation correctly simulates the global features of stall and surge, but requires some improvement in the simulation of the reverse flow behavior to properly capture the choking that occurs in the centrifugal stage.

3. The measurement results presented herein provide a new insight into the development of stall and surge. These phenomena can be directly related to the characteristics of flow over an airfoil and to the pressure balance between compressor stages. All of the measured effects can be explained in terms of known flow physics and, as a result, the measurements performed in these axial-centrifugal compression systems can be extended to axial compressors or to centrifugal compressors.

4. The measurement results provide new information on the limitations of both active and passive stability control systems. As a result, the evaluation of these systems in terms of the true interstage flow physics can be examined.

11.0 REFERENCES

Adamczyk, J. J., and Carta, F. O., 1973, “Unsteady Fluid Dynamic Response of an Axial-Flow Compressor Stage with Distorted Inflow,” Project Squid Technical Report UARL-2-PU, United Aircraft Research Laboratories, East Hartford, CT.

Boyer, K. M., and O’Brien, W. F., 1989, “Model Predictions for Improved Recoverability of a High-Speed Ten-Stage Axial-Flow Compressor, AIAA Paper #89-2684.

Breuer T., and Servaty, S., 1996, “Stall Inception and Surge in High-Speed Axial Flow Compressors,” NASA Technical Report Document ID #96N26989.

Bright, M. M., Qammar, H. K., Weigl, H. J., and Paduano, J., 1997, “Stall Pre-cursor Identification in High-Speed Compressor Stages Using Chaotic Time Series Analysis Methods,” Journal of Turbomachinery, Vol. 119, Issue #3, pp. 491-499.

Cheng, R., Ekerol, H., and Railly, J. W., 1984, “Relative Flow Structure at Exit from an Axial Compressor Rotor in Rotating Stall,” ASME Paper #84-GT-240.

Cousins, W. T., and O’Brien, W. F., 1985, “Axial-Flow Compressor Post-Stall Analysis,” AIAA Paper #85-1349.

Cousins, W. T., 1985, “Summary of Some Applications and Analysis Techniques of High-Response Data,” Internal AlliedSignal Presentation.

Cousins, W. T., Jones, M. G., and Belling, T. L., 1995, “Surge and Stall Characteristics of Axial-Centrifugal Compressors: The Enhancement to Engine Stability,” AGARD Symposium on *Loss Mechanisms in Turbomachinery*, Derby, UK.

Davis, Jr., M. W., 1991, “Parametric Investigation into the Combined Effects of

Pressure and Temperature Distortion on Compression System Stability," AIAA Paper 91-1895, Presented at the 27th Joint Propulsion Conference, Sacramento, CA.

Davis, Jr., M. W., and O'Brien, W. F., 1991, "Stage-by-Stage Poststall Compression System Modeling Technique," AIAA Journal of Propulsion and Power, Vol. 7, No. 6, pp. 997-1005.

Day, I. J., 1976, "Axial Compressor Stall," Ph.D. Dissertation, Christ's College, University of Cambridge.

Day, I. J., and Cumpsty, N. A., 1978, "The Measurement and Interpretation of Flow within Rotating Stall Cells in Axial Compressors," Journal of Mechanical Engineering Science, Vol. 20, pp.101-114.

Day, I. J., Greitzer, E. M., and Cumpsty, N. A., 1978, Prediction of Compressor Performance in Rotating Stall," Journal of Engineering for Power, Vol. 100.

Day, I. J., 1993, "The Unstable Behavior of Low and High Speed Compressors," ASME Paper #93-GT-26, also Journal of Turbomachinery, Vol. 116, Issue 2, pp. 194-201.

Emmons, H. W., Pearson, C. E., and Grant, H.P., 1955, "Compressor Surge and Stall Propagation," Transactions of the ASME, pp. 455-469.

Garnier, V. H., Epstein, A. H., and Greitzer, E. M., 1990, "Rotating Waves as a Stall Inception Indication in Axial Compressors," ASME Paper # 90-GT-156.

Gorrell, S. E., and Davis, Jr., M. W., 1993, "Application of a Dynamic Compression System Model to a Low Aspect Ratio Fan: Casing Treatment and Distortion," AIAA Paper 93-1871, Presented at the 29th Joint Propulsion Conference and Exhibit, Monterey CA.

Greitzer, E. M., 1978a, “Surge and Rotating Stall in Axial-Flow Compressors - Part 1: Theoretical Compression System Model,” ASME Journal of Engineering for Power, Vol. 98, pp. 190-198.

Greitzer, E. M., 1978b, “Surge and Rotating Stall in Axial-Flow Compressors - Part 2: Experimental Results and Comparison With Theory,” ASME Journal of Engineering for Power, Vol 98.

Hale, A. A., and Davis, Jr., M. W., 1992, “DYNamic Turbine Engine Compressor Code: DYNTECC — Theory and Capabilities,” AIAA Paper 92-3190, Presented at the 28th Joint Propulsion Conference and Exhibit, Nashville, TN.

Haynes, J. M., Hendricks, G. J., and Epstein, A. H., 1994, “Active Stabilization of Rotating Stall in a Three-Stage Axial Compressor,” Journal of Turbomachinery, Vol. 116, Issue 2, pp. 226-239.

Kimzey, W. F., 1977, “An Analysis of the Influences of Some External Disturbances on the Aerodynamic Stability of Turbine Engine Axial Flow Fans and Compressors,” AEDC-TR-77-80 (AD-A043543).

Koch, C. C., 1981, “Stalling Pressure Rise Capability of Axial Flow Compressor Stages,” ASME Paper #81-GT-3.

Moore, F. K., 1983, “A Theory of Rotating Stall of Multistage Axial Flow Compressors,” NASA CR-3685, Lewis Research Center, Cleveland, OH.

Owen, A. K., and Davis, Jr., M. W., 1994, “Modeling the Dynamic Behavior of an Axial-Centrifugal Compression System,” AIAA Paper 94-2802, Presented at the AIAA /ASME/SAE/ASEE Joint Propulsion Conference, Indianapolis, IN.

Owen, A. K., Le, Dzu K., Braun, Donald C., and Mattern, Duane L., 1996, “Forced Response Testing of an Axi-Centrifugal Turboshaft Engine,” AIAA Paper #96-2573.

Owen, A. K., Mattern, Duane L., and Le, Dzu K., 1996, “Comparison of Rig and Engine Dynamic Events in the Compressor of an Axi-Centrifugal Turboshaft Engine,” ASME Paper #96-GT-239.

Sexton, M. R., and O’Brien, W. F., 1981, “A Model for Dynamic Loss Response in Axial-Flow Compressors,” ASME Paper #81-GT-154.

Takata, H., and Nagano, S., 1972, “Nonlinear Analysis of Rotating Stall,” Journal of Engineering for Power.

12.0 VITA

William T. Cousins was born in Orange, New Jersey on October 14, 1954. He attended the elementary and secondary schools in Basking Ridge, New Jersey. In 1973, he began studies at Virginia Polytechnic Institute and State University, where he entered into the cooperative education program, being employed in the power production industry. He completed a Bachelor of Science Degree in Mechanical Engineering in 1978 and a Master of Science Degree in Mechanical Engineering in 1979. Over the next six years, he taught as an instructor in the Mechanical Engineering Department while fulfilling the coursework requirements for the Doctor of Philosophy Degree in Mechanical Engineering. In 1985, he accepted a position at AlliedSignal Engines in Phoenix, Arizona, where he has been for the past 13 years, both in a supervisory capacity and also as a technical specialist. Currently, he holds the position of Senior Engineering Specialist in the Performance & Operability Department. He has published extensively in the area of aircraft engine compressor system aerodynamic stability and dynamic operation, and is currently listed in *Who's Who In Science and Engineering*. In addition to his technical duties, he is a Corporate Certified Facilitator/Trainer for the AlliedSignal Total Quality Program. He regularly teaches classes and lectures on different aspects of total quality, such as team building, cycle time reduction, and culture change. Active in ASME International for over 14 years, he has held all the offices in the Arizona Section, is the past ASME Vice President of Region XII, and is currently the ASME Vice President for Professional Development.